ACS OMEGA

Open Access

http://pubs.acs.org/journal/acsodf

Review

Carbon Dots and Their Polymeric Nanocomposites: Insight into Their Synthesis, Photoluminescence Mechanisms, and Recent Trends in Sensing Applications

Dilip Kumar Kar, Praveenkumar V, Satyabrata Si, Harekrishna Panigrahi,* and Smrutirekha Mishra*

Cite This: *ACS Omega* 2024, 9, 11050−11080

Read Online

ACCESS | Metrics & More | Article Recommendations

ABSTRACT: Carbon dots (CDs), a novel class of carbon-based nanoparticles, have received a lot of interest recently due to their exceptional mechanical, chemical, and fluorescent properties, as well as their excellent photostability and biocompatibility. CDs' emission properties have already found a variety of potential applications, in which bioimaging and sensing are major highlights. It is widely acknowledged that CDs' fluorescence and surface conditions are closely linked. However, due to the structural complexity of CDs, the specific underlying process of their fluorescence is uncertain and yet to be explained. Because of their low toxicity, robust and wide optical absorption, high chemical stability, rapid transfer characteristics, and ease of modification, CDs have been recognized as promising carbon nanomaterials for a variety of sensing applications. Thus, following such outstanding properties of CDs, they have been mixed and imprinted onto different polymeric components to achieve a highly efficient nanocomposite with improved functional groups and properties. Here, in this review, various approaches and techniques for the preparation of polymer/CDs nanocomposites have been elaborated along with the individual characteristics of CDs. CDs/polymer nanocomposites recently have been highly demanded for sensor applications. The insights from this review are detailed sensor applications of polymer/CDs nanocomposites especially for detection of different chemical and biological analytes such as metal ions, small organic molecules, and several contaminants.

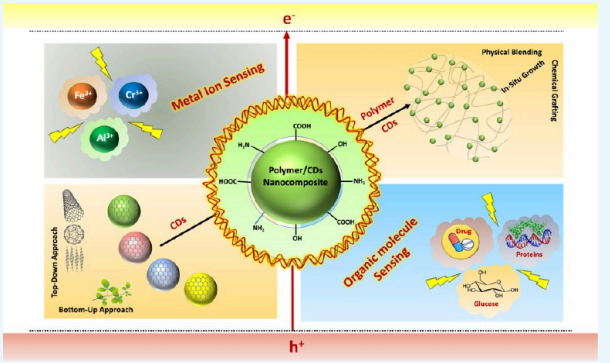

1. INTRODUCTION

Nanostructured materials are currently an area of interest for individual academics as well as research groups around the world because of their enormous potential to improve life and society.[1] In his article "There's plenty of room at the bottom," Feynman (1960) emphasized the benefits of being able to construct structures atom by atom, pointing out that if a bit of information only requires 100 atoms, then all books ever written could be stored in a cube 0.02 in. (0.05 cm) on each side.[2] Even though these nanomaterials have been a part of several applications and products since the dawn of civilization/time, it is currently becoming possible to get better control of their systematic synthesis process and variable application fields.[3,4] By using modern characterization techniques,[5] we have gained a better conception of various nanomaterials which have been discovered earlier as well as have existed in the past. Nanomaterials are classified based on the dimensions of a material, that is, above the nanoscale (<100 nm) range.[6] These are classified as 0D (nanoparticles), 1D (nanowires, nanorods, nanofibers, and nanotubes), 2D (graphene, nanofilms, nanosheets, and nanocoatings), and 3D (bulk powder, dispersions, bundles of nanowires and nanotubes).[7] There are several "top-down" and "bottom-up" methods for generating nanomaterials of various sizes, and these have a vast range of applications.[8] In the healthcare field,[9] these are mostly used for drug delivery including delivery of chemotherapeutic medications for cancerous growth directly along with delivery into the damaged regions of arteries in the case of cardiovascular disease.[10] Additionally, efforts are being made to generate carbon nanotubes for applications such as creating bacterial sensors by fusing antibodies into nanotubes.[11] In the cosmetics industry, titanium oxide nanoparticles are used in sunscreen due to their excellent UV protection properties.[12] These have potential applications in electronic and computing industries,[13,14] and also in the energy industry, these may increase the effectiveness and efficiency along with lowering the cost of

Received: October 1, 2023
Revised: February 1, 2024
Accepted: February 8, 2024
Published: February 26, 2024

conventional techniques of energy generation, such as solar panels,[15,16] while also creating new opportunities for energy storage[17] and harnessing.[18]

The most promising outcomes of nanotechnology are carbon-based materials, which have intriguing features that make them suitable for a large range of usages, from medication to electronics.[19] Recent years have witnessed a rapid growth in the field of research being done on carbon-based nanomaterials, which includes carbon nanotubes, graphene, and its derivatives, fullerenes, nanodiamonds, and other nanosized carbon allotropes.[20] Dimensionally these are divided into 0D, which include nanodiamonds, carbon dots (CDs), and GQDs, and 1D, which include single-walled carbon nanotubes (SWCNTs) and multiwalled carbon nanotubes (MWCNTs), and 2D containing graphene and its derivatives like GO and reduced graphene oxide (RGO).[21] Among the carbon-based nanomaterials, carbon nanotubes (CNTs) are the strongest and stiffest materials with respect to tensile strength and elastic modulus until now. CNTs are chemically bound together with sp^2 bonds, an exceptionally strong type of molecular interaction, just like its fundamental constituent, graphene.[22,23] Another remarkable carbon-based nanomaterial is graphene, in which carbon atoms are bound together in a hexagonal configuration. It is the strongest substance known to us, which is also one of the most electrically and thermally conductive substances.[24] Since graphene is expensive and rather difficult to generate, tremendous efforts are made to develop efficient and affordable processes for producing and using graphene derivatives or similar materials. One such material is graphene oxide (GO), a single-atomic layered substance produced by the potent oxidation of graphite, a resource that is both inexpensive and abundant. Infused with oxygen-containing groups, GO is an oxidized version of graphene having good water dispersibility.[25,26] Due to their small size, significant thermal and electrical conductivity, large specific area, superior mechanical properties, and special optical properties, carbon nanomaterials have nearly endless potential for modification and tailoring, which further opens the door for a wide variety of applications in different fields.[27−29]

Currently, nanomaterials having fluorescent properties have emerged as a result of the fast growth of nanotechnology during the last two decades. These fluorescent nanomaterials have unique optical characteristics due to their nanoscale size, which is crucial in several fluorescent-related applications like bioimaging and detection. The phenomenon of fluorescence is simply the process of emitting light upon absorption of light of a specific wavelength in the case of any molecule. Most of the time, the wavelength of the emitted light is longer than that of the absorbed light.[30,31] There are different types of fluorescent nanomaterials with diversified features and properties. Starting from the inorganic class, semiconductor quantum dots (QDs), silicon/functionalized silicon-based nanomaterials, and metal nanoclusters are the most used, whereas from the organic class carbon-based nanomaterials including graphene quantum dots (GQDs), carbon quantum dots (CQDs), and carbon dots (CDs) along with certain polymeric nanoparticles are well-known. Semiconductor QDs are renowned for their size-dependent fluorescence emission, known as quantum confinement, and by controlling the composition and size of these dots, their emission wavelengths can be precisely tuned. Silicon-based nanomaterials, such as silicon nanocrystals, also exhibit fluorescent properties and demonstrate efficient light emission in the visible and infrared region, which is valuable for silicon-based optoelectronics. Metal nanoclusters are small assemblies of a few several hundred atoms, and these nanoclusters exhibit strong fluorescence emission due to quantum size effects and surface plasmon resonance.[32] CDs, CQDs, and GQDs are carbon-based nanomaterials that exhibit bright fluorescence emission, and the fluorescence properties of these dots basically arise from the presence of sp^2 carbon domains and functional surface groups. As there is still a lot of misconception and debate going on for the exact reason for fluorescence in these carbon-based nanomaterials, we will have a detailed discussion regarding this in the following sections. It is important to note that the fluorescent properties of these nanomaterials can be further enhanced or modified through surface modifications, such as coating them with specific ligands or functionalizing them with biomolecules. These modifications enable the fluorescent nanomaterials to target specific biological or chemical entities for various sensing applications, which is the central focus of this review.

As fluorescence emission is highly sensitive to the immediate microenvironment of a fluorophore, it has been exploited in the development of several sensing applications. The fluorescence would be impacted by any parameter that may have a molecular interaction with the fluorophore.[30] Talking about sensors, the detection system of signals is based on the recording of an alternation in any one of the physical characteristics (such as mechanical, optical, electrical, or thermal) of sensing materials brought on by the interaction with the analyte. The idea for optical sensor systems can be based on the major benefit of employing these fluorescent nanoparticles, such as altering their optical characteristics like intensity, emission color, emission kinetics, or polarization. Fluorescent nanomaterials may be used to detect analytes via a variety of techniques, such as nonradiative Förster resonance energy transfer (FRET), emission quenching from nanomaterials, and increments in emission as a result of the analyte passivating the surface of the nanomaterial.[32] Comparing these fluorescent nanomaterial-based sensors to other small molecule-based ones, there are several benefits that can be obtained. Their benefits include customizable fluorescence characteristics, simple biofunctionalization, the capacity to detect multiple analytes, and being able to detect ultrasensitively even at the nanomolar and picomolar levels of particle concentration, which is not achievable with small molecules.

As discussed earlier, while all these nanomaterials exhibit fluorescence properties, their characteristics differ based on their composition, size, and surface properties. CDs have gained significant attention as fluorescent nanomaterials due to several advantages over others. Notably, CDs being emerging nanomaterials in the nanocarbon family are gradually replacing semiconductor QDs and others on the grounds of their superior biocompatibility, high water solubility, high photostability, excellent cell permeability, excitation-dependent multicolor emissions, and preferable surface modification flexibility.[33] Therefore, a brief history and detailed specifications are mentioned in the next section about CDs.

2. CARBON DOTS (CDs)

CDs were initially identified in 2004 during the preparative electrophoresis purification of SWCNTs.[34] CDs, considered quasispherical carbon nanoparticles, are composed of carbon, oxygen, and hydrogen atoms with a size of fewer than 10 nm. Although there are two fundamental methods for the synthesis

https://doi.org/10.1021/acsomega.3c07612
ACS Omega 2024, 9, 11050−11080

of CDs, i.e., breaking down large carbonaceous materials (top-down) and pyrolysis of small organic molecules (bottom-up); we have witnessed almost a dozen synthetic pathways for this task throughout the years.[35,36] Nearly every carbon-containing precursor has been used to create CDs, including citrates and amines, phenylenediamines, graphite, ionic liquid, polymers, saccharides, biomass, human hair, and human urine.[35,37] CDs have been prepared using a variety of top-down approaches including laser ablation,[38,39] arc discharge,[40,41] electrochemical/acidic oxidation,[42−44] electrochemical exfoliation,[45,46] combustion/thermal microwave-assisted heating,[47,48] and other supported syntheses; however, among these, several techniques are of the complex treatment process and need complex equipment. Having easy operational steps and a lower economic nature, bottom-up methods like hydrothermal,[49,50] solvothermal,[51,52] ultrasonication,[53,54] and MWA (microwave assist)[55,56] synthesis are the most significant. Numerous surface functionalities like high flexibility and tenability of CDs generated employing bottom-up methods, which are, in the case of top-down approaches, difficult to achieve. Aside from their low cost, facile synthesis, and ease of functionalization characteristics, CDs exhibited extraordinary fluorescence properties that have earned them the title "carbon nano lights", and thus a variety of applications can be assigned for these nanomaterials. CDs have exceptional photochemical and physiochemical stability,[57,58] increased water dispersibility, intense and tunable photoluminescence,[59−61] excellent biocompatibility,[62,63] and minimal toxicity. CDs are classified into three distinct classes, namely, carbon nanodots (CNDs), which possess graphite or amorphous-like structure, graphene quantum dots (GQDs), which consist of one or 2−3 graphene layers, and polymer dots that consist of aggregated linear polymer chains around or inside a carbon core, respectively. CDs are widely used in the optical, energy, and biomedical fields and also have great electrical and optical properties with a minimal production cost and good biocompatibility. CDs have a huge range of applications in several scientific disciplines which include catalysis,[64,65] CO_2 reduction,[66] sensors,[67] information encryption,[68,69] light-emitting diodes (LEDs),[70] and promising biomedical applications like phototherapy,[71] bioimaging,[72] drug/gene delivery,[73] and nanomedicines[74] and as nanofillers.[75]

2.1. Synthesis of CDs. Initially, inorganic nanoparticles have frequently been produced from solid substrates using laser ablation, in which the earliest direct demonstrations of CDs were carried out by Sun and co-workers. The synthesized CDs did not possess fluorescent properties initially, and to achieve that, surface passivation/functionalization with hydrocarbon chains (more particularly with PEG) was performed to get the desired photoluminescence.[76] Since surface passivation might render CDs' hydrophilic nature, i.e., water solubility and being amenable to biological applications including bioimaging, this contributed a significant role in the growth of CD investigations. Li et al. reviewed CDs having fluorescence using different solvents through laser irradiation and further doping with metal ions.[77] Although the effect of doping with inorganic salts on the luminescence of CDs was intriguing from a synthetic perspective, this era of study has not advanced significantly due to the fact that one of the quite notable "selling points" of CDs is that they are made from organic building blocks, resulting in less toxicity in CDs than inorganic nanoparticles.

Wet chemistry had been used in CD synthesis like other several synthetic processes, which outline a conventional solution-based approach. The method was created by Liu and co-workers, and it was based on incorporating the carbon source, i.e., phenol/formaldehyde resin within the host matrix of porous silica colloids.[78] CDs were synthesized using the pyrolysis process and released after the silica scaffold was broken down. Surface functionalization then led to the development of the characteristic luminescent features of the CDs. Ngu et al. synthesized CDs using a bottom-up approach, which simply involved the carbonization of considerably inexpensive rice husks with sulfuric acid.[79]

A rather simple and less complex synthesis method was introduced by Ray and colleagues by taking carbon soot as a natural carbon precursor source and refluxing them in strong acid (nitric acid).[80] However, the resulting CDs possessed a comparatively low quantum yield, which was probably due to the larger particles generated and the wide size range. In this same significant field, Qiao et al. effectively created CDs using activated carbon as a natural source through an acid-induced oxidation process.[81] Following chemically derived CD purification, surface functionalization was performed using various amine-terminated organic agents, resulting in water-soluble luminous CDs.

Other solution-based procedures have been developed concurrently with the growth of "chemical oxidation" approaches in the field of CD synthesis. Particularly, the process of generating CDs by the hydrothermal method has probably become the most popular one. The key of this method is to induce condensation of carbonaceous building components at elevated temperatures and further crystallization of the graphitic core of the precursor materials.

Wang et al. studied a straightforward hydrothermal refluxing approach for the synthesis of multicolor CDs using this technique.[82] Amino acids and carbohydrates are converted to luminous CDs using the Millard reaction. By adjusting the amount of base (NaOH) in the precursor solution, CDs of different vibrant colors were created. Through the hydrothermal treatment of aloe plants, Xu et al. devised a simple and green approach for the production of fluorescent CDs.[83] Sahu et al. prepared highly photoluminescent CDs from orange juice using a one-step hydrothermal process, having a pretty high level of quantum yield of 26%.[84] Here, it is demonstrated that the large-scale, easy, environmentally friendly synthesis of CDs is possible using a natural precursor. A study by Jana et al. reported the synthesis of CDs doped with nitrogen utilizing citric acid and 3-aminophenyl boronic acid using the hydrothermal method.[85] By combining $ZnCl_2$ and sodium citrate, Xu et al. synthesized blue-light-emitting CDs (CZnO−Dots), and those were employed as potential biosensors.[86] Cheng and co-workers combined citric acid and zinc chloride in toluene to obtain yellow fluorescent CDs, which were further used in certain applications like fluorescent microfibers and bifunctional photonic crystal films.[87] In another study, Pawar et al. reported the synthesis of nitrogen-doped red-emitting CDs (NRCDs) using *para*-phenylenedimine through the hydrothermal method.[88]

Other methods of generating CDs include a microwave-based synthesis technique, which may be the most affordable and simplest way of synthesizing CDs. It is noteworthy that this facile synthetic approach, developed by Zhang and co-workers, demonstrated the synthesis of N-doped CDs (N-CDs) through a microwave-assisted approach using citric acid

https://doi.org/10.1021/acsomega.3c07612
ACS Omega 2024, 9, 11050−11080

and amino compound-containing hydroxyls like ethanolamine and tris(hydroxyl-methyl)aminomethane.[89] The resulting CDs have significant luminescence blue emissions in solution phases. Wang et al. prepared highly fluorescent CDs through the microwave irradiation method in which polyethylenimine (PEI) was carbonized.[90] The synthesized CDs had a greater intercellular transport efficiency, superior biocompatibility, and stability. Sun et al. described a microwave synthesis approach for the production of red-emitting CDs (RCDs) utilizing phenylenediamine as the carbon source.[91] Particularly *p*-phenylenediamine was dissolved in an ethanol/water mixture followed by sonication and further heating in a domestic microwave oven.

Ju and co-workers reported a one-step carbonization method for the synthesis of red-emitting nitrogen-doped CDs (RN-CDs).[92] The main criteria to synthesize the N-CDs were that acidic conditions should be maintained, and the red emission of N-CDs is pH-dependent, suggesting proton-controlled synthesis and emission. Ding et al. also synthesized red-emitting CDs (RCDs) from pulp-free lemon juice by the process of solvothermal heating.[93] This simple, cost-effective, and ecofriendly way synthesis resulted in highly red luminescent CDs with a remarkable quantum yield of 28%.

One step forward, Bhati and co-workers outlined a simpler method of synthesis of CDs embedded with magnesium−nitrogen (r-Mg-N-CD) having red emission by using the leaves extract of the widely accessible bougainvillea plant through a microwave carbonization process.[94] The excitation-independent emissions from the CDs were detected at ∼678 nm with a higher quantum yield (40%) and remarkable photostability. Khare et al. also synthesized red-emitting zinc-doped CDs (CZnO-Dots) from bougainvillea leaves with remarkable photostability, better water solubility, and high quantum yield (50%).[95] Miao et al. synthesized multiple color emissive CDs using citric acid and urea through the thermal pyrolysis method.[96] As an application, CDs/epoxy resin composite discs were prepared along with pure white LED devices. Hu et al. studied the synthesis of full-color emitting CDs using CA and urea through a solvothermal approach and utilized those in LED applications.[97] Using the same precursors, Tian et al. obtained full-color emissive CDs by tuning the solvents under solvothermal conditions and employed them as CDs phosphors for the fabrication of white LEDs.[98]

The higher production cost and intrinsic poor yield of CDs became the significant bar that substantially restricts their practical usage, preventing CDs as a reality for commercial use.[99,100] So instead of using commercial chemicals and elements as precursors, coal and heavy oil may serve as an alternate source due to their large-scale availability. Heavy oil is an unfavorable feedstock in the conventional refining market owing to its poor yield of fuel products. Still, the presence of plentiful natural aromatic structures and heteroatom compounds enable them to serve as a precursor for the bulk fabrication of carbon products.[100,101] For instance, Hu et al. integrated acid oxidation corrosion and carbonization to turn inexpensive coal into fluorescent CDs, which were then used for copper ion detection.[102] Shao et al. used acid oxidation corrosion to turn petroleum coke into green fluorescent CDs, which were then used in the photocatalytic application.[103] However, coal and lignin have been documented as precursor sources, and the differences and nonrepeatability prevent CDs from being produced in large quantities having a greater quantum yield.[100] To overcome these hurdles, studies in the field of mass production of CDs and characteristic improvement of photoluminescent quantum yield (PLQY) have recently emerged. Heavy oils, particularly the enormous amounts of generated asphalt following solvent extraction, are abundant in heteroatoms and rich aromatic compounds, which might make them possible CD precursors. Ma et al. particularly focused on the mass production of CDs with a high quantum yield through new simple and cost-effective methods for the feasible use of CDs in practical applications. Following a simple hydrothermal approach, they were able to synthesize four highly fluorescent multicolor petroleum-based CDs. With a higher quantum yield (i.e., 64%) and a wide range of photoluminescence (350−650 nm), these CDs were synthesized with a bulk amount from heavy oil and its three solvent deasphalting (SDA) products (i.e., heavy deasphalted oil (HDAO), light deasphalted oil (LDAO), and asphalt).[103] Zhu et al. reported a novel quick magnetic hyperthermia (MHT) approach for large-scale production of luminescent Zn^{2+}, Na^{+}, and K^{+} doped CDs employing corresponding citrate and carbamide as precursors. With an outstanding product yield of 85 g/h and a quantum yield of 50%, the resulting multicolor emissive CDs exhibited exceptional wound healing properties and offered enhanced mechanical performance when utilized as nanofillers.[99] Li et al. was not only able to fabricate CDs in the kilogram-scale (1.4975 kg) but also achieved a stable PLQY of 10.64%. Having low cytotoxicity and consistent photoluminescence range within the biological pH range, these CDs showed multiple applications such as bioimaging and Fe^{3+} ion sensing.[104] Liu et al. synthesized CDs with an outstanding higher absolute PLQY of 67% and a large production output of 25.37 g (from a single batch) from citric acid and carbamide using the MHT method. These resulting CDs significantly improved the overall mechanical properties of nanofiber films of polymers and polymer mixtures when embedded within the polymer matrix.[105] Also, the inclusion of AI and machine learning in the process optimization of chemical reactions has brought revolutionary advancement in the case of experimentation. Tang et al. have developed a regression model on hydrothermally grown CDs to improve process-related features such as PLQY. For getting CDs with a higher quantum yield, ideal possible reaction conditions were obtained from the trained XGBoost-R model, and using those results as reaction parameters, CDs with PLQY of 55.5% were surprisingly achieved. This is one of the highest achieved QY despite having a relatively low heteroatom doping ratio of the precursors.[106]

2.2. Structure of CDs. Understanding CD structures is essential for comprehending their main characteristics, such as fluorescence. Although the precise structure of CDs varies depending on the precursors and the synthesis process, it is widely agreed that CDs are made up of amorphous clusters and carbon crystalline cores comparable to sp^2 carbon. The core of a CD structure can be either crystalline or amorphous. The surface shell that surrounds the core of a CD structure can include a wide range of polar or nonpolar groups, ranging in size from small functional groups to lengthy atomic chains. Different functional groups are often added to CDs in addition to the basic carbon framework by surface passivation or functionalization, which protects the surface and improves the fluorescence of the CDs. Based on the impact of surface passivation, both amorphous and crystalline CDs exhibit comparable optical phenomenology. It is easily comprehensible that the core has almost no influence on the process of

https://doi.org/10.1021/acsomega.3c07612
ACS Omega 2024, 9, 11050−11080

fluorescence emission and that the surface is the sole important component.[107] Different analytical techniques are often used to describe CDs, and their physical characteristics reveal the crystalline structure of the carbon atoms, and to investigate the kind and quantity of functional units that are present on the CDs' surface. The primary method for visualizing CDs has been transmission electron microscopy (TEM), which offers crucial details on particle morphology, size distribution, and crystalline structure. As a result of the graphitic core's crystalline form, high-resolution TEM (HRTEM) studies have been employed to validate the graphitic core's periodicity.

2.3. Photoluminescence of CDs. Excitation-dependent photoluminescence, also known as excitation-dependent emission, is one of the most notable characteristics of CDs. The multicolor characteristics of CDs are highlighted by the broad-spectrum range and relatively high intensities of the emission peaks. In fact, one of the special characteristics of CDs used in various applications is the ability to tailor the emission color by the excitation wavelength.[108] Figure 1 shows typical excitation-dependent luminescence spectra and the related colors.

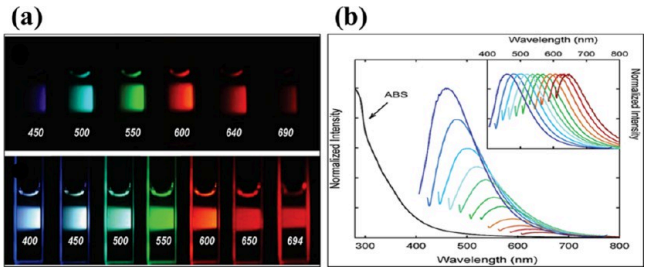

Figure 1. Excitation-dependent luminescence of CDs. (a) Photographs of CDs that have been passivated with polyethylene glycol (PEG) and excited at 400 nm and captured using various bandgap emission filters, or stimulated at the given wavelengths. (b) Fluorescence emission spectra of the carbon dots excited at 20 nm increasing increments. The emission spectra at normalized intensities are displayed in the inset. Reprinted with permission from ref 76. Copyright 2006 American Chemical Society.

It is widely acknowledged that CDs' fluorescence and surface conditions are closely connected. Nevertheless, the precise underlying process of CDs' fluorescence is uncertain and has to be clarified due to the structural complexity of CDs.[109] Even CDs synthesized from identical ingredients (mixtures containing the same amount of formamide and citric acid) might have different optical characteristics depending on the microwave hydrothermal method's applied heat temperature and time. In other words, the fluorescence spectra of two independent CDs samples might differ. While CDs synthesized over extended periods of reaction time at low temperatures had a blue color when exposed to the same wavelength of light, those made over brief periods of reaction time at high temperatures displayed a whole color spectrum.[110] This could be explained by the different sizes of the CDs, which have an impact on their emission profiles because, like semiconductor QDs, CDs' emission is governed by quantum confinement effects, meaning that as QDs get smaller, the energy gap between their valence shell and conduction band widens and their emission wavelength shrinks. Investigation indicated that the full-colored CDs contained more functional groups, including C═N/C═O and C−N groups, on their surfaces than the other sample, suggesting that the differences may be related to the CDs' surface states.[111]

Until now, the photoluminescence properties of CDs have different controversial origin causes. Certain major points are pointed out in the earlier/following sections briefly, but the most common misconception for the actual origination of fluorescence properties in CDs after synthesis pointed out by Essner et al. has created a question about the purification process associated with CDs and whether the real fluorescence is due to the CDs or due to the organic byproducts or impurities or generated surface organic fluorophore.[112] From their study, it can be clearly pointed out that the current proposed purification processes (i.e., filtration or membrane dialysis) are not totally effective toward the complete separation of actual CDs from the synthesized products (especially in the case of bottom-up synthesis), which contains CDs along with impurities, organic fluorophore, and artifacts. It is significant since the top-down CDs production results in fewer molecular byproducts. Taking artifacts into consideration, the authors also explained this by observing the improper fluorescent emission peaks of CDs, and visual red emissions which further revealed that this red color was due to the visual artifact arising from illumination of a concentrated solution already brick red in color. On the contrary, it is demonstrated that the fluorescence from organic fluorophores having small molecular weight dominates the CDs emission in unpurified products generated through bottom-up approaches. A similar aspect is also explained by Javed et al. in which they also identified the long-term impact of fluorescence impurities in CDs resulted in a gradual decrease of quantum yield. From the experimental results, it was clear that the continuous decomposition of impurities caused a deposition on the particles with respect to time, which as a result increased the particle size following the gradual decay of photoluminescent emission. Impurities in CDs samples can affect the photoluminescent capabilities of CDs. Impurities can introduce artifacts and influence PL behavior in a variety of ways. Impurities in the CDs might cause defects or trap states. These defects and traps can serve as nonradiative recombination locations, effectively suppressing PL emission.[113] Impurities can also influence charge carrier dynamics, influencing recombination rates and PL lifetimes. Impurities on the surface of CDs can either inhibit or improve surface state passivation. Surface passivation is essential for efficient light emission from CDs. Impurities that interfere with the passivation process can introduce nonradiative electron relaxation routes, lowering the total photoluminescent quantum yield. Impurities can operate as energy acceptors or donors, resulting in energy transfer mechanisms that compete with the PL-causing radiative recombination. Impurities with energy levels near the excited states of CDs, for example, can enable nonradiative energy transfer, resulting in a drop in photoluminescent intensity.

Comprehending the stability of carbon dots (CDs) is crucial for their various applications. The characteristics of CDs, including structure, fluorescence, and solubility, are influenced by factors such as synthesis method, precursors, and synthetic parameters (e.g., temperature, time, pH). Thermal stability refers to a material's ability to remain stable under elevated temperatures. Typically, the chemical structure of fluorescent materials undergoes changes at higher temperatures, leading to a decline in emission. Therefore, it is essential for carbon dots to exhibit high thermal photostability to endure applications

https://doi.org/10.1021/acsomega.3c07612
ACS Omega 2024, 9, 11050−11080

involving elevated temperatures. In a study conducted in 2014 by Kim et al.,[114] the thermal stability of synthesized silica-based carbon dots was tested at 80 °C. Over a testing period of 264 h, these CDs demonstrated less photoluminescence intensity degradation under heat compared to exposure to UV light. In less than an hour, CDs in silica experienced a 20% reduction in initial photoluminescence (PL) intensity, while it took over 6 h for KBr S-CDs (identified as the most thermally stable) to reach the same level of degradation. At the conclusion of the thermal stability assessment, it was noted that CDs in silica, S-CDs in KCl, and S-CDs in NaCl retained 20%, 40%, and 60%, respectively, of their initial PL intensity. The most favorable outcome was observed for S-CDs in KBr, where approximately 80% of the original PL intensity was retained. All samples exhibited rapid degradation of PL intensity within the first 4 h of temperature exposure, likely due to the presence of retained oxygen and water. However, once water was evaporated from the crystals, degradation either slowed down or stabilized. In 2014, Wang et al.[115] also observed that the emission intensity of the as-prepared carbon dots (CDs) was strongly influenced by temperature. The emission spectra of the CDs, however, did not shift with temperature, as depicted. The intensity decreased by 52% as the temperature increased from 15 to 90 °C, and the PL intensity of the obtained CDs exhibited a somewhat linear change as the temperature increased from 15 to 60 °C. The intriguing aspect of these CDs lies in their suitability for in vivo temperature monitoring applications, given that the temperature range they can withstand exceeds physiological temperatures. In 2016, Liu et al.[116] conducted thermal stability tests on N-CDs in two scenarios: (1) a broad temperature range heating test, and (2) a constant temperature heating test for a set duration. Results indicated that the initial fluorescence intensity of N-CDs remained stable between 25 and 65 °C. Further increasing the temperature from 75 to 95 °C resulted in a slight 2% increment in fluorescence intensity. Additionally, a heating test conducted for 360 min at fixed temperatures of 70 °C, 80 °C, and 90 °C provided further insights into the thermal stability of N-CDs. No decline in fluorescence intensity was observed at any of the fixed temperatures throughout the heating process compared to the initial fluorescence intensity. However, after 360 min, increases in fluorescence intensity of 2%, 7%, and 5%, respectively, were noted at temperatures of 70 °C, 80 °C, and 90 °C. The exceptional stability performance is attributed to the constitution and steric effects of Tris, which contains numerous dendritic hydroxyl-methyl groups.

Similarly, focusing on the pH and ion solution, it is highly required for ensuring the practical applicability of CDs hinges on their stability concerning ions, pH, and time. To assess ion stability, the impact of specific common cations at various concentrations on the synthesized fluorescent CDs was examined. Similarly, pH stability is evaluated by monitoring photoluminescence quenching under different pH conditions. Time stability indicates the duration over which CDs maintain their properties, a critical parameter from an application standpoint since the longevity of CDs-integrated systems directly relies on their time stability. In 2014, Wang et al.[115] explored the ion stability of freshly prepared carbon dots (CDs). In this investigation, 20 mM solutions of NaCl, KNO_3, NH_4Cl, $ZnCl_2$, $Ba(NO_3)_2$, $FeCl_2$, $Ca(NO_3)_2$, $MgSO_4$, $Cu(NO_3)_2$, $Ni(NO_3)_2$, $(CH_3COO)_2Mn$, $Co(NO_3)_2$, $Cd(NO_3)_2$, $PbCl_2$, and $(CH_3COO)_3Cr$ were introduced to 1.0 mL of the produced CDs and mixed for 3 min. The impact of cations such as Na^+, K^+, NH_4^+, Zn^{2+}, Ba^{2+}, Fe^{2+}, Ca^{2+}, Mg^{2+}, Cu^{2+}, Ni^{2+}, Mn^{2+}, Co^{2+}, Cd^{2+}, Pb^{2+}, and Cr^{3+} on the emission response of the synthesized CDs was measured using a fluorescence spectrophotometer. By comparing the fluorescence intensities of the CDs solution in the presence and absence of interfering ions, the relative fluorescence intensity was calculated. The results indicated that the majority of common cations exhibited either no interference or negligible interference, suggesting that the fluorescence intensity of the prepared CDs was not significantly hindered by these cations. Based on pH fluctuations, the reversibility of the switching action of carbon dots was also evaluated. The manufactured CDs were subjected to cycles between pH values of 3 and 9, using acid and base as modulators, and the resulting photoluminescence (PL) intensity was observed. The switching procedure was repeated six times consecutively, showcasing the robust reversibility of the two-way switching operations. The findings suggested that the CDs prepared in this manner could be employed for monitoring liquid temperature and pH. Additionally, the research group assessed the time stability of CDs and observed no significant variation in fluorescence intensity after preserving the synthesized CDs for one month under normal conditions, as described scientifically.

2.4. Factors Affecting Photoluminescence of CDs. Unquestionably one of the most remarkable things about CDs is their PL characteristics, which set them apart from other members of the nanocarbon family. The conjugation effect, the surface state, and the synergistic effect are elements impacting the optical behavior of CDs. Here, we explore how the carbon core and surface state affect PL. Contrarily, a few elements of CD's PL behavior have profoundly confounded the study community.

2.4.1. Quantum Confinement Effect. We begin by describing the quantum confinement effect because the word "quantum" is incorporated into the names of CDs (CQD and GQD). The distance between an electron and a hole inside of an exciton is known as the Bohr radius, and it is generated by the Coulombic interaction of an electron−hole pair. The mobility of the electrons and holes is firmly restrained to the dimension of the material if it decreases to the Bohr radius of the exciton (<10 nm), and significant quantum confinement predominates, leading to unusual optical features. In this case, the fluorescence emission band must be narrowed and excitation independent. The excitonic transition energy and bandgap energy rise with decreasing nanoparticle size, which causes a blue shift in the emission wavelength and a reduction in radiation less energy loss. However, actual experimentation is still needed to confirm the existence of quantum confinement in CDs.[117]

In recent years, scientists have been investigating various methods for synthesizing carbon dots (CDs) that bring about significant changes in their structure, properties, and fluorescence mechanisms. These methods are broadly classified into two categories: top-down and bottom-up techniques. The top-down techniques involve laser irradiation, electrochemical synthesis, and chemical oxidation, while the bottom-up techniques include microwave irradiation and hydrothermal heating. Notably, the microwave irradiation method has emerged as a preferred synthesis approach due to its simplicity and the ability to produce highly luminescent CDs. This method, utilizing electromagnetic irradiation with wavelengths ranging from 1 mm to 1 m in a reaction medium containing

https://doi.org/10.1021/acsomega.3c07612
ACS Omega 2024, 9, 11050−11080

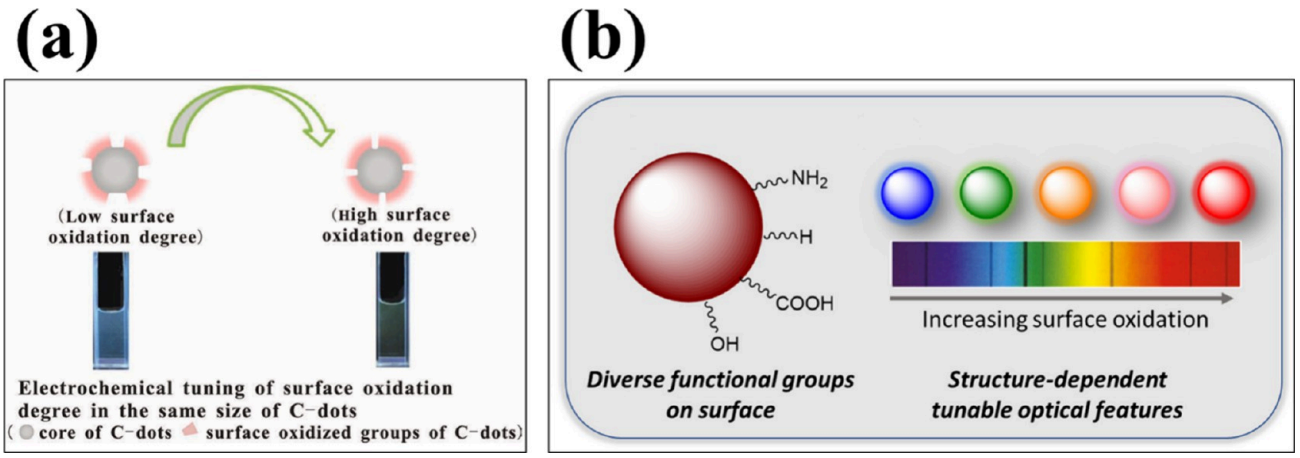

Figure 2. Surface state/defects. (a) Diagram showing the differences in CDs' emissions caused by various levels of surface oxidation. Reproduced with permission from ref 127. Copyright 2011 Wiley. (b) Diagram showing how altering the surface functional groups' oxidation or reduction influences the luminescence of CDs. Reproduced with permission from ref 130. Under the Creative Common Attribution 4.0 International License.

precursor molecule, is a rapid and cost-effective means of synthesizing CDs.

Several studies have successfully demonstrated the synthesis of CDs with a high quantum yield through microwave irradiation, making them suitable for applications such as cell imaging, metal detection, and fluorescence sensors. For instance, He et al. proposed a straightforward microwave-assisted production of CDs with a quantum yield of 51%, which was then applied in the biological cell imaging of BT-474 cells. Additionally, Yang et al.[118] conducted a study where fluorescent CDs were prepared from low-cost xylan via microwave synthesis, requiring low energy consumption (200 W) and completing within 10 min. Collectively, these studies provide compelling evidence that microwave irradiation is an effective, economical, low-cost, and environmentally friendly method for synthesizing CDs. The characteristics and optical features of carbon dots (CDs), particularly the quantum yield and photoluminescence (PL) intensity, are influenced by various synthesis parameters such as pH, temperature, choice of reaction media, types of dopants and carbon precursors, and the ratio of carbon source to reaction medium. The duration of the reaction time plays a crucial role in the formation of CDs from their precursors, ultimately affecting the optical properties of the CDs. For example, Yoshinaga et al.[119] observed an increase in the quantum yield of CDs from 0.7% to 3.0% as the hydrothermal duration extended from 30 to 120 min. Conversely, some reports indicate that prolonged synthesis durations may lead to the destruction of the CDs' structure due to uncontrolled carbonization.

In contrast, So et al.[120] reported the absence of fluorescence in CDs synthesized with microwave irradiation times less than 5 min, suggesting that inadequate synthesis duration results in incomplete carbonization of the precursors. Indeed, manipulating the reaction duration can provide insights into the formation mechanism of CDs, which is crucial for understanding the specific processes involved in complete CDs formation. However, this aspect of study has received limited attention and is rarely investigated due to its complex experimental requirements, necessitating systematic characteristic measures to identify the specific formation mechanism of CDs. Papaioannou et al.[121] outlined a formation mechanism of CDs by varying the reaction duration from 2 to 12 h, proposing four stages, including the decomposition of glucose (precursor), followed by aromatization, nucleation, and growth of CDs.

2.4.2. Conjugation Effect. The conjugation effect is also related to this quantum confinement effect, otherwise known as the size effect. This is a commonly acknowledged PL mechanism where "size" refers to the sp^2 (graphene) domain—the effective conjugation length—rather than the actual particle size.[122] Quasicontinuous electronic levels close to the Fermi level become discrete energy levels as the "size" becomes smaller until it reaches the nanoscale. A greater "size" for CDs results in a smaller bandgap and a longer PL emission wavelength. The energy gap between the highest occupied molecular orbital (HOMO) and the lowest unoccupied molecular orbital (LUMO) diminishes as the CDs' interior graphene domain increases, causing greater delocalization and more even distribution of energy. The PL of CQDs and GQDs with lattice structures or a high level of graphitization may be explained by this paradigm.[123]

2.4.3. Particle Size-Dependent and Independent PL. The particle size-dependent PL of CDs has been examined by several research teams. Li et al. produced CQDs with four distinct particle sizes by electrolyzing aqueous ethanol using graphite electrodes in an alkaline environment.[124] They verified that PL characteristics changed with particle size: tiny (1.2 nm) CQDs were situated in the UV area (about 350 nm), medium (1.5−3 nm) CQDs were found in the visible range (400−700 nm), and big (3.8 nm) CQDs were found in the near-infrared region (around 800 nm). The quantum confinement effect is consistent with this particle size dependency. Kim et al. came to the same conclusion that particle size affects the absorption spectra of GQDs.[125] Many circumstances, nevertheless, go against this dependency. By carefully controlling the thermal pyrolysis of citric acid (CA) and urea, Miao et al. synthesized CDs with multicolor emission, concentrating on CDs with average particle sizes of (3.96 0.54), (4.12 0.68), and (4.34 0.49 nm).[96] Red-shifting in emission wavelength was ascribed to the increasing graphitization or longer effective conjugation lengths rather than size since X-ray diffraction and Raman spectroscopy examinations showed that the degree of graphitization did not match the increasing CDs size trend. By hydrothermally treating a combination of phenylenediamine and urea, Ding et al. also found particle size independent PL of CDs that are

https://doi.org/10.1021/acsomega.3c07612
ACS Omega 2024, 9, 11050−11080

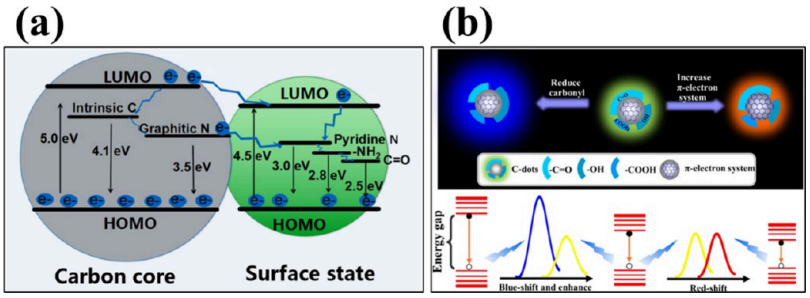

Figure 3. Synergistic effect. (a) An illustration of the energy associated with the luminescence pathway. Reproduced with permission from ref 133. Under the Creative Common Attribution 4.0 International License (b) π-electron and functional group-containing diagram of the putative PL mechanism. Reprinted with permission from ref 134. Copyright 2019 American Chemical Society.

manufactured with various colors, with four samples having fluorescent hues blue, green, yellow, and red with an average particle size of 2.6 nm.[126] The level of surface oxidation is what is responsible for this variance in this case.

2.4.4. Surface States/Defects. In the CDs solution, trap states are generated within the bandgap where the photo-excited electrons and holes can be captured, and after their recombination, fluorescence emission occurs. These trap states are caused by surface defects, functional groups, adsorbed molecules, or impurities. As the excitation wavelength rises, the material under this phenomenon often shows excitation-dependent fluorescence that shifts consistently toward longer wavelengths. The surface state model essentially describes how variations in luminous sites correlate to variations in electronic energy levels. Here, we focus on two types of surface states: surface configurations and doping atoms. The former may be thought of as a general surface structure type in which essential factors include polymers, functional groups (with various degrees of oxidation), defects, and edge states. In the latter, heteroatoms like nitrogen, fluorine, sulfur, phosphorus, or selenium have an impact on PL. Changes in surface arrangements may affect the light-emitting sites or electron energy levels of CDs, maybe even causing emissions in CDs which are nonluminous previously. Redox processes, amino modification/amino passivation, and molecular modification can all influence surface configurations. For having a clear view, we are considering the PL mechanism of CDs synthesized by Bao and co-workers through the electrochemical etching of carbon fibers.[127] Contrary to the conjugation effect, red-shifted emission was observed with CDs produced at higher potentials and also smaller in size. Additional research showed that greater potentials enhance surface oxidation with equivalent increases in emission wavelength. This may be because higher degrees of oxidation increase surface-defect density and trap more excitons, resulting in red-shifted radiation from their recombination. Thus, CDs with significant surface oxidation exhibited green PL (Figure 2a). Another interesting fluorescence on−off phenomenon was observed by Liu and co-workers from the CDs which when fluoresced in dissolved alkaline condition and quenched under acidic conditions. This behavior is due to hydrogen bonds that formed in acid conditions; block emissions which are originated from hydroxyl groups. As a result, hydroxyl-group coatings on CDs improve PL, which is a result of radiative recombination. When hydroxyl or carboxyl groups are embedded on CDs' surfaces, electrons and holes undergo radiative recombination while being illuminated by excitation light, leading to PL.[128] Carboxyl groups, for example, absorb some of the radiation signals, decreasing the PL, whereas hydroxyl groups, which donate electrons, encourage PL. In support of this, Zheng et al. verified that surface groups that donate electrons (on hydrothermally synthesized CDs from candle soot) increase PL by reducing surface carbonyl and epoxy moieties to hydroxyl groups using sodium borohydride. An increase in CDs' luminescence was the outcome of their method i.e., the considerable increase in surface hydroxyl groups without diminishing other species (e.g., C=C and −COOH groups).[129] Further it can note that −OH, −COOH, −CO, and NH_2 are the most prominent functional groups and the characteristics of CDs' surface and core may be altered through functional group modification and doping, respectively[130] (Figure 2b).

The surface configuration of CDs can be altered through amino modification, often known as "amino passivation". It is hypothesized by Li et al. that the level of surface amination affects the PL excitation dependency of CDs. If amino groups passivate all surface states, emissions take place through a single mode of sp^2 carbon's radiative transition, independent of the excitation wavelength. Functional groups like C−O, C=O, and O=CO-H generate a range of various energy levels when surface states are not as passivated, and the fluorescence emission then depends on the excitation energy.[131] Kwon et al. further demonstrated the use of organic compounds with amino groups in the modification of CDs surfaces to modulate their PL. CDs are given additional energy levels via surface functionalization, which results in them exhibiting long-wavelength (up to 650 nm) PL with a very narrow spectral width.[132]

A common technique for changing CDs' electronic structures is heteroatom doping, which involves using elements like nitrogen, fluorine, boron, sulfur, phosphorus, and certain heavy atoms, among which nitrogen and sulfur are common dopants. Doping may be thought of as a surface-state technique even if it is often considered in terms of dopant atoms rather than surface configurations since both procedures basically affect the electronic structure. In conclusion, surface modification and the addition of heteroatoms provide control over the electronic structure and energy levels of CDs, with a broadly applicable PL mechanism at the core.

2.4.5. Synergistic Effect. The interplay between the surface state and the carbon core must be taken into account, and knowing how they work together (the synergistic effect) is crucial to comprehending CDs' PL emissions. Models are frequently interconnected, making it difficult for a single effect to fully explain observed data. Therefore, as will be explained

https://doi.org/10.1021/acsomega.3c07612
ACS Omega 2024, 9, 11050−11080

below, research has concentrated on the synergistic impact of the combined effects of PL mechanisms.

According to certain research, CDs' photoluminescence is caused by both the carbon core and surface state. In support of this theory, Yu et al. synthesized six distinct types of CDs with varying carbon and nitrogen levels using a microwave fabrication technique. They observed that the diverse CDs structures are linked to variable emissions and excitations. In accordance with electron transitions of intrinsic C (4.1 eV), graphitic N (3.5 eV), pyridine N (3.0 eV), amino N (2.8 eV), and C═O (2.5 eV), five CDs emission bands centered at 305, 355, 410, 445, and 500 nm, respectively, correspond to these electron transitions (Figure 3a). These energy-transfer processes are due to the synergy between carbon cores and surface states.[133]

In order to produce CDs PL, surface functional groups typically work in synergy with the conjugation effect. Liu et al. synthesized CDs using oxidized carbonized fiber and further post-treatment with sodium hydroxide and sodium borohydride. According to their research, the electron system and carbonyl group were coupled, and the QY was dependent on the carbonyl group (Figure 3b). Overall, the π-electron system and functional groups worked synergistically to influence CDs PL.[134] In terms of radiation recombination, defects are frequently thought of as a common category of surface configurations that, along with the conjugation effect, explain luminescence. Gan et al. studied the PL of CDs derived hydrothermally and observed weakening blue and slightly variable green emissions as the reaction time increased. The former may have been caused by carbon defects (such as vacancies and irregular rings) and the latter by the radiative recombination of electron−hole pairs in the carbon network (the size effect). Fundamentally, impacts resulting from both carbon cores and surface states are integrated and interact to produce internal factors-dominated emissions.[135,136]

2.4.6. Solvent Effect. The synthesis and characterization of CDs depend heavily on solvents since they have an impact on both particle dissolution and synthesis. Varied solvents result in CDs with various optical characteristics and different structures. The solvent employed in the study is frequently crucial if the CDs fluoresces toward the wavelength of a higher region. Mostly using the H-bonding hypothesis, CDs' solvatochromic phenomenon was elucidated[137−139] (Figure 4a). The fluorescence was observed in polar protic solvents via H-bonding between the solvent molecules and the CDs' surface functional groups (Figure 4b). In contrast, the fluorescence behavior of the CDs has been explained in aprotic solvents by considering factors like dipole moments (interactions at the excited state), Kamlet−Taft parameters, the refractive index, and the permittivity of the solvent molecules.[140,141] This is similar to how CDs excited states are more stable in aprotic solvents, yielding greater quantum yield. Other supported phenomena like solvent relaxation are well described by Ai et al. through which it can be obtained that a more polar solvent was found to better stabilize the excited state of CDs while having little to no impact on the ground state, red shifting the emission.[123]

2.4.7. Heteroatom Doping and Their Effect in QY Enhancement. Usually, the quantum yield of CDs is influenced by various factors which have been described briefly in the following sections. As CDs have a graphitic sp^2 hybridized carbon core, this can be favorable for both functionalization and doping. In the process of heteroatom

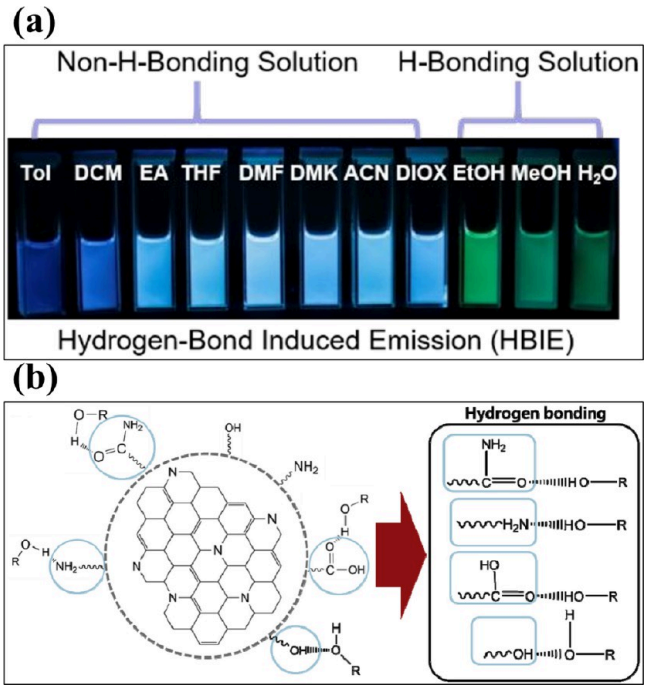

Figure 4. Solvent effect. (a) The influence of hydrogen bonding on luminescence between solvent molecules and CDs. Reproduced with permission from ref 139. Copyright 2017 The Royal Society of Chemistry. (b) Schematic representation of the hydrogen bonding interaction between the surface functional groups of CDs with polar protic solvent molecules (R = H, alkyl chain). Reproduced with permission from ref 140. Copyright 2020 Elsevier.

doping, certain carbon atoms in the graphitic structure are swapped out for the heteroatoms (other than carbon). Introducing atomic impurities (such as nitrogen, boron, sulfur, phosphorus, and so on) onto CDs may alter their electronic structures, yielding n-type or p-type carriers. As a result, by applying different types and quantities of doping atoms, the optical and electrical characteristics of CDs can be modified.[142] The introduction of heteroatoms into carbon materials having graphitic carbon networks, regardless of whether the dopants have a higher electronegativity (as nitrogen) or lower electronegativity (as boron, sulfur, or phosphorus) than that of carbon, could cause electron modulation to change the charge distribution and electronic properties of carbon skeletons. This in turn affects their work function for electronic applications and enhances their efficiency.[143] Following a one-step or multistep synthesis process, there are several top-down (arc discharge, laser ablation, electrochemical/chemical oxidation, etc.) and bottom-up (hydrothermal/solvothermal, microwave, pyrolysis, ultrasonication, etc.) strategies that have been employed to synthesize single-atom doped or multiatom codoped CDs.[142] CDs doped with heteroatoms have recently gained popularity due to their exceptional photoluminescence properties and wide range of applications. Because of the similarities of nitrogen and carbon atoms, N-doping is one of the most commonly utilized ways to promote the photoluminescence property of CDs. The introduction of the nitrogen atom clearly changes the environment of internal electronics, which can impact the photoluminescence of CDs.[144] For instance, Zhang et al. synthesized N-doped CDs with an exceptional quantum yield of 15.7% from folic acid using a one-step hydrothermal method.[145] Zhao et al.

https://doi.org/10.1021/acsomega.3c07612
ACS Omega 2024, 9, 11050−11080

synthesized N, S-*co*-doped CDs having a quantum yield of 17.5% having outstanding optical properties and chemical and biological stability through a hydrothermal method.[146] Similarly, sulfur atoms can modify the electronic structures of CDs providing energy or emissive trap states for photoexcited electron capture. S-Doped CDs possess all the advantages similar to blank CDs, adding the extra feature of avoiding self-quenching, which is due to its large ensemble Stokes shift. Sulfur doping also results in a higher quantum yield like in the case of S-doped CDs, synthesized by Xu et al. through the hydrothermal method, which possessed an outstanding quantum yield of 67%.[147] The peculiar electrical structure created by the synergistic impact between the heteroatoms and CDs has received a lot of interest, and the number of active spots for codoping CDs has expanded significantly. Furthermore, the band structure of CDs may be engineered by incorporating metal atoms and metal carbonite into the CDs matrix. Doped metal atoms, such as Zn, Mn, and Gd, can aid in electron and hole radiative recombination on the CDs' surface. Furthermore, the presence of valence electrons in dopant metal atoms or metal carbonates can boost the charge electron transfer, resulting in an increase in QY. For a better view and with an application perspective, Xu et al. explained the advantage of heteroatom doping of CDs. From their study, it can be observed that specific surface area and nitrogen doping on typical carbon materials can result in higher supercapacitor characteristics.[148] In a very recent study, Liu et al. explained the impact of boron doping in CDs, which resulted in achieving an ultrahigh quantum yield of 99.6%. To investigate the mechanism of heteroatom doping impact on CDs, electron density difference and first-principle calculations of doping element states in spherical modified CDs with Ba atom were performed. It was concluded that the charge transfer generated through hetero atoms was most likely the cause of the high quantum yield Ba-CDs, which was particularly favorable for enhanced photoluminescence mechanism of CDs.[149]

2.4.8. Software for Quantum Yield Simulation. Quantum yield (QY) is the proportion of emitted photons to absorption photons generated by the fluorescent material. The QY of quinine sulfate can be used as a reference fluorescent material to compare QY CDs. The quantum yield of carbon dots can range from less than 1% to over 50%, with some reports of even higher values. Achieving high quantum yields in carbon dots is an active topic of research, with numerous ways being investigated to improve their efficiency. These strategies include optimizing the synthesis conditions, surface passivation, and engineering the carbon dot structure to reduce nonradiative decay pathways and enhance radiative recombination. There are various software tools available for modeling quantum yield, which is a measure of a light-emitting process's efficiency. NWChem is an impressive computational chemistry program for calculating quantum yields. It provides a variety of quantum mechanical techniques and can calculate both ground and excited states. VASP (Vienna Ab initio Simulation Package) may be used to examine quantum yields in addition to electronic structure studies. It simulates excited states and luminescent characteristics using density functional theory (DFT) and many-body perturbation theory (MBPT). Q-Chem is a complete quantum chemistry software suite that allows us to calculate quantum yields. It is compatible with a variety of approaches, including time-dependent density functional theory (TDDFT), which is often used to simulate excited states and emission processes.

2.5. Polymer/CDs Nanocomposites. *2.5.1. Physical Blending.* Commonly, the term "blending" refers to the process of combining two or more chemicals without initiating a chemical reaction or the formation of additional industrial chemicals. It is the process of making a polymer blend by mechanically mixing different polymers together in the melt. Since the majority of polymer pairs are immiscible, blends between them are not formed spontaneously. Additionally, the phase structure of polymer blends is not equilibrium and is dependent on the method of synthesis. Melt mixing, solution blending, latex mixing, partial block or graft copolymerization, and the fabrication of interpenetrating polymer networks (IPN) are the five techniques known to produce polymer blends. On a laboratory scale, solution blending is commonly used to fabricate polymer blends. In a typical solvent, the blend's constituent parts are dissolved, then vigorously stirred. The blend is separated by precipitation or evaporation of the solvent. The procedure has certain advantages like the ability to prevent unfavorable chemical reactions while mixing the system rapidly and with less energy usage. In general, the most common technique for producing polymer blends is melt mixing. In extruders or batch mixers, the blend's component parts are combined in their molten state.

2.5.2. Chemical Grafting. In polymer chemistry, the term "grafting" describes the attachment of polymer chains to a surface. Grafting is a desirable method for adding various functional groups to a polymer. Therefore, it has been demonstrated that under certain circumstances, a variety of amendment procedures can enhance the inherent properties of the standard polymer backbone. Graft polymerization involves covalently bonding and polymerizing monomers as side chains onto the primary polymer chain (the backbone).[150] Free radical initiators including dibenzoyl peroxide, potassium permanganate ($KMnO_4$), potassium persulfate (KPS - $K_2S_2O_8$), ammonium persulfate (APS), azobis-(isobutyronitrile) (AIBN), ceric ammonium nitrate (CAN), and Fenton's reagent, together, can be used to initiate free radicals on the backbone during chemical grafting.

2.5.3. In-Situ Growth. As a reference to in situ growth, it means that growth is taking place without isolating it from the place of its formation and if one can characterize it without isolating it. In situ polymerization methods often include the mixing of nanomaterials in a neat monomer (or multiple monomers) or a solution of monomer, followed by polymerization in the presence of the dispersed nanomaterials.[151] In situ polymerization has a number of advantages. First of all, this method may be used to synthesize thermoplastic and thermoset-based nanocomposites. Additionally, it allows for the grafting of polymers onto the surface of the filler, which can typically enhance the final composite's characteristic properties. Due to the fillers' excellent dispersion and intercalation in the polymer matrix, partially exfoliated structures may be produced with this technique.[152]

Numerous methods have been used to synthesize polymer/CDs nanocomposites, including stirring, sol−gel,[153] drop casting,[154] conventional solution casting,[155] in situ chemical polymerization,[156] polymer-assisted self-assembly, stirring,[157] interfacial polymerization, solution blending,[158] reverse microemulsion polymerization, cross-linking reaction, photopolymerization, bulk polymerization, Schiff base reaction, electrospinning, hydrothermal treatment,[159] thermal treatment-in

https://doi.org/10.1021/acsomega.3c07612
ACS Omega 2024, 9, 11050−11080

situ,[160,161] nonsolvent driven phase inversion, and free radical dispersion polymerization.

2.6. Synthesis and Applications of Polymer/CDs Nanocomposites. Issa et al. used a composite film made of poly(vinyl alcohol) (PVA) and nitrogen-doped CDs to remove harmful cadmium ions. The empty fruit bunch wastes from oil palm trees were used to produce carboxymethylcellulose (CMC), which was then combined with polyethylenimine (PEI) to create the CDs. PVA was then employed to embed the CDs. The resulting polymer composite film had a bright blue color, a higher QY of 47%, and an increased Cd^{2+} removal percentage of 91.1%.[162] Wang et al. developed a facile procedure to synthesize CDs/MIPs (molecularly imprinted polymers combined with CDs, a fluorescent composite material for the detection of trace amounts of 4-nitrophenol (4-NP). First, using anhydrous citric acid as a carbon source and AEAPMS as a surface modification, a hydrothermal synthesis was used to produce fluorescent CDs with a high quantum yield (QY) of 51.8%. Then, utilizing 4-NP as a template, (3-aminopropyl) triethoxysilane (APTES) as a functional monomer, tetraethoxysilane (TEOS) as a cross-linker, and CDs as signal sources, respectively, CDs were synthesized with MIPs (CDs/MIPs) using the sol−gel technique.[163]

Generally, CDs have the capacity to enhance or modify the characteristics or functionalities of materials already in use for specific purposes. Consequently, the fundamental framework and attributes of CD/polymer nanocomposites are dictated by the type of polymer matrix employed, which can be either thermoplastic (linear or branched) or thermoset (cross-linked polymer). CDs may be either covalently bonded to or mixed noncovalently with the polymer matrix. The selection of the polymer matrix is contingent on the intended application. The strength of secondary interactions between the polymer and CDs, as well as the feasibility of covalently attaching CDs, is influenced by the chemical structure of the polymer or thermoset resin. This, in turn, affects the dispersion of CDs and the overall preparation cost. The current methodologies for creating CD/polymer nanocomposites can be categorized into physical blending, chemical grafting, and in situ growth. CDs, as a burgeoning category of carbon nanomaterials, exhibit significant promise across a wide range of applications owing to their facile preparation, distinctive properties, and diverse structures and compositions. The advantageous attributes, coupled with abundant surficial polar functionalities, bestow CDs with considerable potential for further development into CD/polymer nanocomposites. These nanocomposites have the capacity to enhance performance and introduce novel functionalities. Recently, CD/polymer nanocomposite materials have found applications in various fields, with a particular focus on energy storage, environmental concerns, and biomedical applications, prompting extensive research efforts. Consequently, this section will comprehensively outline and emphasize the advancements in employing CD/polymer nanocomposites in these forefront areas. Depending on the intended application, distinct criteria govern the final properties of CD/polymer nanocomposites. In the energy sector, optimal electron charge transfer and ionic conductivity are imperative, whereas in environmental applications, the nontoxicity and reusability of the nanocomposites play a pivotal role. For biomedical purposes, considerations such as hydrophilicity, biocompatibility, nontoxicity, and biodegradability become crucial factors.

MIPs are a fascinating class of materials designed to mimic the highly specific recognition capabilities of natural antibodies and receptors. These synthetic polymers possess tailor-made binding sites that can selectively recognize the bind to target molecules with high affinity and specificity. These materials are created through the polymerization of functional and cross-linked monomers around a template molecule, which ultimately led to a highly cross-linked three-dimensional network polymer. The template molecule is subsequently removed, leaving behind cavities that possess a complementary shape, size, and chemical functionality to the target molecule. This imprinting process results in the creation of artificial recognition sites within the polymer matrix, enabling the selective binding of the target molecule (i.e., CDs) even in complex mixtures. Molecular recognition is often driven by intermolecular interactions such as hydrogen bonds, ionic and dipole−dipole interactions between the template molecule and functional groups present within the polymer matrix.[164−167]

Wu et al. synthesized yellow emitting polymer/CDs composite using carboxy methyl cellulose/polyvinyl alcohol and chitosan. CDs were prepared via one-step hydrothermal process, and further polymer nanocomposites were fabricated through a drop casting method.[168] In order to fabricate the polymer/CDs nanocomposites, Devadas et al. established a viable in situ chemical oxidative polymerization process employing the conducting polymers polypyrrole (PPy) and polyaniline (PANI). The in situ chemical oxidative polymerization approach that was presented was the ideal way of achieving the synergistic interaction between polymers and CDs. As a result, adding adequate CDs improved the specific capacitance values of both polymers by up to double or more. The polymer/CDs hybrid is thus the ideal electrode material for use in supercapacitors and prototype energy storage/conversion systems.[169] Wang et al. utilized magnetic covalent organic frameworks (MCOFs), MIPs, and CDs to develop a composite material that can be used as a fluorescence sensor. MCOFs were employed as sorbents and supporting materials in the fabrication of the MCOFs/MIPs/CDs, while MIPs served as selective sorbents, and CDs were chosen as the fluorescence sensor element. Using a one-pot reverse microemulsion polymerization technique, the MCOFs/MIPs/CDs were effectively synthesized and used for the selective, sensitive, and rapid detection of TNP.[170] Wang et al. fabricated solid-white-light-emitting phosphors by combining blue and orange emissive CDs with polystyrene nanospheres, resulting a polymer/CDs composite (WCDs/PS). A warm WLED and temperature-sensory device were designed based on the superior stability and high-quality lighting performance of WCDs/PS.[171] By dispersing the CDs nanoparticles in various amounts into aqueous solution using interfacial polymerization (IP) of *m*-phenylenediamine (MPD) and t chloride monomers, Li et al. synthesized a novel CDs-TFN RO membrane (TMC). Further, the CDs-TFN RO membrane was fabricated by interfacial polymerization on the PSf membrane (microporous polysulfone support). The desalination performance of the TFN membrane with 0.02 wt % CDs inclusion was promising, with a water flux of 87.1 $L/m^2/h$ and salt rejection of 98.8%.[172] Zheng et al. utilized hexamethylenetetramine (HMT) and polycarbonate as precursors to synthesize CDs and CDs-polymer composite in a facile one-step hydrothermal process. The powdered dried polymer/CDs nanocomposites have remarkable optical stability, and no luminescence quenching was found. This fluorescent polymer/CDs nano-

https://doi.org/10.1021/acsomega.3c07612
ACS Omega 2024, 9, 11050−11080

composite has potential application in metal-less white LED phosphors.[159] Li et al. synthesized an alginate (Alg) hydrogel that responds to pyrophosphate ions (PPi), demonstrating its potential as a fluorescence sensing platform for ALP detection. This hydrogel was fabricated utilizing CDs as a visual indicator and Cu^{2+} as a cross-linker to produce Cu/Alg gel. The CDs were immobilized in the Cu/Alg gel matrix to fabricate the composite of CDs/Cu/Alg that has green fluorescence.[173] A hybrid microgel system composed of up-conversion CDs embedded in a network of polymer microgels with boronic acid functionalization was reported by Wang et al. In particular, the functional comonomers of 4-vinylphenyl boronic acid (VPBA) and acrylamide (AAm) combined in one pot can be easily synthesized into spherical hybrid microgel particles by one-step free radical polymerization in water.[174] An ecofriendly approach was proposed by Kazemifard et al. to synthesize CDs from rosemary leaves, which were then used as a fluorophore in an optical sensor after being modified with MIPs for the detection of thiabendazole (TBZ). For this, a reverse microemulsion approach was used to stabilize a silica shell utilizing tetraethoxysilane (TEOS) as a silica source on the surface of CDs. Then, employing 3-aminopropyl triethoxysilane as a functional monomer and TEOS as a cross-linker, MIPs were synthesized in the presence of TBZ as a template.[175] Koulivand et al. developed a novel mixed matrix nanofiltration membrane by incorporating CDs into a poly(ether sulfone) (PES) matrix. A simple hydrothermal technique was successfully employed to produce CDs, which were then used to enhance the hydrophilicity, permeability, antifouling characteristics, and dye rejection efficiency of PES. The phase inversion method was used to add CDs into the PES casting solution. In terms of membrane shape, porosity, hydrophilicity, permeability, nanofiltration performance, and fouling factors, the impacts of adding CDs to the membrane matrix were investigated.[176] Yuan et al. developed novel composite membranes based on the polymer/CDs active layer for organic solvent nanofiltration. The CDs with tailored functional groups were facilely synthesized and embedded into polyethylenimine (PEI) matrix, and then dip-coated on polyacrylonitrile support to prepare composite membranes through interfacial polymerization. The hydrolyzed polyacrylonitrile (PAN) support was coated with a cross-linked PEI-CDs layer to form a thin, defect-free composite membrane.[177]

3. MECHANISM AND SENSING APPLICATIONS OF CDs AND POLYMER/CDs NANOCOMPOSITES

3.1. Mechanism and Sensing Applications of CDs.

3.1.1. Designing of CDs in Sensing Applications. The potential for employment as a sensor is illustrated by any phenomena of fluorescence change (intensity, wavelength, anisotropy, or lifespan) connected to the concentration of various analytes. The majority of CDs-based sensing technologies are based on analyte-induced fluorescence quenching. Many CDs need to be functionalized with desired recognition elements, such as antibodies and aptamers, in order to provide high specificity toward analytes of interest, like proteins, even though some CDs exhibit selectivity toward interesting analytes such as Fe^{3+}, Cu^{2+}, ascorbic acid, glucose, hydroxyl radicals, tartrazine, iodide, DNA, cells, and bacteria.[178] The hydrophilicity and fluorescence of CDs are associated with the surface functional groups; therefore, the functionalization of CDs must be tuned with regard to biocompatibility, sensitivity, and selectivity[67] as shown in detailed description in Table 1 for different types of materials used for preparation of CDs and their sensing applications.

It has been observed that carbon dots (CDs) exhibit the potential for quenching when exposed to heavy ions such as Fe^{3+} and Hg^{2+}. This phenomenon introduces an intriguing dimension to the study of carbon dot interactions, suggesting that the presence of these heavy ions can influence and modulate the fluorescence properties of CDs. The quenching effect over heavy ions underscores the dynamic nature of CD interactions with various elements, expanding the scope of their applications in sensing and other related fields. Further exploration of these interactions could lead to innovative approaches for utilizing carbon dots in diverse analytical and detection technologies. The quenching of carbon dots by heavy ions represents a dynamic process wherein the fluorescence of CDs is reduced or completely extinguished upon interaction. The underlying mechanisms involve complex interactions between the heavy metal ions and the surface functional groups of CDs, leading to alterations in the electronic structure and optical properties. One significant implication of the quenching phenomenon is its potential application in fluorescence sensing, which is well described in the review. Studies have explored the use of CDs as sensitive probes for detecting and quantifying heavy metal ions in aqueous solutions. The quenching effect serves as a basis for developing selective and responsive sensors with applications in environmental monitoring, water quality assessment, and industrial safety. Despite progress in understanding the quenching of CDs by heavy ions, challenges remain, including the need for a deeper mechanistic understanding and the exploration of real-world applications. Future research directions may involve investigating the impact of environmental conditions, exploring additional heavy metal ions, and advancing the integration of CDs into practical sensing devices.

3.1.2. Sensing Mechanism of CDs. One of the most recent quantum nanomaterials, CDs, are synthesized from carbon-based materials. Since their discovery, these nanomaterials have drawn a lot of attention due to their superior qualities, including simple surface functionalization, green and simple synthetic routes, excellent water solubility, good photostability, great biocompatibility, bright fluorescence, and tunable surface functionalities as previously discussed in section 1. CDs can be used in place of semiconductor quantum dots to achieve highly sensitive detection in the field of biosensing because of their nontoxic nature.[179,180] CDs have been utilized for drug delivery, bioimaging, and analyte detection. These applications were based on the concept that interactions between analytes and CDs can cause quenching, which lowers fluorescence or suppress quenching, which enhances fluorescence. CDs, which have been used in sensing applications, undergo several different fluorescence-changing processes which are the key features for sensing.[181] The CDs' quenching methods include resonance energy transfer (RET), photoinduced electron transfer (PET), inner filter effect (IFE), and static and dynamic quenching. The three types of energy transmission are surface energy transfer (SET), Förster resonance energy transfer (FRET), and Dexter energy transfer (DET). When CDs and the quencher interact, a nonfluorescent ground-state complex is generated, leading to static quenching. When the quencher and CDs collide owing to energy transfer or charge transfer, the excited state returns to the ground state, and the phenomenon is known as dynamic quenching. A brief view of these phenomenon is well discussed by Sun et al.[178]

https://doi.org/10.1021/acsomega.3c07612
ACS Omega 2024, 9, 11050−11080

Table 1. Detailed Description for Different Types of Materials Used for Preparation of CDs and Their Sensing Applications[a]

Sl no.	material	precursor	method and condition	fluorescence color and quantum yield	selectivity/sensitivity	fluorescence wavelengths (nm)	limit of detection (LOD)	reference
1	CDs	Citric acid (CA), 3-aminophenylboronic acid	Hydrothermal	Blue, 57.8%	Nitrite ion	λ_{ex} - 360, λ_{em} - 420	7.9 nm	85
2	N-CDs	*o*-Phenylenediamine	Carbonization	Red, 12.8%	Hematin	λ_{ex} - 560	0.18 μM	92
3	B-CDs	Boric acid, L-ascorbic acid	Hydrothermal	Blue, -	Pb^{2+}, Cu^{2+}, pyrophosphate ($P_2O_7^{4-}$)	λ_{ex} - 350, λ_{max} - 440	25 nm−250 μM, 50 nm−300 μM, and 25−500 μM	199
4	g-CNQDs	Formamide ($HCONH_2$)	Microwave synthesis	Blue, 29%	Hg^{2+}	λ_{ex} - 340, λ_{max} - 405	1 nM	182
5	CDs	CA, Ethylenediamine	Hydrothermal	Blue, 80%	Fe^{3+}	λ_{ex} - 360, λ_{em} - 443	1 ppm	193
6	CDs	CA, Ethylenediamine	Hydrothermal	Blue, 38−80%	Fe^{3+}	λ_{ex} - 360	0.9 ppb	185
7	CDs	Oxalic acid, urea	Microwave synthesis	Blue, 29%	Fe^{3+}	λ_{em} are red-shifted from 405 to 495	4.8 nM	197
8	S-doped CDs	Sodium citrate, sod thiosulfate	Hydrothermal	Blue, 67%	Fe^{3+}	λ_{max} - 440	0.1 μM	147
9	CDs	Dopamine	Hydrothermal	Blue, green, 6.4%	Fe^{3+}, dopamine	λ_{max} - 400	0−20 μM	194
10	CDs	Pomelo peel	Hydrothermal	Blue, 6.9%	Hg^{2+}	λ_{max} - 444	0.23 nM	187
11	PANI/CDs	Sodium citrate, NH_4HCO_3	Hydrothermal	Blue, -	Hg^{2+}	λ_{max} - 448	0.05−1.0 μM	183
12	ODN-CDs	CA, Ethylenediamine, Sodium chloroacetate	Hydrothermal	-, 75.0%, and 7.19%	Hg^{2+}	λ_{max} - 347	2.6 nM	188
13	N, S codoped CDs	3-Mercaptopropionic acid (as a S source), ethylenediamine, diethylenetriamine, triethylenetetramine (as a N source)	Hydrothermal	Green, 69%	Hg^{2+}	355−370	0.05 nM	190
14	Valine-functionalized GQDs	CA, valine	Pyrolysis	Blue, 28.07%	Hg^{2+}	λ_{max} - 450	0.4 nM	215
15	N-doped CDs	Hydrosoluble chitosan	Hydrothermal	Blue, 31.8%	Hg^{2+}	λ_{max} - 360	80 nM	191
16	Thiourea fun. CdSe/CdS QDs	Core−shell CdSe/CdS QDs, thiourea (TU)	Electrostatic interaction.	-	Hg^{2+}	λ_{max} - 536	0.56 mg/L	184
17	QD/DNA/gold nanoparticle			-	Hg(II)	-	0.4 and 1.2 ppb	216
18	Amino fun. GQDs	Graphene oxide, GQD, ammonia	Hydrothermal	Green, 16.4%	Cu^{2+}	λ_{max} - 320 and 500	6.9 nm	201
19	Polyamine fun. CQDs	CA, branched poly(ethylenimine)	Pyrolysis	Blue, 40%	Cu^{2+}	λ_{ex} - 365	6 nM	200
20	CdTe QDs	$CdCl_2$, Te, and $NaBH_4$ for CdTe QDs, mereaptoactetic acid			Cu^{2+}	-	-	186
21	Mn-doped Ag_2S QDs		Chemical precipitation		Laminin (LN)	-	3.2 pg/mL	206
22	CDs	Fresh aloe	Hydrothermal	Yellow, 10.37%	Tartrazine	λ_{max} - 503	73 nM	83
23	Boronic acid fun. CDs	Phenylboronic acid	Modified hydrothermal carbonization method	Blue, 8.4%	Glucose	λ_{max} - 408	9−900 μM	209
24	CDs	L-Arginine	Hydrothermal	Blue, 16%	4-Chloroethcathinone	λ_{max} - 430	1.73 mM and 0.14 mM	203
25	CDs and CdTe QDs	Spinach, CdTe QD	Hydrothermal	Blue and red	Spermine	λ_{max} - 470 for blue CDs, λ_{max} - 690 for red CDs	76 nM	207
26	Eu-fun. CDs	Citric acid monohydrate, urea	Microwave synthesis	Green and red	Point-of-care testing (POCT) of dipicolinic acid (DPA)	λ_{max} - 530	0.8 nM	205
27	CDs	CA, Ethylenediamine (EDA)	Hydrothermal	Blue	Trinitrotoluene	λ_{max} - 455	10 nM to 1.5 μM	208
28	CQDs	Citrate and NH_4HCO_3	Hydrothermal	Red, green, blue	Hydrogen peroxide (H_2O_2)	λ_{max} - 604 for red, 550 for green, 445 for blue	0−88.2 mM	204

[a]Abbreviations: CDs - carbon dots, QDs - quantum dots, CQDs - carbon quantum dots, N-CDs - nitrogen doped CDs, B-CDs - boron doped CDs, g-CN - graphite carbon nitride, S - sulfur, PANI - polyaniline, ODN - oligodeoxyribonucleotide, Ag - silver, Cd - cadmium, Se - selenium, Te - tellurium, Mn - manganese, Eu - europium, CA - citric acid.

https://doi.org/10.1021/acsomega.3c07612
ACS Omega 2024, 9, 11050−11080

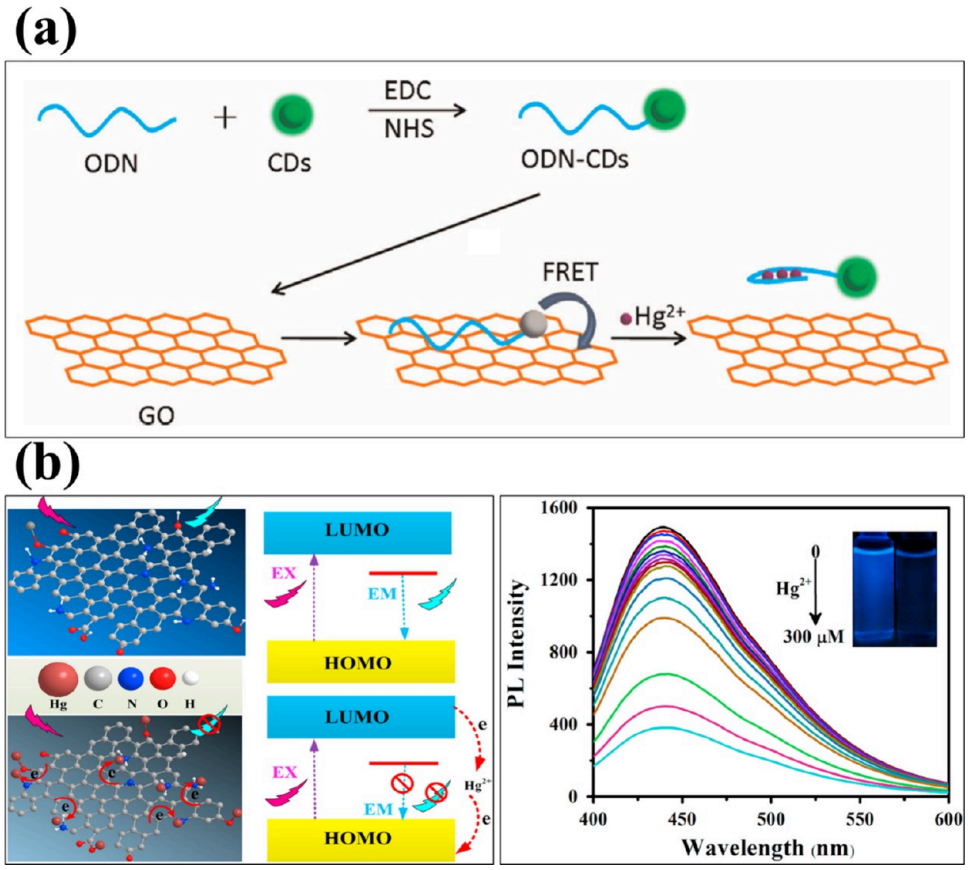

Figure 5. (a) Schematic illustration of GO quenched ODN labeled CDs and the GO-CDs-ODN system for Hg^{2+} detection due to the fluorescence recovery. Reproduced with permission from ref 188. Copyright 2015 Elsevier. (b) A plausible mechanism for fluorescence quenching of N-doped CDs by Hg^{2+} and representative PL emission with increasing Hg^{2+} concentration. Reprinted with permission from ref 191. Copyright 2016 Elsevier.

3.1.3. Design of Sensor for CDs. Typically, there are three approaches used in the design of fluorescent CDs-based sensors. One involves the direct interaction of analytes with CDs, which changes the fluorescence signals of the CDs. Next, CDs that have been postfunctionalized are used for sensing. The third is the use of CDs as sensing materials by integrating them with additional components (such as quenchers, fluorophores, substrates, etc.).

3.1.4. Sensing Applications of CDs. With the aid of the recognizable fluorescence quenching effect, CDs have recently received extensive evaluation as fluorescent probes to quantitatively identify trace chemical pollutants in aquatic systems. A wide variety of analytes, including ions, small molecules, macromolecules, cells, and germs, could be detected by CDs because of their special fluorescence properties. The sensing of various analytes using CDs is discussed in the sections that follow.

3.1.4.1. Metal Ion Sensing. CDs frequently experience electron transfer and the inner filter effect during fluorescence quenching of analytes. For detecting metal ions including Ag^{+}, Hg^{2+},[182−184] Fe^{3+},[185] Cr^{6+}, and Cu^{2+},[186] CDs have been adopted. CDs synthesized from carboxylic acids, amines, and amino acids exhibit selectivity for some metal ions through interactions like the coordination of their surface functional groups, including carboxylate and amino, with metal ions. When the CDs come into contact with the metal ions, either the inner filter effect or electron transfer can quench their fluorescence.

3.1.4.2. Mercury and Ferric Ion Sensing. One of the most harmful and widespread pollutants that poses risks to both the environment and human health is mercury(II) ion (Hg^{2+}). It is well-known that Hg^{2+} can readily pass through epidermal, respiratory, and digestive tissues, causing permanently harming the central nervous system, damaging DNA, and impairing mitosis. Lu et al. reported an affordable, environmentally friendly, and quite easy method for producing water-soluble, fluorescent CDs with a quantum yield of around 6.9% and a size of 2−4 nm via a hydrothermal process employing cheap pomelo peel waste as the carbon source. With a detection limit as low as 0.23 nM, these CDs have also been employed as a novel sensing probe for the label-free, sensitive detection of Hg^{2+} ions based on Hg^{2+}-induced fluorescence quenching. This sensing device has been successfully utilized to analyze a lake water sample and also has great selectivity for Hg^{2+} detection.[187] A fluorometric biosensor for Hg^{2+} detection based on GO and CDs-labeled oligonucleotide was developed by Cui et al. In the suggested system, GO functioned as the FRET acceptor, and CDs labeled T-rich 22-mer oligonucleotide served as the energy donor and molecular recognition probe. Oligonucleotides would be adsorbed on GO surfaces in the absence of Hg^{2+} ions, quenching the fluorescence of CDs (Figure 5a). The current GO-based sensor device has a detection limit of 2.6 nM and is highly selective toward Hg^{2+} over a broad range of metal ions. This simple and efficient technology will demonstrate a possible use in the Hg^{2+} monitoring of the environment and food.[188] In order to detect methylmercury, Isabel et al. originally reported a fluorescent

https://doi.org/10.1021/acsomega.3c07612
ACS Omega 2024, 9, 11050−11080

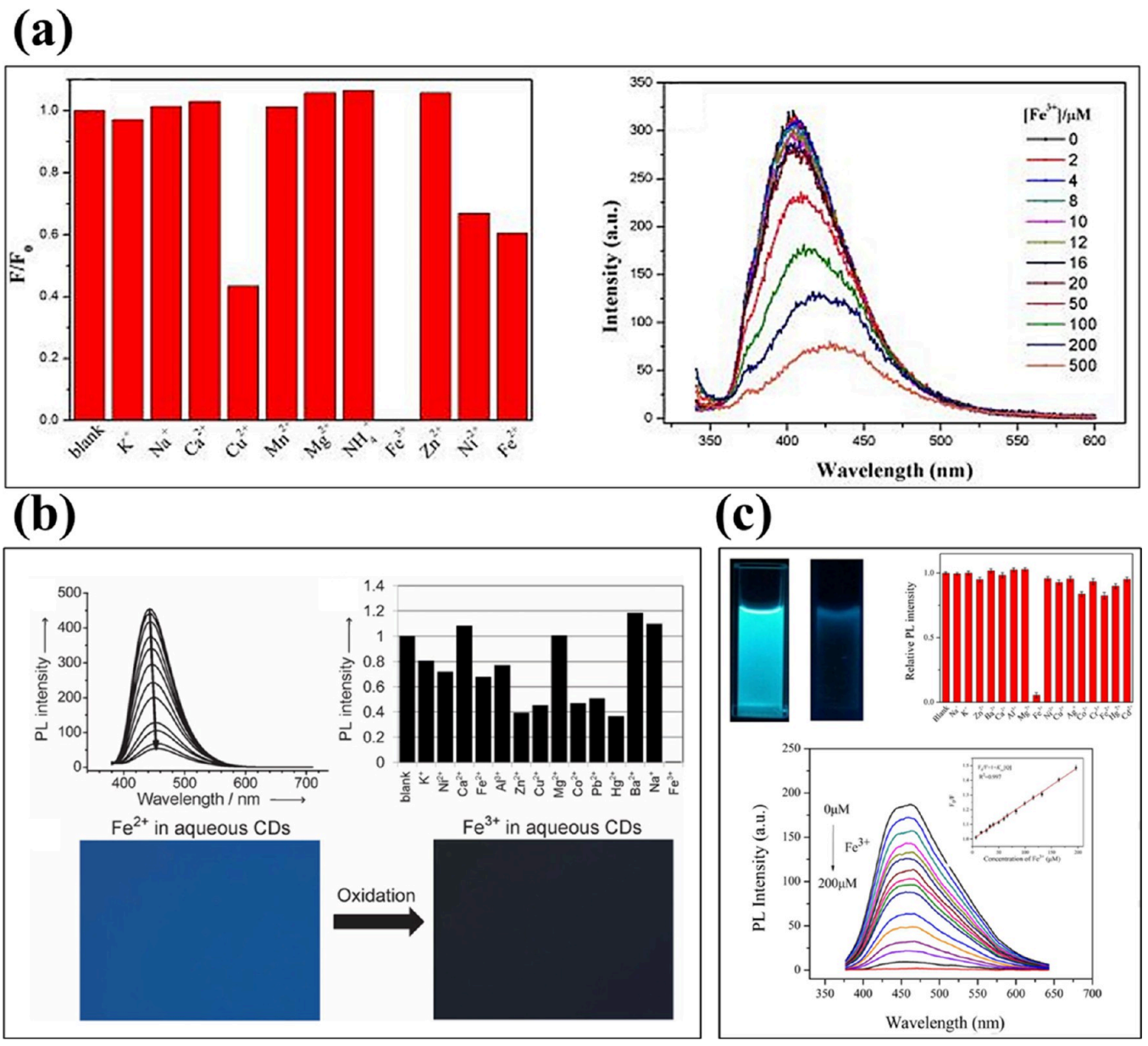

Figure 6. (a) Selectivity of the C-QDs toward Fe^{3+} ions and Representative fluorescence emission spectra of C-QDs in the presence of increasing Fe^{3+} ions concentrations. Reproduced with permission from ref 192. Copyright 2015 Elsevier. (b) Fluorescence quenching in the presence of Fe^{3+} ions and the on/off fluorescence. Reproduced with permission from ref 193. Copyright 2013 Wiley. (c) Selectivity and PL spectra of N-CDs in the presence of various concentration of Fe^{3+} ions. Reproduced with permission from ref 197. Copyright 2015 Elsevier.

assay based on in situ ultrasound-assisted synthesis of CDs utilizing D-fructose as the carbon source. With an average size of 2.5 nm, CDs had a small size distribution, and the results showed a repeatability represented as a relative standard deviation of 2.2% ($N = 7$) and a methylmercury detection limit of 5.9 nM. The basis of the recognition event is hypothesized to be methylmercury's hydrophobicity and its potential to facilitate a nonradiative electron/hole recombination.[189] One-step synthesis of nitrogen and sulfur codoped CDs (NSCDs) with a high photoluminescence quantum yield of 69% was reported by Mohapatra et al., for the selective and sensitive detection of Hg^{2+} in water and live cells. The nonradiative electron transfer from the excited state to the d-orbital of the metal ion is responsible for the switch on−off fluorescence shift with mercury addition. Excellent selectivity is displayed by the detection approach in both tap water and the presence of complex metal ions in the intracellular environment.[190] From hydrosoluble chitosan, Wang and colleagues synthesized N-doped CDs with high yield (38.4 ± 3.4%) and high quantum yield (31.8%). Photoluminescence quenching was used to provide very sensitive and specific Hg^{2+} detection. With a detection limit of 80 nM, the N-doped CDs displayed potential as mercury ion sensors (Figure 5b). The use of MATLAB code and a smartphone app for colorimetric measurement was demonstrated. These tools might be used with portable and relatively inexpensive Hg^{2+} sensors.[191]

Our lives depend heavily on iron, and iron deficiency is the first of three major micronutrient deficits worldwide. It is necessary to effectively manage and monitor the presence of ferric ions in biological systems and the environment. Zhou et al. effectively synthesized CQDs with a high quantum yield and excellent photoluminescence using citric acid and tris as

https://doi.org/10.1021/acsomega.3c07612
ACS Omega 2024, 9, 11050−11080

precursors. The as-synthesized CQDs with a QY as high as 52% are monodispersed spherical particles, and the diameter distribution of CQDs is 2.8 ± 1.1 nm. The CQDs sensing system furthermore provided simple, dependable, and sensitive Fe^{3+} ions detection through fluorescence quenching (Figure 6a). With a detection limit of 1.3 μM and an excellent linear correlation (R^2 = 0.997) throughout the concentration range of 0−50 μM, the CQDs probes offered extremely sensitive studies of Fe^{3+} ions. By employing these probes, the probes were also able to determine the amount of Fe^{3+} ions present in both the lake water and tap water.[192] Zhu et al. addressed a simple and effective hydrothermal approach for the synthesis of CDs, which is suited for industrial-scale production (yield is about 58%) with a QY as high as 80%. By switching from a low to a high synthesis temperature, the polymer-like CDs were transformed into carbogenic CDs. The CDs could be used as a biosensor reagent to detect Fe^{3+} in biological systems. Because of the unique coordination relationship between Fe^{3+} ions and the phenolic hydroxy groups of the CDs, which has been extensively employed for the detection of Fe^{3+} ions or colored processes in classic organic chemistry, the fluorescence of the CDs could be quenched by Fe^{3+} ions (Figure 6b). The estimation for the detection limit was 1 ppm or so. Additionally, oxidation may be used to generate the on/off fluorescence in the detection system using a Fe^{3+}/Fe^{2+} medium, and in the case of Fe, the selectivity was highest among other metal ions.[193] Qu et al. proposed a simple, economic, and green one-step synthesis of photoluminescent CDs via a hydrothermal method. The average size of the as-prepared CDs is about 3.8 nm. Most significantly, the surfaces of the as-prepared CDs have unique catechol groups. It was further shown that such entirely new CDs can function as a very efficient fluorescent sensing platform for label-free sensitive and selective detection of Fe^{3+} ions and dopamine with a detection limit as low as 0.32 mm and 68 nm, respectively, which was due to the special response of catechol groups to Fe^{3+} ions.[194] Lu et al. synthesized water-soluble photoluminescent CDs through one-step microwave pyrolysis of oxalic acid. The as-prepared CDs could be used as a highly efficient nanoprobe for Fe^{3+} as well as Ag^{+} detection. Additionally, CDs have exceptional selectivity over other typical metal ions and exhibit high sensitivity and selectivity to Fe^{3+} and Ag^{+} in complicated environments, thereby making them suitable probes for PL detection of Fe^{3+} and Ag^{+} with detection limits as low as 4.8 and 2.4 nM, respectively.[195] Zhang et al. proposed a simple and efficient solid-phase synthesis method for the fabrication of N-doped, highly fluorescent CDs. With an absolute quantum yield (QY) of up to 31%, the produced N-doped CDs displayed a strong blue emission. The N-doped CDs may be used as a novel fluorescent probe for label-free Fe^{3+} sensing since they were entirely water-soluble and remarkably stable against high pH, ionic strengths, and light illumination. Oxygen-rich groups on N-doped CDs were strongly coordinated to Fe^{3+}, which resulted in fluorescence quenching via nonradiative electron transfer and the quantitative detection of Fe^{3+}. With a detection limit of 2.5 nM, the probe showed a broad linear response concentration range (0.01−500 M) to Fe^{3+}.[196] Lu et al. reported the synthesis of CDs by one-step microwave-assisted pyrolysis of DL-malic acid as the carbon source, ethanolamine and ethanesulfonic acid as N and S dopants, respectively. Additionally, as a fluorescent probe for Fe^{3+} ions, such N-CDs demonstrated a broad detection range and outstanding accuracy (Figure 6c). With a linear range of 6.0−200 M and a limit of detection of 0.80 M, this probe enabled the selective detection of Fe^{3+} ions.[197] Xu et al. used the hydrothermal approach to synthesize S-doped CDs with a high fluorescence quantum yield (67%) utilizing sodium citrate and sodium thiosulfate as the precursors. The average diameter of spherical-shaped S-doped CDs is 4.6 nm, and Fe^{3+} ions could efficiently and selectively quench their fluorescence. As a result, S-doped C-dots were used as probes for the detection of Fe^{3+}, which has a limit of detection of 0.1 M.[147] Ju et al. developed a simple and cost-effective method for the synthesis of nitrogen-doped GQDs (N-GQDs) via the hydrothermal treatment of GQDs with hydrazine. The produced N-GQDs with functional groups rich in oxygen show a bright blue emission with a quantum yield of 23.3%. (QY). The as-prepared N-GQDs were found to be a highly efficient fluorescence sensing platform for the label-free sensitive and selective detection of Fe(III) ions with detection limits as low as 90 nM. Additionally, highlighted is the effective use of N-GQDs for the detection of Fe^{3+} ions in actual water samples. It is also notably observed that the detection of Fe^{3+} by N-GQDs involves both dynamic and static quenching processes, whereas the quenching impact of Fe^{3+} on the fluorescence of GQDs is accomplished by affecting the surface states of GQDs.[198]

3.1.4.3. Copper Ion Sensing. Cu^{2+} is a trace element that is essential for human health and is usually present in untreated natural water. However, it becomes toxic at high concentrations and, following prolonged exposure to high amounts, can harm the liver or kidneys. So, it is necessary to monitor the Cu^{2+} ions in the biosystem as well as in the environment and to understand their complex contributions to health and disease states.

Wang et al. reported the synthesis of boron-doped CDs through a hydrothermal method using ascorbic acid and boric acid as precursors. The as-prepared CDs have an irregular shape with a particle diameter of 10 nm and exhibit strong fluorescence. Since the formation of nonfluorescent metal complexes between chelating oxygen atoms on the surface of the CDs, fluorescence is quenched by Cu(II) and Pb(II) ions. A sensitive B-CDs-based FL analytical system for Cu^{2+} and Pb^{2+} ions was designed by taking advantage of the efficient FL quenching effect of Cu^{2+} and Pb^{2+} ions caused by charge transfer between −COO/OH groups or bidentate OH-donors and Cu^{2+} or Pb^{2+} ions, respectively. It is significant to note that the quenched Cu (II)-quenched B-CDs complexes system exhibits very sensitive and selective detection of PPi by a FL recovery procedure, whereas Pb(II)-quenched B−C-dots enable recovery selective detection of Pb^{2+} and Cu^{2+} ions. A detection range of 8.47−13.56 nM was achieved through this fluorescent probe.[199] Dong et al. developed a novel sensing method for the detection of Cu^{2+} ions based on the quenched fluorescence (FL) signal of branched poly(ethylenimine) (BPEI)-functionalized carbon quantum dots (CQDs). It was observed that the polyamine-functionalized CQDs were efficient FL probes for detecting Cu^{2+} (Figure 7a). The amino groups on the surface of the BPEI-CQDs can interact with Cu^{2+} ions to form an absorbent complex, which then causes the FL of the CQDs to be sensitively quenched by means of an inner filter effect. With a detection limit as low as 6 nM and a dynamic range of 10 to 1100 nM, this simple approach can provide a quick, reliable, and selective detection of Cu^{2+}. The FL-based sensing system based on CQDs has been found to have promising applications in the detection of

https://doi.org/10.1021/acsomega.3c07612
ACS Omega 2024, 9, 11050−11080

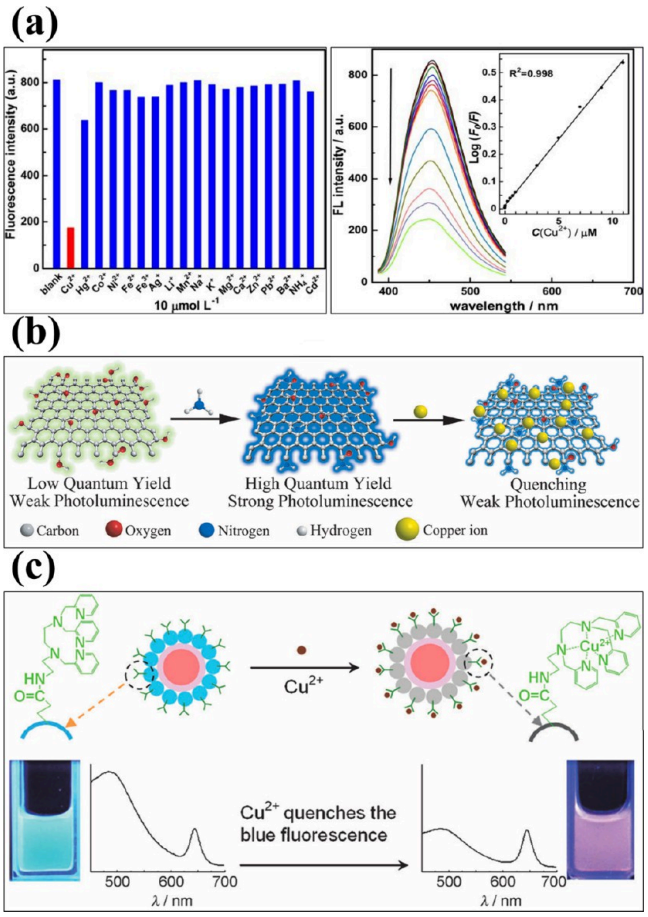

Figure 7. (a) Selectivity and FL response of CQDs for Cu^{2+} ions. Reprinted with permission from ref 200. Copyright 2012 American Chemical Society. (b) Schematic illustration of copper ion sensing by GQDs through quenching. Reproduced with permission from ref 201. Copyright 2013 Wiley. (c) Schematic representation of dual-emission fluorescent sensing of Cu^{2+} ions based on a CdSe/C-TPEA nanohybrid. Reproduced with permission from ref 202. Copyright 2012 Wiley.

Cu^{2+} in environmental water samples and exhibits several benefits including quick detection, high sensitivity, good selectivity, wide linear response range, and low cost.[200] Sun et al. reported the fabrication of a novel, highly fluorescent Cu^{2+} sensing probe using hydrothermal treatment of graphene quantum dots (GQDs). The greenish-yellow fluorescent GQDs (gGQDs) with a low quantum yield (QY, 2.5%) are changed into amino-functionalized GQDs (afGQDs) with a high QY (16.4%) after hydrothermal treatment in ammonia. The selectivity of afGQDs for Cu^{2+} is substantially higher than that of gGQDs because the Cu^{2+} ion has a higher binding affinity and faster chelating kinetics with N and O on the surface than other transition metal ions. Importantly, amination transformed the GQDs' surface charge from negative to positive, thereby making it easier for cells to absorb the of GQDs. In order to detect Cu^{2+} in aqueous solutions and even in live cells, a simple fluorescence sensor can be fabricated by utilizing the aforementioned features having a limit of detection of 6.9 nM[201] (Figure 7b). *N*-(2-Aminoethyl)-*N*,*N*,*N*′-tris(pyridin-2-ylmethyl)ethane-1,2-diamine (AE-TPEA), an organic molecule specific for Cu^{2+} ions, was integrated by Zhu et al. into a hybrid system made of carbon and CdSe/ZnS quantum dots (QDs), leading to the development of a selective and sensitive ratiometric strategy for intracellular sensing of Cu^{2+} ions. As a dual-emission fluorophore (CdSe/C nanohybrid), the CQDs emitting blue fluorescence are hybridized with the CdSe/ZnS QDs emitting red fluorescence (Figure 7c). The CdSe/ZnS QDs embedded in silica shells ($CdSe/SiO_2$) are inert to Cu^{2+} ions and only serve as reference signals for a built-in correction to avoid environmental effects. In the meanwhile, inorganic−organic CdSe/C-TPEA probes are developed by conjugating the specific Cu^{2+} ion receptor AE-TPEA with the responsive CdSe/C nanohybrid. When excited at a single wavelength of 400 nm, the hybrid probe exhibits two emission bands with respective centered at 485 and 644 nm. While the fluorescence of the red $CdSe/SiO_2$ particles does not change, that of the blue CQDs functionalized with AE-TPEA selectively recognizes Cu^{2+} ions. As a ratiometric fluorescent sensor for Cu^{2+} ions, it results as a consequence of the constant color changes caused by the addition of Cu^{2+} ions, which are visible with the naked eye under a UV light when the two fluorescence intensities are varied.[202]

3.1.4.4. Sensing of Organic Molecules. CDs have become a viable and cutting-edge method for detecting organic compounds in recent years. These have exceptional fluorescent properties which make them the ideal choice for identifying and classifying different organic molecules. A brief overview of the detection of certain major organic molecules is mentioned below.

A CDs-based turn-off PL sensing assay for the detection of psychoactive drugs, such as the -conjugated keto compound 4-chloroethcathinone, was reported by Yen et al. L-Arginine was used as the precursor for the CDs using a hydrothermal process. The synthesized CDs were used to measure 4-chloroethcathinone in an aqueous solution and on C-dot-functionalized papers (CDsFPs). The C-dots are selective for misused drugs with a -conjugated keto or ester group when the pH is 7.0. The analyte-induced PL quenching caused by an electron transfer process serves as the basis for the sensing method. According to the research, the 4-chloroethcathinone, its analogues, and popular narcotics like cocaine and heroin can all be detected using the C-dot probe at pH 7.0, whereas cathinones can be detected at pH 11.[203] Using sodium citrate and NH_4HCO_3, Chu and colleagues synthesized water-soluble multicolor luminescent CQDs using a one-step hydrothermal process. For the detection of H_2O_2, these CQDs displayed multicolor emission under a single wavelength excitation. It is demonstrated that red emission CQDs can detect H_2O_2 throughout a linear range of 0−88.2 mM using an LED with a central wavelength of 365 nm as the excitation source, and the H_2O_2 sensitivity of wavelength shift to changes in the H_2O_2 concentration was observed to be 0.18 nm/mM. The multicolor luminescence CQDs for H_2O_2 provide excellent analytical performance with affordable, convenient, and sensitive detection. Figure 8a gives an illustration of experimental set up for the detection of H_2O_2.[204] As a novel ratiometric fluorescent probe for point-of-care testing (POCT) of dipicolinic acid (DPA), a biomarker of anthrax, Wang et al. reported Eu(III) CDs (CDs-Eu). The CDs served as a scaffold for coordination with Eu(III) ions and a luminescence reference in the probe (CDs-Eu). The CDs containing carboxyl and amino groups and Eu(III) ions were easily coordinated to form the probe. Due to the existence of energy transfer when DPA chromophore associated with Eu(III) ions, the inherent red luminescence of Eu(III) ions can be sensitized

https://doi.org/10.1021/acsomega.3c07612
ACS Omega 2024, 9, 11050−11080

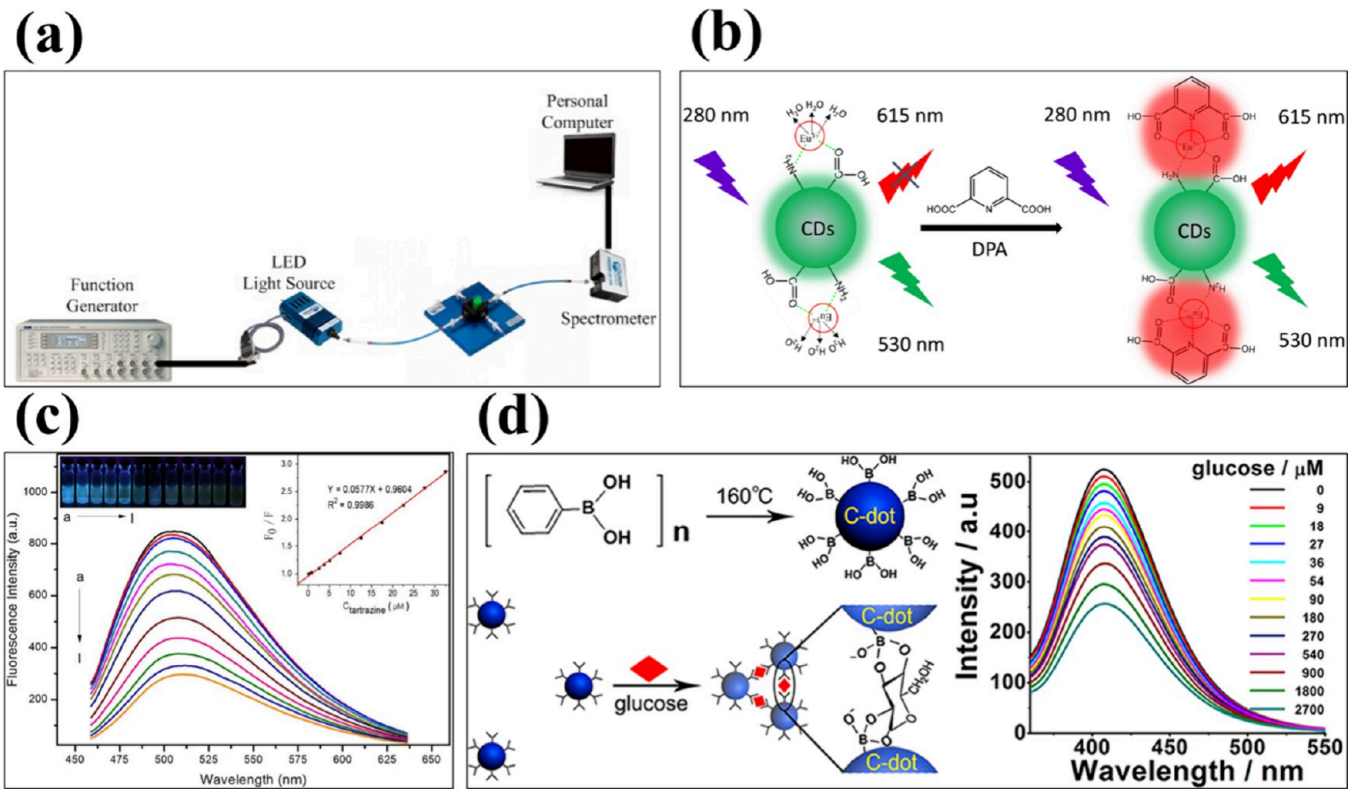

Figure 8. (a) Schematic diagram showing the experimental arrangement for H_2O_2 detection. Reproduced with permission from ref 204. Copyright 2016 Optica Publishing. (b) Schematic illustration of the ratiometric fluorescence probe for the detection of DPA. Reproduced with permission from ref 205. Copyright 2020 Elsevier. (c) Fluorescence emission spectra of C-dots in the presence of different concentrations of tartrazine. Reprinted with permission from ref 83. Copyright 2015 American Chemical Society. (d) The schematic diagram for fluorescent blood sugar sensing. Reprinted with permission from ref 209. Copyright 2014 American Chemical Society.

with the addition of DPA. A ratiometric fluorescence response to DPA was produced as a result of the reference fluorescent peaking at 530 nm being practically constant (Figure 8b). With a linearity range of 0.5 nM to 5 M and a LOD of 0.8 nM, the proposed technique demonstrated sensitive responses.[205] Wu et al. developed a unique low-toxic, water-dispersed Ag_2S quantum dot (Ag_2S: Mn QDs) that was initially used as a type of ECL material and then used as an ECL biosensor for the detection of laminin (LN). As a new signal tracer, BSA-Ag_2S: Mn bioconjugates were easily formed in water using 3-mercaptopropionic acid (3-MPA) as a growth template, Mn as a dopant to increase luminescence efficiency, and BSA as a linking agent to further increase luminescence intensity. This suggested immunosensor, which used a sandwiched immunoassay approach, had a comparatively low detection limit of 3.2 pg/mL for laminin detection and a linear range from 10 pg/mL to 100 ng/mL.[206] Xu et al. reported a simple, affordable, and environmentally friendly approach for the synthesis of water-soluble, highly fluorescent carbon quantum dots (CDs) utilizing a hydrothermal method using aloe as a carbon source. The average diameter of CDs was 5 nm, and they exhibited vivid yellow photoluminescence (PL) with a quantum yield of about 10.37%. The produced CDs were employed as an efficient sensor for sensitive and selective detection of tartrazine, one of the commonly used synthetic food colorants, through a static quenching procedure based on fluorescence quenching (Figure 8c). The reduction in fluorescence intensity allowed tartrazine to be identified throughout a linear range of 0.25 to 32.50 M. In addition, this observation was effectively used to identify tartrazine in food samples collected from nearby markets, indicating its significant potential for routine food analysis.[83] Fu et al. developed a fluorometric probe based on a combination of CDs and CdTe QDs that has excellent selectivity and sensitivity for the detection of spermine. It is highly desired to develop effective, low-cost methods for spermine detection since spermine is an indicator of the freshness of meat. As a result, a fluorometric probe made of red fluorescent cadmium telluride quantum dots (CdTe QDs) and blue fluorescent CDs was developed, with CdTe QDs acting as the response signal and CDs as the internal reference. Spermine effectively maintains the red fluorescence of CDs while effectively quenching the red fluorescence of CdTe QDs, resulting in a recognizable fluorescent color fluctuation of the probe solution from shallow pink to blue. With a low limit of detection (76 nM), this probe can selectively distinguish spermine from other organic amines.[207] Zhang et al. created aqueous N-rich CDs using microwave-assisted pyrolysis, and they used them as sensing platforms for the fluorescence detection of 2,4,6-trinitrotoluene (TNT). The strong TNT-amino interaction that allows the charge transfer mechanism to quench the photoluminescence of amino-functionalized CDs is the fundamental basis of the fluorescent sensing platform. The resulting linear detection has a quick reaction time of 30 s and covers a linear detection range of 10 nM to 1.5 μM.[208] For nonenzymatic blood glucose sensing applications, Shen et al. reported a novel method for fabricating fluorescent boronic acid-modified CDs. Phenylboronic acid serves as the only precursor in the one-step "synthesis modification integration" technique used to synthesize the functionalized CDs. The added glucose selectively leads to the assembly and

https://doi.org/10.1021/acsomega.3c07612
ACS Omega 2024, 9, 11050−11080

Table 2. Detailed Description of Synthesis Approach for Polymer/CDs Nanocomposites and Their Sensing Applications[a]

Sl no.	polymer/CDs nanocomposites	preparation method of nanocomposites	application	sensitivity for contaminant/ analyte	FL color and quantum yield	FL emission Wavelength (nm)	limit of detection (LOD)	References
1	CDs/MIPs	Sol−gel	Chemical sensor	4-nitrophenol	Blue, 51.8%	λ_{ex} - 370	35 nM	163
2	BMIP/CDs	Sol−gel	Chemical sensor	3-nitrotyrosine	Green, -	λ_{ex} - 425	17 nM	153
3	CDs/carboxymethyl cellulose film and CDs/ chitosan film	Drop casting	Chemical sensor	Cu^{2+}	Yellow, 6%	λ_{ex} - 420	10 nM	168
4	CDs/PVA	Drop casting	Chemical sensor	Fe^{3+}	Green, 8.64%	λ_{ex} - 370	-	155
5	CDs/cellulose	Solution blending	Chemical sensor	-	Bright green, 50%	λ_{max} - 470	-	158
6	CDs/PET film	Drop casting	Chemical sensor	Relative humidity (RH) sensing	-	-	-	154
7	Fe_3O_4/OCMC/CDs	One-pot synthesis	Chemical Sensor	Cu^{2+}	Green, -	λ_{ex} - 340	0.56 μM	220
8	PVA/CDs hydrogels	Physical cross-linking	Chemical Sensor	Fe^{3+}	Green, -	λ_{ex} - 470	10 μm	221
9	CM/CNF/CDs-hydrogel	Radical polymerization	Chemical Sensor	Fe^{3+}	Blue, 23.6%	λ_{ex} - 382, λ_{em} - 462	18 mg/L	222
10	CDs/SiO_2/PAN	Electrospinning, stirring	Chemical Sensor	Fe^{3+}	Blue, -	λ_{ex} - 350	3.95 μM	223
11	Cellulose nanofibril-CDs/ lignin hydrogel	Free-radical polymerization	Chemical Sensor	Cr^{6+}	Blue, -	λ_{ex} - 437, λ_{em} - 515	11.2 mg/L	224
12	CDs/agarose hydrogel	Film casting	Chemical Sensor	Cr^{6+} Fe^{3+}, Pb^{2+}, Mn^{2+}, Cu^{2+}	Multicolor, -	-	1 pM, 0.5 nM, 0.5 μM	225
13	CDs-IPDI	In-situ synthesis	Chemical Sensor	Cr^{6+}	Blue, 30.4%	λ_{ex} - 375	0.42 mg/L	233
14	Pyrene-boronic acid-CDs/ cellulose membrane	Solution casting	Chemical Sensor	F^-	Blue, -	λ_{ex} - 355	0.59 μM	226
15	CDs/silica aerogel	In-situ synthesis	Chemical Sensor	Aromatic VOCs	Yellow, -	λ_{ex} - 450	5 μL/L	227
16	TPU/CDs	In-situ polymerization	Chemical Sensor	Ag^+	Blue, 20%	λ_{ex} − 400	12 μM	228
17	MCOFs/MIPs/CDs	Reverse microemulsion	Chemical Sensor	TNP	Blue, -	λ_{ex} - 370, λ_{em} - 470	0.1 nM	170
18	CDs/Fe_3O_4/MIPs	Reverse microemulsion	Chemical Sensor	TNP	Blue, -	λ_{ex} - 370, λ_{em} - 470	0.5 nM	229
19	ACDs/DNT/MIPs	-	Chemical Sensor	DNT	-	-	0.28 ppm	230
20	CQDs/MIPs	One-pot synthesis	Chemical Sensor	Mesotrione	Blue, -	λ_{ex} - 360, λ_{em} - 453	4.7 nM/L	234
21	Poly(VPBA-Aam)-CDs	Free radical polymerization	Biological Sensor	Glucose	-	NIR-900	2−20 mM	174
22	HMIP/CDs	Microwave assisted	Biological Sensor	Tetracycline	Blue, -	λ_{ex} - 390, λ_{em} - 503	3.1 μg/L	231
23	CDs/MIPs	Sol−gel	Biological Sensor	Caffeic acid	Blue, -	λ_{ex} - 360	0.11 μM	232
24	CDs/SiO_2/MIPs	Reverse microemulsion	Biological Sensor	TBZ	-	λ_{ex} - 300, λ_{max} - 360	8 ng/mL	175
25	CDs-MIP	Reverse microemulsion polymerization	Biological Sensor	EGFR epitopes	-	λ_{ex} - 540, λ_{em} - 610	0.73 μg/mL	235
26	CDs/Cu/Alg	Cross-linking	Biological Sensor	ALP	Green, -	λ_{max} - 513	0.55 mU/ mL	173
27	MIPs-GSCDs	Reverse microemulsion	Biological Sensor	Phenobarbital	-	λ_{ex} - 340, λ_{em} - 410	0.1 nM/L	236

[a]Abbreviations: CDs - carbon dots, MIP - molecularly imprinted polymer, BMIP - bioinspired MIP, PVA - poly vinyl alcohol, PET - polyethylene terephthalate, OCMC - *ortho*-carboxymethyl chitosan, CM/CNF - carboxymethylated cellulose nanofibrils, PAN - polyacrylonitrile, IPDI - isophorone diisocynate, VOC - volatile organic compound, TPU - thermoplastic polyurethane, MCOF - magnetic covalent organic framework, ACDs - amino functionalized CDs, DNT - dinitrotoluene, VPBA - vinyl phenyl boronic acid, Aam - acrylamide, HMIP - hollow MIP, TBZ - thiabendazole, ALP - alkaline phosphate, GSCDs - green source CDs.

fluorescence quenching of the CDs (Figure 8d). These fluorescent responses may be utilized to accurately detect glucose in the 9−900 μM range. The CDs exhibit excellent selectivity and can effectively withstand interference from diverse biomolecules due to their "inert" surface. The suggested sensor technology has been utilized to measure

https://doi.org/10.1021/acsomega.3c07612
ACS Omega 2024, 9, 11050−11080

glucose in human serum with effectiveness.[209] Similarly, Zhu et al.[210] showed a strategy to integrate Bi-doped carbon quantum dots (CQDs) with liposomes to produce fluorescence visualization and therapeutic effects, namely lipo/Bi-doped CQDs. Lipo/Bi-doped CQDs show good water solubility and physicochemical properties, which can be used for in vitro labeling of colon cancer (CT26) cells and in vivo imaging localization tracking tumors for monitoring. Simultaneously, thanks to the excellent pH sensitivity and ion doping characteristic of Bi-doped CQDs, lipo/Bi-doped CQDs can be used to reveal the drug release rate of liposomes at different pH values and exhibit potential effects in vivo antitumor therapy.

3.1.4.5. Sensing of Proteins. Since proteins are essential to many biological processes, it is crucial to identify and quantify them in biomedical research and diagnosis. By exploiting the unique characteristics of CDs, researchers have made remarkable strides in developing sensitive, specific, and real-time protein detection methods.

The first test using aptamer-functionalized CDs as a sensory platform for protein identification was presented by Xu et al. Through a particular protein/aptamer interaction, the presence of thrombin can cause the aptamer-modified fluorescent CDs to create a sandwich structure with aptamer-functionalized silica nanoparticles. The test exhibited good specificity for thrombin. Compared to several previously reported fluorescence-based thrombin detection assays, a detection limit of 1 nM was attained, which is a substantial improvement.[211] A sensitive fluorescent test for the protein biomarker mucin 1 (MUC1) has been developed by Ma et al. Its foundation was the accumulation of functionalized CDs when MUC1 is present. The MUC1 aptamer and antibodies were covalently conjugated to CDs, and the immunoreaction between the CDs-labeled aptamer to MUC1 and the CDs-labeled antibodies to MUC1 produced a sandwich structure that was accompanied by CDs aggregation and fluorescence quenching. With a detection limit of 2 nM, the change in fluorescence is directly linked to the MUC1 concentration in the range of 5 to 100 nM.[212] Collectively creating a label-free sensor array for protein discrimination, Xu et al. devised a simple one-step method for quickly (within 1 min) producing four different types of nitrogen doped CDs. Eight proteins with different isoelectric points and molecular weights may be concurrently and successfully differentiated at nanomolar concentration using linear discrimination analysis (LDA) based on various fluorescence intensity responses patterns. It was also possible to identify proteins in mixtures or with varying amounts. Furthermore, even with a human urine sample present, several proteins could still be accurately identified without any overlap. Additionally, the ability to distinguish between serums from persons with rectal cancer, people with Alzheimer's disease, and healthy people is very promising for auxiliary clinical diagnosis.[213] In another research study, Freire et al. described the creation and use of polyethylenimine, ethylenediamine branched-functionalized CQDs (CQDs.BPEI) for protein sensing. It was discovered that these carbon-based nanoparticles function as a platform for protein response. Based on this, the CQDs.BPEI system could, depending on the analyte protein, identify eight distinct proteins (four metallic and four nonmetallic) even at concentrations as low as 5−40 nM. Furthermore, it was also possible to create a quick "nose"-based method to distinguish proteins by mixing components like copper ions and EDTA with CQDs.BPEI.[214]

3.2. Mechanism and Sensing Applications of Polymer/CDs Nanocomposites. *3.2.1. Mechanism for Polymer/CDs Nanocomposites in Sensing Applications.* The liquid-state fluorescent probe has typically been prepared by dispersing the CDs in an aqueous solution, even though the fluorescent probes may also be built up using only the CDs. However, this has obvious drawbacks including limited mobility and relatively low recovery efficiency. Additionally, the interaction of various ambiguous elements like pH value and salt content in actual aquatic settings may damage CDs' dispersion stability, which may cause the CDs to aggregate. This might lead to the fluorescence self-quenching phenomena.[217,218] The construction of solid-state fluorescent probes via CDs injection into the polymer matrix has been developed to address these issues. A solid-state fluorescence probe is more stable, portable, and compatible with small-footprint devices than a liquid-state fluorescent probe. A solid-state probe also has the specific benefit of having a reversible response to the analytes and comparatively higher recovery efficiency due to the easier washing step.[219] Additionally, by interacting with the active sites of the polymers through secondary interactions or covalent bonding, CDs can be evenly diffused in the proper polymer matrix, thereby reducing the agglomeration issue and improving the stability and accuracy of the analysis. Beyond that, it has been demonstrated that the presence of a polymer increases the PL intensity and QYs of CDs,[162] with plausible explanations as follows: (1) the agglomeration of CDs may be effectively inhibited due to the physiochemical interaction between CDs and polymer; (2) in accordance with the assumptions that the photoluminescence originates from the radiative recombination between the excited electron located at the surface energy trap and the holes, as well as the surface states[218] as shown in Table 2 regarding synthesis approach for polymer/CDs nanocomposites and their sensing applications.

3.2.2. Sensing Applications of Polymer/CDs Nanocomposites. Currently, CDs have been incorporated into polymeric matrixes to fabricate various fluorescent sensors, including membranes, hydrogels, aerogels, test paper, and electrospun nanofibrous films. These sensors have remarkable functions in the detection of heavy metals and organic contaminants, including Ag^{+}, Cu^{2+}, Fe^{3+}, Cr^{6+}, 2,4,6-trinitrophenol (TNP), 4-nitrophenol (4-NP), mesotrione, and 2,4-dinitrotoluene (DNT). As biosensors, these polymer/CDs nanocomposites are applicable in the detection of alkaline phosphatase (ALP), epidermal growth factor receptor (EGFR) epitopes, caffeic acid, thiabendazole (TBZ), 3-nitrotyrosine (3-NT), tetracycline, and glucose.

Wu et al. developed polymer/CDs composite films for the detection of Cu^{2+} ions using yellow-emitting CDs (y-CDs), which are synthesized through a one-step hydrothermal process. The as-prepared y-CDs possessed prominent fluorescent properties and high-water disparities. The two types of polymer/y-CDs composite sensors that are depicted here are (a) carboxy methyl cellulose/poly(vinyl alcohol) and (b) chitosan. Fluorescence intensity and time stability can both be enhanced in (a). Even though both (a) and (b) have selectivity, sensor (b)'s response is noticeably more sensitive than (a)'s, i.e., due to the chelation mechanism of chitosan with Cu^{2+} ions. The detection limit for Cu^{2+} ions is 10 nM/1.3 ppm owing to an optimized sample of system (b).[168] In a one-pot synthesis, Kumar et al. created a novel magnetic fluorescent nanoparticle by encapsulating CDs on Fe_3O_4

https://doi.org/10.1021/acsomega.3c07612
ACS Omega 2024, 9, 11050−11080

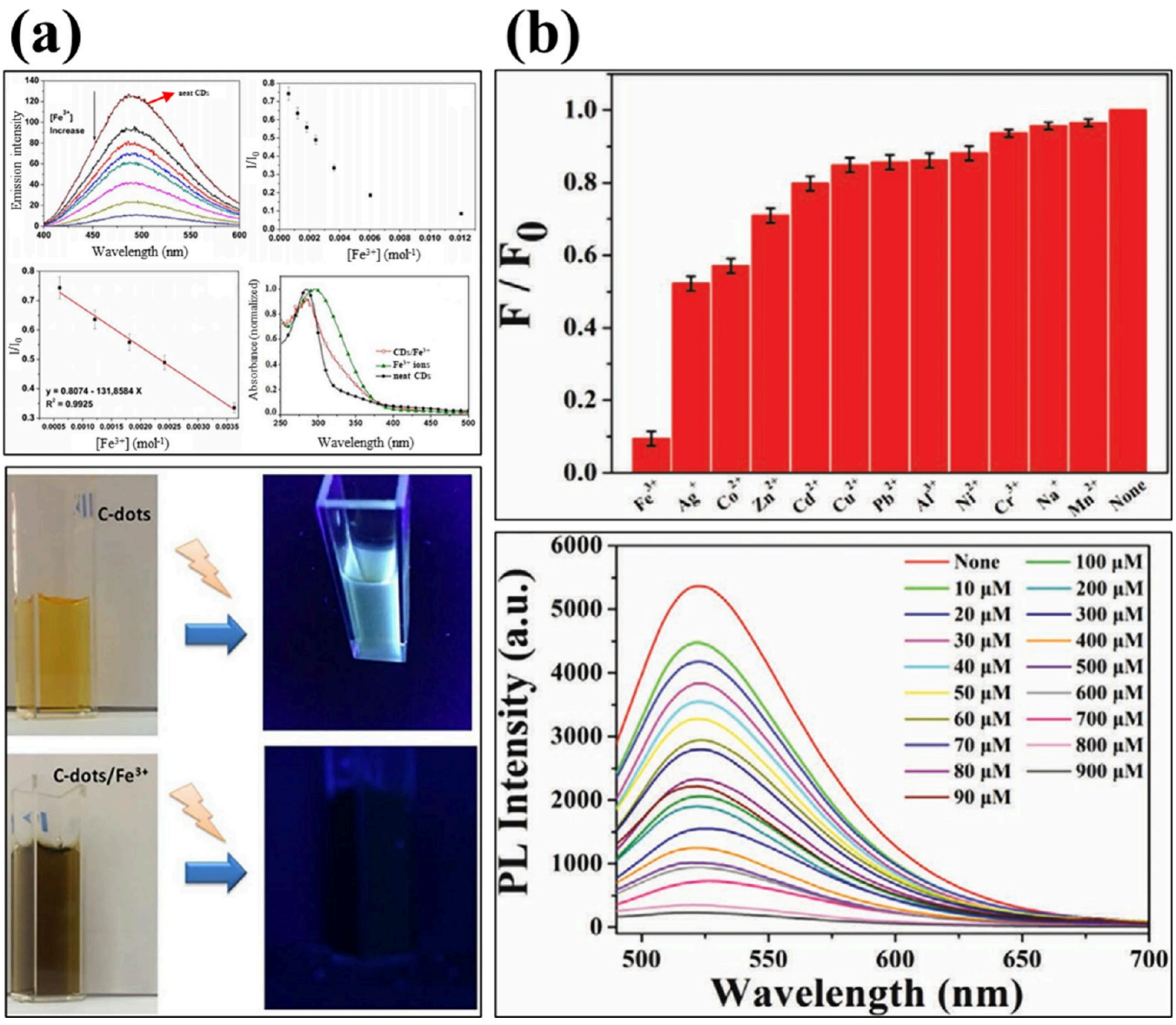

Figure 9. (a) PL emission spectra of CDs with varying concentration of Fe^{3+} and visual detection under both normal light and under UV. Reproduced with permission from ref 155. Under the Creative Common Attribution 4.0 International License. (b) The maximum fluorescence intensity ratio of PVA-CNDs hydrogel; fluorescence spectra (λ_{ex} = 470 nm) of the hydrogel with different concentrations of Fe^{3+}. Reproduced with permission from ref 221. Copyright 2019 Wiley.

nanoparticles modified with chitosan (Fe_3O_4@OCMC@CDs). More crucially, a weak magnet may be used to readily separate the produced magnetic fluorescent nanoparticle using an external magnetic field. Excellent selectivity is demonstrated by the fluorescent magnetic nanoparticles for the detection of Cu^{2+} ions over other metal ions. The inclusion of various concentrations of Cu^{2+} ions was found to successfully quench the fluorescence intensity. With a detection limit of 0.56 μM and a signal-to-noise ratio of 3, the decrease in fluorescence intensity here demonstrates the detection of Cu^{2+} ions in the linear range of 0.01−200 μM.[220] Carvalho et al. synthesized water-stable luminescent CDs from acerola fruit (Malpighiae-marginta) via a hydrothermal process. These CDs were further successfully used to fabricate CDs/poly(vinyl alcohol) luminescent nanocomposites (CDs/PVA) by blending CDs with PVA aqueous solution. The use of a colorimetric visual sensor for the detection of Fe^{3+} metal ions allowed examination of CDs/PVA composite films' application as an effective sensor having a strong green emission. In the presence of Fe^{3+} ions, the composite's emission spectra were quenched. Sensing is revealed to be sensitive to Fe^{3+} ions as the fluorescence intensity decreases indicating a linear response with the increasing Fe^{3+} ions concentration in the range of 0.001−0.012 mol L^{-1}. Consequently, utilizing fluorescent CDs/PVA composite films, highly specific "turn off" fluorescence detection of Fe^{3+} was accomplished[155] (Figure 9a). Shao et al. synthesized a high-strength fluorescent hydrogel by physically cross-linking carbon nanodots (CNDs) with poly(vinyl alcohol) (PVA). By freezing and thawing PVA and CNDs, luminous PVA-CND hydrogels were produced. The resultant hydrogel displays fluorescence quenching in the presence of Fe^{3+} owing to the high selectivity and sensitivity fluorescence properties of CNDs, which can be used as a solid detection platform for Fe^{3+}. The PVA-CNDs luminous hydrogel can be employed as an effective Fe^{3+} detection platform, with a detection limit of 10 μM for Fe^{3+}

https://doi.org/10.1021/acsomega.3c07612
ACS Omega 2024, 9, 11050−11080

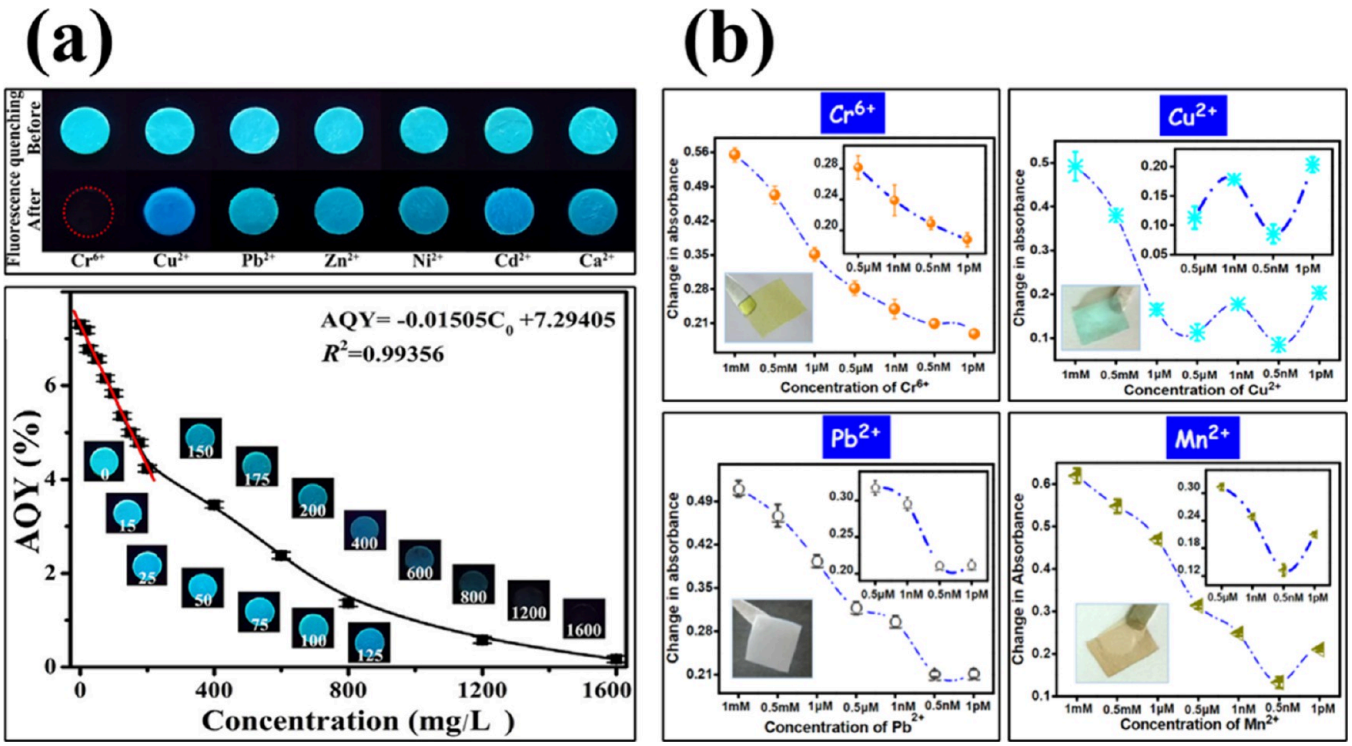

Figure 10. (a) Fluorescent selectivity of the lignin-based hydrogel (FLH) after the addition of different metal ions at the concentration of 2000 mg/L and gradual fluorescence decrease of FLH-3 with the increase of the Cr (VI) concentration. Reproduced with permission from ref 224. Copyright 2021 Elsevier. (b) The net change in absorbance value of chitosan-metal chelate peak on binding of metal ion of different concentration Inset: The enlarged view of the graph from 0.5 μM to 1 pM concentration range of metal ions and the photograph of the Agr/CDs hydrogel film after binding with the respective metal ions. Reprinted with permission from ref 225. Copyright 2015 American Chemical Society.

determined by fluorescence investigations[221] (Figure 9b). Guo et al. developed a novel fluorescent nanocellulosic hydrogel based on CNDs and CNFs that functions as both an optical sensor for measuring the concentration of heavy metals and an efficient adsorbent for removing them. The synthesized fluorescent nanocellulosic hydrogel (CM/CNF/CDs/hydrogel) showed excellent sensitivity for the detection of Fe^{3+} and strong blue fluorescence with a fluorescence quantum yield of 23.6%. The CNFs modified with CDs in this hydrogel not only facilitated the hydroxyl-induced aggregation of heavy metals as the adsorption-aggregator but also permitted a quick visual response to heavy metals as the optical sensor, increasing the adsorption capacity of heavy metals and enhanced the stability of the fluorescence signal and sensitivity for determining the concentration of heavy metals. In this case, fluorescence changed from bright blue to a deep black as the concentration of Fe^{3+} ions surged, and also the LOD was calculated to be 18 mg L^{-1}.[222] Li et al. assessed a novel turn-off and label-free fluorescence sensor based on a carbon quantum dot encapsulated mesoporous silica/polyacrylonitrile (CDs/meso-SiO_2/PAN) electrospun nanofibrous membrane for the detection of Fe(III). The micro- and mesopore-sized CDs/mesoSiO_2/PAN membrane are highly hydrophilic in nature. The membrane exhibits good sensing capability for the linearity range selective detection of Fe(III) with the detection limit estimated to be 3.95 μM. For the detection of Fe(III), the CDs can be employed as a "turn-off" sensor. Only Fe(III) quenched the fluorescent signal in the CDs/mesoSiO_2/PAN membrane, whereas other metal ions barely impacted the luminosity. The CDs/mesoSiO_2/PAN composite nanofibrous membrane exhibits strong fluorescence sensing capability for the selective detection of Fe(III) in tap water sample analysis, with recoveries ranging from 100 to 110%, offering it a novel sensing platform.[223]

Yuan et al. created a new fluorescent lignin-based hydrogel containing cellulose nanofibers and CDs for the high-value utilization of lignin and control of hexavalent chromium (Cr(VI)). A wide linear range from 15 to 200 mg/L and a high sensitivity to Cr(VI) were both displayed by this new hydrogel, with a limit of detection of 11.2 mg/L. Furthermore, this hydrogel was utilized as a solid-state fluorescence probe to detect Cr(VI) (Figure 10a). The highly effective adsorption and detection of Cr(VI) were further validated by XPS and FTIR investigations. This is because the 3D porous structures formed by lignin and CCN-CDs provide multiple ion transport channels and active sites, hence stabilizing the fluorescence signal.[224] In order to detect heavy metal ions, Gogoi et al. developed a hybrid solid sensing platform based on chitosan-based CDs-rooted agarose hydrogel film. Simple electrostatic interaction between NH^{3+} groups in CDs and OH- groups in agarose is the basis for the development of the solid sensing platform. For the colorimetric-optical detection of the quintet heavy metal ions Cr^{6+}, Cu^{2+}, Fe^{3+}, Pb^{2+}, and Mn^{2+}, agarose hydrogel rooted with CDs acted as an interesting sensing platform. Agr/CDs hydrogel thin film color variations were found that matched the colors of the individual metal ion solutions: Cr^{6+} yellow, Cu^{2+} blue, Fe^{3+} brown, Pb^{2+} white, and Mn^{2+} tan brown (Figure 10b). This color shift can be attributable to the strategic formation of colored chitosan-metal chelates. The minimum detection limit was determined to be 1 pM for Cr^{6+}, 0.5 nM for Fe^{3+}, Pb^{2+}, and Mn^{2+}, and 0.5 M for Cu^{2+}.[225] Li et al. developed a novel sensing platform for

https://doi.org/10.1021/acsomega.3c07612
ACS Omega 2024, 9, 11050−11080

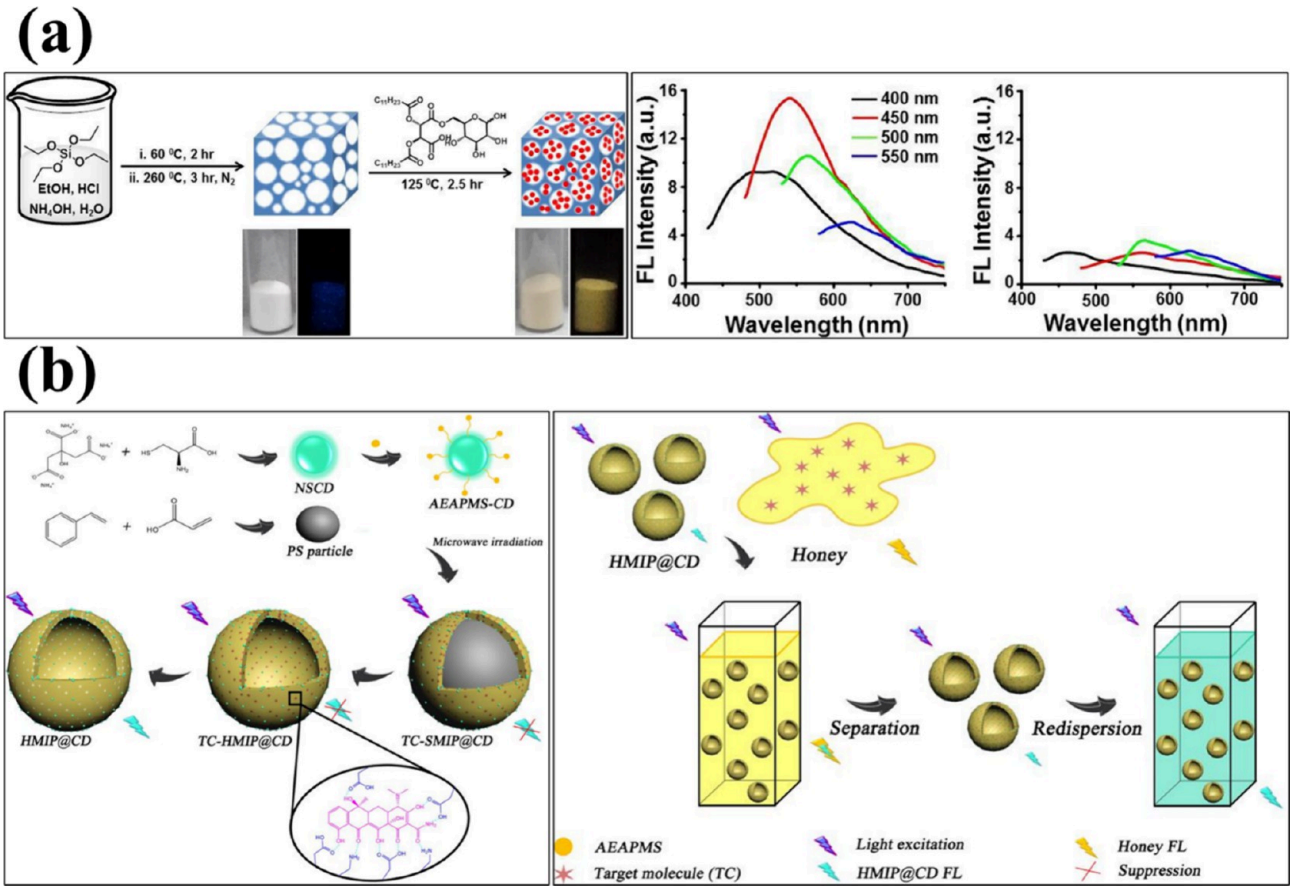

Figure 11. (a) Schematic illustration of fabrication of CDs/aerogel and detection of aniline. Reproduced with permission from ref 227. Copyright 2017 Elsevier. (b) Schematic illustration of HMIP@CDs and their fluorescence detection process of tetracycline. Reproduced with permission from ref 231. Copyright 2018 Elsevier.

the selective detection and removal of fluoride (F^-) ion at environmentally relevant levels utilizing pyrene boronic acid and CDs. On the surface of water-soluble CDs, pyrene-boronic acid (PyB) moieties have been immobilized to form the probe. Due to the high selectivity and sensitivity of F^-, in particular, the affinity of a boron atom toward it constitutes an attractive strategy. Additionally, an amino-modified cellulose membrane containing CDs/PyB has been fabricated for the efficient removal of F^-. The cellulose membrane-based sensor exhibits outstanding F^- adsorption and removal efficiency of 90.2%, as well as the considerable potential for the detection of F^-. The pyrene-boronic acid−based CDs (CDs/PyB) provide a sensor with strong selectivity for F^- over other anions that respond linearly for F^- concentrations throughout a range of 0 to 200 M and a detection limit of 5.9×10^{-5} M (0.59 μM).[226]

Aromatic volatile organic compound (VOC) detection is critical for monitoring environmental applications, industrial safety, and occupational hazards. Further, Dolai et al. reported the development of an aromatic VOC detection platform using silica aerogel embedding fluorescent CDs. Different aromatic VOCs were detected using the CDs/aerogel; specifically, it was found that different aromatic VOCs caused differential shifts and quenching of the fluorescence signals linked to the aerogel-embedded CDs. Particularly, both aniline and *p*-phenylenediamine resulted in considerable positive shifts of the fluorescence signal as well as significant fluorescence quenching[227] (Figure 11a). Bai et al. synthesized high-performance thermoplastic polyurethane elastomer/CDs (TPU/CDs) bulk nanocomposites with vibrant luminescence by using in situ polymerization. The CDs were produced using 2-aminothiophenol and citric acid. Through the interaction between active hydrogen and NCO from the isocyanate monomers of TPU, these many hydrogen-containing functional groups enabled covalent bonding with the TPU matrix during polymerization. All of the nanocomposites had more prominent luminescence behavior as compared to the initial solid-state CDs (absolute photoluminescence quantum yields (QY: 20%). Ag^+ detection studies for the composite film were carried out due to the good Ag^+ detection performance of the CDs (LOD = 12 μM), the high QY, and the processability of the nanocomposites.[228] Wang et al. used a reverse microemulsion technique to fabricate a new magnetic fluorescent composite material consisting of CDs, Fe_3O_4 as a conucleus, and MIPs as specific recognition sites. The synthesized CDs/Fe_3O_4/MIPs exhibited significant magnetic and fluorescence capabilities for the separation and detection of 2,4,6-trinitrophenol (TNP). These nanocomposites also had a spherical and homogeneous core−shell structure. The novel fluorescent material showed a strong linear range of 1 nM−100 M and a low LOD of 0.5 nM for TNP detection, indicating the CDs/Fe_3O_4/MIPs had exceptional TNP sensitivity. As a result, the CDs/Fe_3O_4/MIPs were successfully used to detect TNP in samples of lake water and tap water. This fluorometric TNP assay has a 0.5 nM detection limit. The technique worked well to identify TNP in samples of spiked tap water and river water, with recoveries ranging from 89.4% to 108.5%.[229] Dai et al.

https://doi.org/10.1021/acsomega.3c07612
ACS Omega 2024, 9, 11050−11080

synthesized amino-functionalized CDs (AC-dots) and used them to fluorescently label a MIP made using 2,4-dinitrotoluene (DNT) as a template. With a detection limit of 0.28 ppm, the fluorescence sensor had a quick response and was able to produce quantitative readings in the linear range between 1 and 15 ppm. With relatively accurate predictions of DNT concentrations, selectivity tests further demonstrated the MIPs' strong identification of the target molecule even in the presence of possible interferences (structural analogs). In addition, the material can be retrieved following measurement and regenerated for ongoing usage, which lowers costs and offers a noninvasive technique of examination (no nanomaterials are left in the sample). It has good reusability for up to 5 cycles.[230]

Wang et al. synthesized a novel fluorescent composite material based on MIPs that included CDs for the sensitive and selective detection of 4-nitrophenol (4-NP) (CDs). First, utilizing anhydrous citric acid as a carbon source and AEAPMS as a surface modification, hydrothermal synthesis was used to produce luminous CDs with a high quantum yield (QY) of 51.8%. Then, utilizing 4-NP as a template, (3-aminopropyl) triethoxysilane (APTES) as a functional monomer, tetraethoxysilane (TEOS) as a cross-linker, and CDs as signal sources, respectively, CDs were made with MIPs (CDs@MIPs) using the sol−gel technique. As it combined the benefits of CDs and MIPs, the CDs@MIPs demonstrated excellent fluorescence properties and good selectivity to 4-NP. Under ideal circumstances, from 0.025 gmL^{-1} to 5 gmL^{-1} of 4-NP, the relative fluorescence intensity of CDs@MIPs dropped linearly. For 4-NP, the limit of detection (LOD) was 5 ng mL^{-1} (35 nM).[163] Li et al. reported the preparation of single-hole hollow molecularly imprinted polymers embedded CDs (HMIP@CDs) via a microwave-assisted sol−gel method for the detection of tetracycline (TC) in honey. Because honey's autofluorescence overlaps with CDs' fluorescence emission spectrum, CDs cannot be used to directly detect TC in honey. Within 3 min, the diluted honey sample's TC was adsorbed by the HMIP@CDs; following this, the HMIP@CDs and TC were centrifuged from the honey sample and redistributed into phosphate buffer solution. It was avoided that honey's autofluorescence would disrupt the HMIP@CDs fluorescence signal (Figure 11b). The approach demonstrated excellent linearity within 10−200g L^{-1} and a modest 3.1 g L^{-1} detection limit.[231] Xu et al. created a simple approach for the detection of caffeic acid (CA) by combining the excellent selectivity of MIPs with the robust and stable photoluminescence of CDs. First, silane-functionalized CDs were synthesized using citric acid as the carbon source and aminosilane as the coordinating solvent. These CDs provided the signal of fluorescence and served as the carrier for the subsequent imprinting technique. The CDs@MIPs demonstrated exceptional selectivity, high binding affinity, and good reusability toward CA templates. Under ideal circumstances, the amount of CA between 0.5 and 200 M caused a linear reduction in the fluorescence intensity of CDs@MIPs. The detection limit was 0.11 μM. Finally, the suggested technique was used to detect CA in human plasma with success.[232]

4. CONCLUSIONS AND FUTURE OUTLOOK

Numerous synthesis approaches, properties (especially optical PL properties), and applications of CDs and polymer/CDs nanocomposites have been demonstrated, but the development of CDs and polymer/CDs nanocomposite-based fluorescence sensors are the major emphasis of this review paper. CDs are more biocompatible than semiconductor quantum dots but have lower QYs. It has been discovered that doping CDs with additional elements (such nitrogen, sulfur, and phosphorus) can improve the photoluminescence, like broad visible spectrum emission. Future studies will need the synthesis of CDs with wide visible emission. It is anticipated that by modifying precursors and doping agents, a wide range of CDs might be developed, opening up a new path to a number of unanticipated uses beyond sensing, including catalysis, bioimaging, disease diagnosis, energy storage, etc. A summary of the sensing processes, sensor architecture, and sensing characteristics for diverse targets is provided. Numerous areas of detection have been considered, including chemical and biological analytes such as metal ions, small organic molecules, and several contaminants along with temperature, pH, cations, cancer cells, and antibiotics. For a variety of targets, polymer/CDs nanocomposites have demonstrated good performance as chemical, biological, and physical sensors. The sensing capabilities of polymer/CDs nanocomposites might be expanded and enhanced by increasing their sensitivity and selectivity for different targets. The majority of the polymer/CDs nanocomposites' sensing applications are based on their FL quenching process. Despite the significant prospects provided by polymer/CDs nanocomposites, there are still certain challenges in studying their significant potential.

More studies are required for the development of polymer/CDs nanocomposites from cheap and natural polymer sources and simple one-step synthesis techniques as most of the nanocomposites result from synthetic polymer precursors. More work could expand toward doped/functionalized polymer/CDs nanocomposites as they can possess a wide visible spectrum emission for better applications. Specifically, in the sensing part, there are a lot of new analytes/targets can be explored, and sensitivity along with selectivity can be improved. More focus has to be put forward for the visual and solid probe for detection. There are only a few research works and no such progress in the physical sensors like temperature, light humidity etc. along with other specific carcinogenic metals such as Hg, Pd, Ni, As, Cd, etc. The fluorescence mechanism is still a topic of debate, and as the PL properties of polymer nanocomposites clearly depend on CDs, clear insight into the fluorescence mechanism is much needed. Multiple sensing capabilities of different analytes using the same probe could be a ground breaking factor in this research.

AUTHOR INFORMATION

Corresponding Authors

Smrutirekha Mishra − *Institute of Chemical Technology (ICT), Indian Oil Campus (IOC), Bhubaneswar 751013 Odisha, India;* orcid.org/0000-0002-8258-063X; Email: s.mishra@iocb.ictmumbai.edu.in, smruti.wisdom@gmail.com

Harekrishna Panigrahi − *School of Chemical Technology, Kalinga Institute of Industrial Technology, Bhubaneswar 751024 Odisha, India;* orcid.org/0000-0002-7527-0254; Email: harekrishna.panigrahi@kiitbiotech.ac.in, harekrishnapanigrahi91@gmail.com

https://doi.org/10.1021/acsomega.3c07612
ACS Omega 2024, 9, 11050−11080

Authors

Dilip Kumar Kar − *School of Chemical Technology, Kalinga Institute of Industrial Technology, Bhubaneswar 751024 Odisha, India*

Praveenkumar V − *Institute of Chemical Technology (ICT), Indian Oil Campus (IOC), Bhubaneswar 751013 Odisha, India*

Satyabrata Si − *School of Chemical Technology, Kalinga Institute of Industrial Technology, Bhubaneswar 751024 Odisha, India*

Complete contact information is available at: https://pubs.acs.org/10.1021/acsomega.3c07612

Notes

The authors declare no competing financial interest.

■ ACKNOWLEDGMENTS

S.R.M. acknowledges H.K.P. as the cocorresponding author of this manuscript. S.R.M. is thankful to H.K.P. for giving an informative and scientific skeleton to the manuscript and adding new references to the manuscript.

■ REFERENCES

(1) Baig, N.; Kammakakam, I.; Falath, W.; Kammakakam, I. Nanomaterials: A Review of Synthesis Methods, Properties, Recent Progress, and Challenges. *Mater. Adv.* **2021**, 1821−1871, DOI: 10.1039/d0ma00807a.

(2) Ramesh, K. T. *Nanomaterials: Mechanics and Mechanisms*; Springer: US, 2009. DOI: 10.1007/978-0-387-09783-1.

(3) Kolahalam, L. A.; Kasi Viswanath, I. V.; Diwakar, B. S.; Govindh, B.; Reddy, V.; Murthy, Y. L. N. Review on Nanomaterials: Synthesis and Applications. *Materials Today: Proceedings* **2019**, *18*, 2182−2190, DOI: 10.1016/j.matpr.2019.07.371.

(4) Mazari, S. A.; Ali, E.; Abro, R.; Khan, F. S. A.; Ahmed, I.; Ahmed, M.; Nizamuddin, S.; Siddiqui, T. H.; Hossain, N.; Mubarak, N. M.; Shah, A. Nanomaterials: Applications, Waste-Handling, Environmental Toxicities, and Future Challenges - A Review. *J. Environ. Chem. Eng.* **2021**, *9* (2), 105028.

(5) Kaliva, M.; Vamvakaki, M. Nanomaterials Characterization. In *Polymer Science and Nanotechnology: Fundamentals and Applications*; Elsevier, 2020; pp 401−433. DOI: 10.1016/B978-0-12-816806-6.00017-0.

(6) Buzea, C.; Pacheco, I. Nanomaterials and Their Classification. In *Advanced Structured Materials*; Springer Verlag, 2017; Vol. *62*, pp 3−45. DOI: 10.1007/978-81-322-3655-9_1.

(7) Awan, T. I.; Ahmad, A.; Bibi, S.; Tehseen, A.; Bashir, A. Nanomaterials. In *Chemistry of Nanomaterials: Fundamentals and Applications*; Elsevier, 2020; pp 225−269. DOI: 10.1016/B978-0-12-818908-5.00009-3.

(8) Das, S.; Mukherjee, A.; Sengupta, G.; Singh, V. K. Overview of Nanomaterials Synthesis Methods, Characterization Techniques and Effect on Seed Germination. In *Nano-Materials as Photocatalysts for Degradation of Environmental Pollutants: Challenges and Possibilities*; Elsevier, 2019; pp 371−401. DOI: 10.1016/B978-0-12-818598-8.00018-3.

(9) Pirzada, M.; Altintas, Z. Nanomaterials for Healthcare Biosensing Applications. *Sensors (Switzerland)* **2019**, *19*, 5311 DOI: 10.3390/s19235311.

(10) Srinivas, V. *What Are the Uses and Applications of Nanoparticles?*; 2021. https://creativecommons.org/licenses/by-nc-sa/4.0/.

(11) Bekyarova, E.; Ni, Y.; Malarkey, E. B.; Montana, V.; McWilliams, J. L.; Haddon, R. C.; Parpura, V. Applications of Carbon Nanotubes in Biotechnology and Biomedicine. *J. Biomed Nanotechnol* **2005**, *1* (1), 3−17.

(12) Trivedi, M.; Murase, J. Titanium Dioxide in Sunscreen. In *Application of Titanium Dioxide*; InTech, 2017. DOI: 10.5772/intechopen.68886.

(13) Allsopp, M.; Walters, A.; Santillo, D. *Nanotechnologies and Nanomaterials in Electrical and Electronic Goods: A Review of Uses and Health Concerns; Use of Nanomaterials in Fuel Cells and Photovoltaic Cells; 3.6 Use of Nanomaterials in Electric Double-Layer Capacitor (EDLC); 3.7 Use of Nanomaterials in Lead-Free Solder*; 2007.

(14) Semeniuk, M.; Yi, Z.; Poursorkhabi, V.; Tjong, J.; Jaffer, S.; Lu, Z. H.; Sain, M. Future Perspectives and Review on Organic Carbon Dots in Electronic Applications. *ACS Nano* **2019**, *13* (6), 6224−6255.

(15) Fu, X.; Xu, L.; Li, J.; Sun, X.; Peng, H. Flexible Solar Cells Based on Carbon Nanomaterials. *Carbon* **2018**, 1063−1073, DOI: 10.1016/j.carbon.2018.08.017.

(16) Kumar, S.; Nehra, M.; Deep, A.; Kedia, D.; Dilbaghi, N.; Kim, K. H. Quantum-Sized Nanomaterials for Solar Cell Applications. *Renewable and Sustainable Energy Reviews* **2017**, *73*, 821−839, DOI: 10.1016/j.rser.2017.01.172.

(17) Chen, C.; Fan, Y.; Gu, J.; Wu, L.; Passerini, S.; Mai, L. One-Dimensional Nanomaterials for Energy Storage. *Journal of Physics D: Applied Physics* **2018**, *51*, 113002 DOI: 10.1088/1361-6463/aaa98d.

(18) Rasal, A. S.; Yadav, S.; Yadav, A.; Kashale, A. A.; Thagare Manjunatha, S.; Altaee, A.; Chang, J.-Y. Carbon Quantum Dots for Energy Applications: A Review. *ACS Appl. Nano Mater.* **2021**, *4*, 6515.

(19) Dresselhaus, M. S.; Terrones, M. Carbon-Based Nanomaterials from a Historical Perspective. *Proc. IEEE* **2013**, *101*, 1522−1535, DOI: 10.1109/JPROC.2013.2261271.

(20) Nasir, S.; Hussein, M. Z.; Zainal, Z.; Yusof, N. A. Carbon-Based Nanomaterials/Allotropes: A Glimpse of Their Synthesis, Properties and Some Applications. *Materials* **2018**, *11*, 295 DOI: 10.3390/ma11020295.

(21) Xin, Q.; Shah, H.; Nawaz, A.; Xie, W.; Akram, M. Z.; Batool, A.; Tian, L.; Jan, S. U.; Boddula, R.; Guo, B.; Liu, Q.; Gong, J. R. Antibacterial Carbon-Based Nanomaterials. *Adv. Mater.* **2019**, *31* (45), 1804838 DOI: 10.1002/adma.201804838.

(22) Zhang, C.; Wu, L.; de Perrot, M.; Zhao, X. Carbon Nanotubes: A Summary of Beneficial and Dangerous Aspects of an Increasingly Popular Group of Nanomaterials. *Front. Oncol.* **2021**, *11*, DOI: 10.3389/fonc.2021.693814.

(23) Rathinavel, S.; Priyadharshini, K.; Panda, D. A Review on Carbon Nanotube: An Overview of Synthesis, Properties, Functionalization, Characterization, and the Application. *Mater. Sci. Eng. B: Solid-State Mater. Adv. Technol.* **2021**, *268*, 115095 DOI: 10.1016/j.mseb.2021.115095.

(24) Allen, M. J.; Tung, V. C.; Kaner, R. B. Honeycomb Carbon: A Review of Graphene. *Chem. Rev.* **2010**, *110* (1), 132−145.

(25) Singh, R. K.; Kumar, R.; Singh, D. P. Graphene Oxide: Strategies for Synthesis, Reduction and Frontier Applications. *RSC Adv* **2016**, *6*, 64993−65011, DOI: 10.1039/c6ra07626b.

(26) Compton, O. C.; Nguyen, S. T. Graphene Oxide, Highly Reduced Graphene Oxide, and Graphene: Versatile Building Blocks for Carbon-Based Materials. *Small.* **2010**, *6*, 711−723.

(27) Zaytseva, O.; Neumann, G. Carbon Nanomaterials: Production, Impact on Plant Development, Agricultural and Environmental Applications. *Chem. Biol. Technol. Agric* **2016**, *3*, 17 DOI: 10.1186/s40538-016-0070-8.

(28) Cha, C.; Shin, S. R.; Annabi, N.; Dokmeci, M. R.; Khademhosseini, A. Carbon-Based Nanomaterials: Multifunctional Materials for Biomedical Engineering. *ACS Nano* **2013**, *7*, 2891−2897.

(29) Sabzehmeidani, M. M.; Mahnaee, S.; Ghaedi, M.; Heidari, H.; Roy, V. A. L. Carbon Based Materials: A Review of Adsorbents for Inorganic and Organic Compounds. *Mater. Adv* **2021**, *2*, 598−627, DOI: 10.1039/d0ma00087f.

(30) Chandra, A.; Prasad, S.; Gigli, G.; del Mercato, L. L. Fluorescent Nanoparticles for Sensing. *Front. Nanosci.* **2020**, *16*, 117−149, DOI: 10.1016/B978-0-08-102828-5.00006-1.

(31) Wolfbeis, O. S. An Overview of Nanoparticles Commonly Used in Fluorescent Bioimaging. *Chem. Soc. Rev.* **2015**, *44*, 4743−4768, DOI: 10.1039/c4cs00392f.
(32) Halicka, K.; Meloni, F.; Czok, M.; Spychalska, K.; Baluta, S.; Malecha, K.; Pilo, M. I.; Cabaj, J. New Trends in Fluorescent Nanomaterials-Based Bio/Chemical Sensors for Neurohormones Detection A Review. *ACS Omega* **2022**, *7* (38), 33749−33768.
(33) Zuo, P.; Lu, X.; Sun, Z.; Guo, Y.; He, H. A Review on Syntheses, Properties, Characterization and Bioanalytical Applications of Fluorescent Carbon Dots. *Microchimica Acta* **2016**, *183*, 519−542, DOI: 10.1007/s00604-015-1705-3.
(34) Xu, X.; Ray, R.; Gu, Y.; Ploehn, H. J.; Gearheart, L.; Raker, K.; Scrivens, W. A. Electrophoretic Analysis and Purification of Fluorescent Single-Walled Carbon Nanotube Fragments. *J. Am. Chem. Soc.* **2004**, *126* (40), 12736−12737.
(35) Liu, J.; Li, R.; Yang, B. Carbon Dots: A New Type of Carbon-Based Nanomaterial with Wide Applications. *ACS Cent Sci.* **2020**, *6* (12), 2179−2195.
(36) Xia, C.; Zhu, S.; Feng, T.; Yang, M.; Yang, B. Evolution and Synthesis of Carbon Dots: From Carbon Dots to Carbonized Polymer Dots. *Adv. Sci* **2019**, *6*, 1901316 DOI: 10.1002/advs.201901316.
(37) Chu, K. W.; Lee, S. L.; Chang, C. J.; Liu, L. Recent Progress of Carbon Dot Precursors and Photocatalysis Applications. *Polymers* **2019**, *11*, 689 DOI: 10.3390/polym11040689.
(38) Reyes, D.; Camacho, M.; Camacho, M.; Mayorga, M.; Weathers, D.; Salamo, G.; Wang, Z.; Neogi, A. Laser Ablated Carbon Nanodots for Light Emission. *Nanoscale Res. Lett.* **2016**, *11* (1), No. 424, DOI: 10.1186/s11671-016-1638-8.
(39) Kurian, M.; Paul, A. Recent Trends in the Use of Green Sources for Carbon Dot Synthesis-A Short Review. *Carbon Trends* **2021**, *3*, 100032.
(40) Chao-Mujica, F. J.; Garcia-Hernández, L.; Camacho-López, S.; Camacho-López, M.; Camacho-López, M. A.; Reyes Contreras, D.; Pérez-Rodríguez, A.; Peña-Caravaca, J. P.; Páez-Rodríguez, A.; Darias-Gonzalez, J. G.; Hernandez-Tabares, L.; Arias de Fuentes, O.; Prokhorov, E.; Torres-Figueredo, N.; Reguera, E.; Desdin-García, L. F. Carbon Quantum Dots by Submerged Arc Discharge in Water: Synthesis, Characterization, and Mechanism of Formation. *J. Appl. Phys.* **2021**, *129* (16), No. 163301, DOI: 10.1063/5.0040322.
(41) Das, R.; Shahnavaz, Z.; Ali, M. E.; Islam, M. M.; Abd Hamid, S. B. Can We Optimize Arc Discharge and Laser Ablation for Well-Controlled Carbon Nanotube Synthesis? *Nanoscale Research Letters* **2016**, *11*, No. 510, DOI: 10.1186/s11671-016-1730-0.
(42) Deng, J.; Lu, Q.; Mi, N.; Li, H.; Liu, M.; Xu, M.; Tan, L.; Xie, Q.; Zhang, Y.; Yao, S. Electrochemical Synthesis of Carbon Nanodots Directly from Alcohols. *Chem.—Eur. J.* **2014**, *20* (17), 4993−4999.
(43) Ming, H.; Ma, Z.; Liu, Y.; Pan, K.; Yu, H.; Wang, F.; Kang, Z. Large Scale Electrochemical Synthesis of High Quality Carbon Nanodots and Their Photocatalytic Property. *Dalton Transactions* **2012**, *41* (31), 9526−9531.
(44) Desai, M. L.; Jha, S.; Basu, H.; Singhal, R. K.; Park, T. J.; Kailasa, S. K. Acid Oxidation of Muskmelon Fruit for the Fabrication of Carbon Dots with Specific Emission Colors for Recognition of Hg2+ Ions and Cell Imaging. *ACS Omega* **2019**, *4* (21), 19332−19340.
(45) Li, X.; Ge, F.; Li, X.; Zhou, X.; Qian, J.; Fu, G.; Shi, L.; Xu, Y. Rapid and Large-Scale Production of Carbon Dots by Salt-Assisted Electrochemical Exfoliation of Graphite Rods. *J. Electroanal. Chem.* **2019**, *851*, 113390.
(46) Joseph, J.; Anappara, A. A. White-Light-Emitting Carbon Dots Prepared by the Electrochemical Exfoliation of Graphite. *ChemPhysChem* **2017**, *18* (3), 292−298.
(47) Li, D.; Liang, C.; Ushakova, E. V.; Sun, M.; Huang, X.; Zhang, X.; Jing, P.; Yoo, S. J.; Kim, J. G.; Liu, E.; Zhang, W.; Jing, L.; Xing, G.; Zheng, W.; Tang, Z.; Qu, S.; Rogach, A. L. Thermally Activated Upconversion Near-Infrared Photoluminescence from Carbon Dots Synthesized via Microwave Assisted Exfoliation. *Small* **2019**, *15* (50), No. 1905050, DOI: 10.1002/smll.201905050.
(48) Singh, R. K.; Kumar, R.; Singh, D. P.; Savu, R.; Moshkalev, S. A. Progress in Microwave-Assisted Synthesis of Quantum Dots (Graphene/Carbon/Semiconducting) for Bioapplications: A Review. *Mater. Today Chem.* **2019**, *12*, 282−314, DOI: 10.1016/j.mtchem.2019.03.001.
(49) Shabbir, H.; Tokarski, T.; Ungor, D.; Wojnicki, M. Eco Friendly Synthesis of Carbon Dot by Hydrothermal Method for Metal Ions Salt Identification. *Materials* **2021**, *14* (24), 7604.
(50) Wang, B.; Yu, J.; Sui, L.; Zhu, S.; Tang, Z.; Yang, B.; Lu, S. Rational Design of Multi-Color-Emissive Carbon Dots in a Single Reaction System by Hydrothermal. *Adv. Sci.* **2021**, *8* (1), 2001453 DOI: 10.1002/advs.202001453.
(51) Zhao, P.; Li, X.; Baryshnikov, G.; Wu, B.; Ågren, H.; Zhang, J.; Zhu, L. One-Step Solvothermal Synthesis of High-Emissive Amphiphilic Carbon Dots: Via Rigidity Derivation. *Chem. Sci.* **2018**, *9* (5), 1323−1329.
(52) Wang, C.; Yang, K.; Wei, X.; Ding, S.; Tian, F.; Li, F. One-Pot Solvothermal Synthesis of Carbon Dots/Ag Nanoparticles/TiO_2 Nanocomposites with Enhanced Photocatalytic Performance. *Ceram. Int.* **2018**, *44* (18), 22481−22488.
(53) Ma, Z.; Ming, H.; Huang, H.; Liu, Y.; Kang, Z. One-Step Ultrasonic Synthesis of Fluorescent N-Doped Carbon Dots from Glucose and Their Visible-Light Sensitive Photocatalytic Ability. *New J. Chem.* **2012**, *36* (4), 861−864.
(54) Kumar, R.; Kumar, V. B.; Gedanken, A. Sonochemical Synthesis of Carbon Dots, Mechanism, Effect of Parameters, and Catalytic, Energy, Biomedical and Tissue Engineering Applications. *Ultrasonics Sonochemistry* **2020**, *64*, No. 105009, DOI: 10.1016/j.ultsonch.2020.105009.
(55) Liu, Q.; Zhang, N.; Shi, H.; Ji, W.; Guo, X.; Yuan, W.; Hu, Q. One-Step Microwave Synthesis of Carbon Dots for Highly Sensitive and Selective Detection of Copper Ions in Aqueous Solution. *New J. Chem.* **2018**, *42* (4), 3097−3101.
(56) De Medeiros, T. V.; Manioudakis, J.; Noun, F.; Macairan, J. R.; Victoria, F.; Naccache, R. Microwave-Assisted Synthesis of Carbon Dots and Their Applications. *J. Mater. Chem. C Mater.* **2019**, *7* (24), 7175−7195.
(57) Fatahi, Z.; Esfandiari, N.; Ehtesabi, H.; Bagheri, Z.; Tavana, H.; Ranjbar, Z.; Latifi, H. Physicochemical and Cytotoxicity Analysis of Green Synthesis Carbon Dots for Cell Imaging. *EXCLI J.* **2019**, *18*, 454−466.
(58) Sachdev, A.; Matai, I.; Gopinath, P. Implications of Surface Passivation on Physicochemical and Bioimaging Properties of Carbon Dots. *RSC Adv.* **2014**, *4* (40), 20915−20921.
(59) Hu, S.; Trinchi, A.; Atkin, P.; Cole, I. Tunable Photoluminescence across the Entire Visible Spectrum from Carbon Dots Excited by White Light. *Angewandte Chemie - International Edition* **2015**, *54* (10), 2970−2974.
(60) Zhang, Y.; Yuan, R.; He, M.; Hu, G.; Jiang, J.; Xu, T.; Zhou, L.; Chen, W.; Xiang, W.; Liang, X. Multicolour Nitrogen-Doped Carbon Dots: Tunable Photoluminescence and Sandwich Fluorescent Glass-Based Light-Emitting Diodes. *Nanoscale* **2017**, *9* (45), 17849−17858.
(61) Yue, J.; Zhang, K.; Yu, H.; Yu, L.; Hou, T.; Chen, X.; Ge, H.; Hayat, T.; Alsaedi, A.; Wang, S. Mechanism Insights into Tunable Photoluminescence of Carbon Dots by Hydroxyl Radicals. *J. Mater. Sci.* **2019**, *54* (8), 6140−6150.
(62) Dias, C.; Vasimalai, N.; Sárria, M. P.; Pinheiro, I.; Vilas-Boas, V.; Peixoto, J.; Espiña, B. Biocompatibility and Bioimaging Potential of Fruit-Based Carbon Dots. *Nanomaterials* **2019**, *9* (2), 199.
(63) Xu, X.; Zhang, K.; Zhao, L.; Li, C.; Bu, W.; Shen, Y.; Gu, Z.; Chang, B.; Zheng, C.; Lin, C.; Sun, H.; Yang, B. Aspirin-Based Carbon Dots, a Good Biocompatibility of Material Applied for Bioimaging and Anti-Inflammation. *ACS Appl. Mater. Interfaces* **2016**, *8* (48), 32706−32716.
(64) Hutton, G. A. M.; Martindale, B. C. M.; Reisner, E. Carbon Dots as Photosensitisers for Solar-Driven Catalysis. *Chem. Soc. Rev.* **2017**, *46*, 6111−6123, DOI: 10.1039/c7cs00235a.

https://doi.org/10.1021/acsomega.3c07612
ACS Omega 2024, 9, 11050−11080

(65) Chen, B. B.; Liu, M. L.; Huang, C. Z. Carbon Dot-Based Composites for Catalytic Applications. *Green Chem.* **2020**, *22*, 4034−4054, DOI: 10.1039/d0gc01014f.
(66) Domingo-Tafalla, B.; Martínez-Ferrero, E.; Franco, F.; Palomares-Gil, E. Applications of Carbon Dots for the Photocatalytic and Electrocatalytic Reduction of CO_2. *Molecules* **2022**, *27*, 1081 DOI: 10.3390/molecules27031081.
(67) Xu, D.; Lin, Q.; Chang, H. T. Recent Advances and Sensing Applications of Carbon Dots. *Small Methods* **2020**, *4*, No. 1900387, DOI: 10.1002/smtd.201900387.
(68) Tan, J.; Li, Q.; Meng, S.; Li, Y.; Yang, J.; Ye, Y.; Tang, Z.; Qu, S.; Ren, X. Time-Dependent Phosphorescence Colors from Carbon Dots for Advanced Dynamic Information Encryption. *Adv. Mater.* **2021**, *33* (16), 2006781 DOI: 10.1002/adma.202006781.
(69) Muthamma, K.; Sunil, D.; Shetty, P. Carbon Dots as Emerging Luminophores in Security Inks for Anti-Counterfeit Applications - An up-to-Date Review. *Appl. Mater. Today* **2021**, *23*, No. 101050, DOI: 10.1016/j.apmt.2021.101050.
(70) Zhao, B.; Tan, Z. Fluorescent Carbon Dots: Fantastic Electroluminescent Materials for Light-Emitting Diodes. *Adv. Sci* **2021**, *8*, No. 1001977, DOI: 10.1002/advs.202001977.
(71) Li, B.; Zhao, S.; Huang, L.; Wang, Q.; Xiao, J.; Lan, M. Recent Advances and Prospects of Carbon Dots in Phototherapy. *Chem. Eng. J* **2021**, *408*, No. 127245, DOI: 10.1016/j.cej.2020.127245.
(72) Li, H.; Yan, X.; Kong, D.; Jin, R.; Sun, C.; Du, D.; Lin, Y.; Lu, G. Recent Advances in Carbon Dots for Bioimaging Applications. *Nanoscale Horizons* **2020**, *5*, 218−234, DOI: 10.1039/c9nh00476a.
(73) Zare, H.; Ahmadi, S.; Ghasemi, A.; Ghanbari, M.; Rabiee, N.; Bagherzadeh, M.; Karimi, M.; Webster, T. J.; Hamblin, M. R.; Mostafavi, E. Carbon Nanotubes: Smart Drug/Gene Delivery Carriers. *Int. J. Nanomed.* **2021**, *16*, 1681−1706, DOI: 10.2147/IJN.S299448.
(74) Wang, B.; Song, H.; Qu, X.; Chang, J.; Yang, B.; Lu, S. Carbon Dots as a New Class of Nanomedicines: Opportunities and Challenges. *Coord. Chem. Rev.* **2021**, *442*, No. 214010, DOI: 10.1016/j.ccr.2021.214010.
(75) Sreenath, P. R.; Mandal, S.; Panigrahi, H.; Das, P.; Dinesh Kumar, K. Carbon Dots: Fluorescence Active, Covalently Conjugated and Strong Reinforcing Nanofiller for Polymer Latex. *Nano-Structures and Nano-Objects* **2020**, *23*, 100477.
(76) Sun, Y. P.; Zhou, B.; Lin, Y.; Wang, W.; Fernando, K. A. S.; Pathak, P.; Meziani, M. J.; Harruff, B. A.; Wang, X.; Wang, H.; Luo, P. G.; Yang, H.; Kose, M. E.; Chen, B.; Veca, L. M.; Xie, S. Y. Quantum-Sized Carbon Dots for Bright and Colorful Photoluminescence. *J. Am. Chem. Soc.* **2006**, *128* (24), 7756−7757.
(77) Li, X.; Fu, Y.; Zhao, S.; Xiao, J. F.; Lan, M.; Wang, B.; Zhang, K.; Song, X.; Zeng, L. Metal Ions-Doped Carbon Dots: Synthesis, Properties, and Applications. *Chemical Engineering Journal* **2022**, *430*, 133101.
(78) Liu, R.; Wu, D.; Liu, S.; Koynov, K.; Knoll, W.; Li, Q. An Aqueous Route to Multicolor Photoluminescent Carbon Dots Using Silica Spheres as Carriers. *Angewandte Chemie - International Edition* **2009**, *48* (25), 4598−4601.
(79) Ngu, P. Z. Z.; Chia, S. P. P.; Fong, J. F. Y.; Ng, S. M. Synthesis of Carbon Nanoparticles from Waste Rice Husk Used for the Optical Sensing of Metal Ions. *Xinxing Tan Cailiao/New Carbon Materials* **2016**, *31* (2), 135−143.
(80) Ray, S. C.; Saha, A.; Jana, N. R.; Sarkar, R. Fluorescent Carbon Nanoparticle: Synthesis, Characterization and Bio-Imaging Application. *J. Phys. Chem. C* **2009**, *3*, 18546−18551.
(81) Qiao, Z. A.; Wang, Y.; Gao, Y.; Li, H.; Dai, T.; Liu, Y.; Huo, Q. Commercially Activated Carbon as the Source for Producing Multicolor Photoluminescent Carbon Dots by Chemical Oxidation. *Chem. Commun.* **2009**, *46* (46), 8812−8814.
(82) Wang, T. Y.; Chen, C. Y.; Wang, C. M.; Tan, Y. Z.; Liao, W. S. Multicolor Functional Carbon Dots via One-Step Refluxing Synthesis. *ACS Sens* **2017**, *2* (3), 354−363.
(83) Xu, H.; Yang, X.; Li, G.; Zhao, C.; Liao, X. Green Synthesis of Fluorescent Carbon Dots for Selective Detection of Tartrazine in Food Samples. *J. Agric. Food Chem.* **2015**, *63*, 6707−6714.
(84) Sahu, S.; Behera, B.; Maiti, T. K.; Mohapatra, S. Simple One-Step Synthesis of Highly Luminescent Carbon Dots from Orange Juice: Application as Excellent Bio-Imaging Agents. *Chem. Commun.* **2012**, *48* (70), 8835−8837.
(85) Jana, J.; Lee, H. J.; Chung, J. S.; Kim, M. H.; Hur, S. H. Blue Emitting Nitrogen-Doped Carbon Dots as a Fluorescent Probe for Nitrite Ion Sensing and Cell-Imaging. *Anal. Chim. Acta* **2019**, *1079*, 212−219.
(86) Xu, Q.; Liu, Y.; Su, R.; Cai, L.; Li, B.; Zhang, Y.; Zhang, L.; Wang, Y.; Wang, Y.; Li, N.; Gong, X.; Gu, Z.; Chen, Y.; Tan, Y.; Dong, C.; Sreeprasad, T. S. Highly Fluorescent Zn-Doped Carbon Dots as Fenton Reaction-Based Bio-Sensors: An Integrative Experimental-Theoretical Consideration. *Nanoscale* **2016**, *8* (41), 17919−17927.
(87) Cheng, J.; Wang, C. F.; Zhang, Y.; Yang, S.; Chen, S. Zinc Ion-Doped Carbon Dots with Strong Yellow Photoluminescence. *RSC Adv.* **2016**, *6* (43), 37189−37194.
(88) Pawar, S.; Kaja, S.; Nag, A. Red-Emitting Carbon Dots as a Dual Sensor for In3+ and Pd2+ in Water. *ACS Omega* **2020**, *5* (14), 8362−8372.
(89) Zhang, Y.; Liu, X.; Fan, Y.; Guo, X.; Zhou, L.; Lv, Y.; Lin, J. One-Step Microwave Synthesis of N-Doped Hydroxyl-Functionalized Carbon Dots with Ultra-High Fluorescence Quantum Yields. *Nanoscale* **2016**, *8* (33), 15281−15287.
(90) Wang, J.; Sheng Li, R.; Zhi Zhang, H.; Wang, N.; Zhang, Z.; Huang, C. Z. Highly Fluorescent Carbon Dots as Selective and Visual Probes for Sensing Copper Ions in Living Cells via an Electron Transfer Process. *Biosens Bioelectron* **2017**, *97*, 157−163.
(91) Sun, Y.; Wang, X.; Wang, C.; Tong, D.; Wu, Q.; Jiang, K.; Jiang, Y.; Wang, C.; Yang, M. Red Emitting and Highly Stable Carbon Dots with Dual Response to PH Values and Ferric Ions. *Microchimica Acta* **2018**, *185* (1), No. 83, DOI: 10.1007/s00604-017-2544-1.
(92) Ju, Y. J.; Li, N.; Liu, S. G.; Liang, J. Y.; Gao, X.; Fan, Y. Z.; Luo, H. Q.; Li, N. B. Proton-Controlled Synthesis of Red-Emitting Carbon Dots and Application for Hematin Detection in Human Erythrocytes. *Anal Bioanal Chem.* **2019**, *411* (6), 1159−1167.
(93) Ding, H.; Ji, Y.; Wei, J. S.; Gao, Q. Y.; Zhou, Z. Y.; Xiong, H. M. Facile Synthesis of Red-Emitting Carbon Dots from Pulp-Free Lemon Juice for Bioimaging. *J. Mater. Chem. B* **2017**, *5* (26), 5272−5277.
(94) Bhati, A.; Anand, S. R.; Gunture, G.; Garg, A. K.; Khare, P.; Sonkar, S. K. Sunlight-Induced Photocatalytic Degradation of Pollutant Dye by Highly Fluorescent Red-Emitting Mg-N-Embedded Carbon Dots. *ACS Sustain Chem. Eng.* **2018**, *6* (7), 9246−9256.
(95) Khare, P.; Bhati, A.; Anand, S. R.; Gunture; Sonkar, S. K. Brightly Fluorescent Zinc-Doped Red-Emitting Carbon Dots for the Sunlight-Induced Photoreduction of Cr(VI) to Cr(III). *ACS Omega* **2018**, *3* (5), 5187−5194.
(96) Miao, X.; Qu, D.; Yang, D.; Nie, B.; Zhao, Y.; Fan, H.; Sun, Z. Synthesis of Carbon Dots with Multiple Color Emission by Controlled Graphitization and Surface Functionalization. *Adv. Mater.* **2018**, *30* (1), No. 1704740, DOI: 10.1002/adma.201704740.
(97) Hu, T.; Wen, Z.; Thomas, T.; Wang, C.; Song, Q.; Yang, M.; Wang, C. Temperature-Controlled Spectral Tuning of Full-Color Carbon Dots and Their Strongly Fluorescent Solid-State Polymer Composites for Light-Emitting Diodes. *Nanoscale Adv.* **2019**, *1* (4), 1413−1420.
(98) Tian, Z.; Zhang, X.; Li, D.; Zhou, D.; Jing, P.; Shen, D.; Qu, S.; Zboril, R.; Rogach, A. L. Full-Color Inorganic Carbon Dot Phosphors for White-Light-Emitting Diodes. *Adv. Opt Mater.* **2017**, *5* (19), No. 1700416, DOI: 10.1002/adom.201700416.
(99) Zhu, Z.; Cheng, R.; Ling, L.; Li, Q.; Chen, S. Rapid and Large-Scale Production of Multi-Fluorescence Carbon Dots by a Magnetic Hyperthermia Method. *Angewandte Chemie - International Edition* **2020**, *59* (8), 3099−3105.
(100) Ma, J.; Zhang, L.; Chen, X.; Su, R.; Shi, Q.; Zhao, S.; Xu, Q.; Xu, C. Mass Production of Highly Fluorescent Full Color Carbon

Dots from the Petroleum Coke. *Chin. Chem. Lett.* **2021**, *32* (4), 1532−1536.
(101) Ye, R.; Xiang, C.; Lin, J.; Peng, Z.; Huang, K.; Yan, Z.; Cook, N. P.; Samuel, E. L. G.; Hwang, C. C.; Ruan, G.; Ceriotti, G.; Raji, A. R. O.; Martí, A. A.; Tour, J. M. Coal as an Abundant Source of Graphene Quantum Dots. *Nat. Commun.* **2013**, *4*, No. 2943, DOI: 10.1038/ncomms3943.
(102) Hu, C.; Yu, C.; Li, M.; Wang, X.; Yang, J.; Zhao, Z.; Eychmüller, A.; Sun, Y. P.; Qiu, J. Chemically Tailoring Coal to Fluorescent Carbon Dots with Tuned Size and Their Capacity for Cu(II) Detection. *Small* **2014**, *10* (23), 4926−4933.
(103) Shao, X.; Wu, W.; Wang, R.; Zhang, J.; Li, Z.; Wang, Y.; Zheng, J.; Xia, W.; Wu, M. Engineering Surface Structure of Petroleum-Coke-Derived Carbon Dots to Enhance Electron Transfer for Photooxidation. *J. Catal.* **2016**, *344*, 236−241.
(104) Li, W.; Liu, Y.; Wang, B.; Song, H.; Liu, Z.; Lu, S.; Yang, B. Kilogram-Scale Synthesis of Carbon Quantum Dots for Hydrogen Evolution, Sensing and Bioimaging. *Chin. Chem. Lett.* **2019**, *30* (12), 2323−2327.
(105) Liu, C.; Cheng, R.; Guo, J.; Li, G.; Li, H.; Ye, H. G.; Liang, Z.-B.; Wang, C. F.; Chen, S. Carbon Dots Embedded Nanofiber Films: Large-Scale Fabrication and Enhanced Mechanical Properties. *Chin. Chem. Lett.* **2022**, *33* (1), 304−307.
(106) Tang, B.; Lu, Y.; Zhou, J.; Chouhan, T.; Wang, H.; Golani, P.; Xu, M.; Xu, Q.; Guan, C.; Liu, Z. Machine Learning-Guided Synthesis of Advanced Inorganic Materials. *Mater. Today* **2020**, *41*, 72−80.
(107) Mosconi, D.; Mazzier, D.; Silvestrini, S.; Privitera, A.; Marega, C.; Franco, L.; Moretto, A. Synthesis and Photochemical Applications of Processable Polymers Enclosing Photoluminescent Carbon Quantum Dots. *ACS Nano* **2015**, *9* (4), 4156−4164.
(108) Jelinek, R. *Carbon Quantum Dots: Synthesis, Properties and Applications*; Carbon Nanostructures Series; Springer, 2017, http://www.springer.com/series/8633.
(109) Zhu, S.; Song, Y.; Zhao, X.; Shao, J.; Zhang, J.; Yang, B. The Photoluminescence Mechanism in Carbon Dots (Graphene Quantum Dots, Carbon Nanodots, and Polymer Dots): Current State and Future Perspective. *Nano Research* **2015**, *8*, 355−381, DOI: 10.1007/s12274-014-0644-3.
(110) Yoo, D.; Park, Y.; Cheon, B.; Park, M. H. Carbon Dots as an Effective Fluorescent Sensing Platform for Metal Ion Detection. *Nanoscale Res. Lett.* **2019**, *14*, No. 272, DOI: 10.1186/s11671-019-3088-6.
(111) Pan, L.; Sun, S.; Zhang, A.; Jiang, K.; Zhang, L.; Dong, C.; Huang, Q.; Wu, A.; Lin, H. Truly Fluorescent Excitation-Dependent Carbon Dots and Their Applications in Multicolor Cellular Imaging and Multidimensional Sensing. *Adv. Mater.* **2015**, *27* (47), 7782−7787.
(112) Essner, J. B.; Kist, J. A.; Polo-Parada, L.; Baker, G. A. Artifacts and Errors Associated with the Ubiquitous Presence of Fluorescent Impurities in Carbon Nanodots. *Chem. Mater.* **2018**, *30* (6), 1878−1887.
(113) Javed, N.; O'Carroll, D. M. Long-Term Effects of Impurities on the Particle Size and Optical Emission of Carbon Dots. *Nanoscale Adv.* **2021**, *3* (1), 182−189.
(114) Kim, T. H.; Wang, F.; McCormick, P.; Wang, L.; Brown, C.; Li, Q. Salt-Embedded Carbon Nanodots as a UV and Thermal Stable Fluorophore for Light-Emitting Diodes. *J. Lumin.* **2014**, *154*, 1−7.
(115) He, G.; Shu, M.; Yang, Z.; Ma, Y.; Huang, D.; Xu, S.; Wang, Y.; Hu, N.; Zhang, Y.; Xu, L. Microwave Formation and Photoluminescence Mechanisms of Multi-States Nitrogen Doped Carbon Dots. *Appl. Surf. Sci.* **2017**, *422*, 257−265.
(116) Liu, Y.; Zhou, L.; Li, Y.; Deng, R.; Zhang, H. Highly Fluorescent Nitrogen-Doped Carbon Dots with Excellent Thermal and Photo Stability Applied as Invisible Ink for Loading Important Information and Anti-Counterfeiting. *Nanoscale* **2017**, *9* (2), 491−496.
(117) Mandal, S.; Das, P. Are Carbon Dots Worth the Tremendous Attention It Is Getting: Challenges and Opportunities. *Appl. Mater. Today* **2022**, *26*, No. 101331, DOI: 10.1016/j.apmt.2021.101331.
(118) Yang, P.; Zhu, Z.; Chen, M.; Chen, W.; Zhou, X. Microwave-Assisted Synthesis of Xylan-Derived Carbon Quantum Dots for Tetracycline Sensing. *Opt Mater. (Amst)* **2018**, *85*, 329−336.
(119) Yoshinaga, T.; Iso, Y.; Isobe, T. Optimizing the Microwave-Assisted Hydrothermal Synthesis of Blue-Emitting L-Cysteine-Derived Carbon Dots. *J. Lumin.* **2019**, *213*, 6−14.
(120) So, R. C.; Sanggo, J. E.; Jin, L.; Diaz, J. M. A.; Guerrero, R. A.; He, J. Gram-Scale Synthesis and Kinetic Study of Bright Carbon Dots from Citric Acid and Citrus Japonica via a Microwave-Assisted Method. *ACS Omega* **2017**, *2* (8), 5196−5208.
(121) Papaioannou, N.; Titirici, M. M.; Sapelkin, A. Investigating the Effect of Reaction Time on Carbon Dot Formation, Structure, and Optical Properties. *ACS Omega* **2019**, *4* (26), 21658−21665.
(122) Ding, H.; Wei, J. S.; Zhang, P.; Zhou, Z. Y.; Gao, Q. Y.; Xiong, H. M. Solvent-Controlled Synthesis of Highly Luminescent Carbon Dots with a Wide Color Gamut and Narrowed Emission Peak Widths. *Small* **2018**, *14* (22), No. 1800612, DOI: 10.1002/smll.201800612.
(123) Ai, L.; Yang, Y.; Wang, B.; Chang, J.; Tang, Z.; Yang, B.; Lu, S. Insights into Photoluminescence Mechanisms of Carbon Dots: Advances and Perspectives. *Sci. Bull.* **2021**, *66*, 839−856, DOI: 10.1016/j.scib.2020.12.015.
(124) Li, H.; He, X.; Kang, Z.; Huang, H.; Liu, Y.; Liu, J.; Lian, S.; Tsang, C. H. A.; Yang, X.; Lee, S. T. Water-Soluble Fluorescent Carbon Quantum Dots and Photocatalyst Design. *Angewandte Chemie - International Edition* **2010**, *49* (26), 4430−4434.
(125) Kim, S.; Hwang, S. W.; Kim, M. K.; Shin, D. Y.; Shin, D. H.; Kim, C. O.; Yang, S. B.; Park, J. H.; Hwang, E.; Choi, S. H.; Ko, G.; Sim, S.; Sone, C.; Choi, H. J.; Bae, S.; Hong, B. H. Anomalous Behaviors of Visible Luminescence from Graphene Quantum Dots: Interplay between Size and Shape. *ACS Nano* **2012**, *6* (9), 8203−8208.
(126) Ding, H.; Yu, S. B.; Wei, J. S.; Xiong, H. M. Full-Color Light-Emitting Carbon Dots with a Surface-State-Controlled Luminescence Mechanism. *ACS Nano* **2016**, *10* (1), 484−491.
(127) Bao, L.; Zhang, Z. L.; Tian, Z. Q.; Zhang, L.; Liu, C.; Lin, Y.; Qi, B.; Pang, D. W. Electrochemical Tuning of Luminescent Carbon Nanodots: From Preparation to Luminescence Mechanism. *Adv. Mater.* **2011**, *23* (48), 5801−5806.
(128) Liu, L.; Li, Y.; Zhan, L.; Liu, Y.; Huang, C. One-Step Synthesis of Fluorescent Hydroxyls-Coated Carbon Dots with Hydrothermal Reaction and Its Application to Optical Sensing of Metal Ions. *Sci. China Chem.* **2011**, *54* (8), 1342−1347.
(129) Zheng, H.; Wang, Q.; Long, Y.; Zhang, H.; Huang, X.; Zhu, R. Enhancing the Luminescence of Carbon Dots with a Reduction Pathway. *Chem. Commun.* **2011**, *47* (38), 10650−10652.
(130) Shabbir, H.; Csapó, E.; Wojnicki, M. Carbon Quantum Dots: The Role of Surface Functional Groups and Proposed Mechanisms for Metal Ion Sensing. *Inorganics (Basel)* **2023**, *11* (6), 262.
(131) Li, X.; Zhang, S.; Kulinich, S. A.; Liu, Y.; Zeng, H. Engineering Surface States of Carbon Dots to Achieve Controllable Luminescence for Solid-Luminescent Composites and Sensitive Be2+ Detection. *Sci. Rep* **2014**, *4*, No. 4976, DOI: 10.1038/srep04976.
(132) Kwon, W.; Do, S.; Kim, J. H.; Jeong, M. S.; Rhee, S. W. Control of Photoluminescence of Carbon Nanodots via Surface Functionalization Using Para-Substituted Anilines. *Sci. Rep.* **2015**, *5*, No. 12604, DOI: 10.1038/srep12604.
(133) Yu, J.; Liu, C.; Yuan, K.; Lu, Z.; Cheng, Y.; Li, L.; Zhang, X.; Jin, P.; Meng, F.; Liu, H. Luminescence Mechanism of Carbon Dots by Tailoring Functional Groups for Sensing Fe^{3+} Ions. *Nanomaterials* **2018**, *8* (4), 233.
(134) Liu, C.; Bao, L.; Yang, M.; Zhang, S.; Zhou, M.; Tang, B.; Wang, B.; Liu, Y.; Zhang, Z. L.; Zhang, B.; Pang, D. W. Surface Sensitive Photoluminescence of Carbon Nanodots: Coupling between the Carbonyl Group and π-Electron System. *J. Phys. Chem. Lett.* **2019**, *10* (13), 3621−3629.
(135) Gan, Z.; Wu, X.; Hao, Y. The Mechanism of Blue Photoluminescence from Carbon Nanodots. *CrystEngComm* **2014**, *16* (23), 4981−4986.

(136) Gan, Z.; Xiong, S.; Wu, X.; Xu, T.; Zhu, X.; Gan, X.; Guo, J.; Shen, J.; Sun, L.; Chu, P. K. Mechanism of Photoluminescence from Chemically Derived Graphene Oxide: Role of Chemical Reduction. *Adv. Opt Mater.* **2013**, *1* (12), 926−932.
(137) Wang, H.; Zhang, T.; Zhu, J.; Zhai, Y.; Wang, H.; Bai, X.; Dong, B.; Song, H. A Novel Mechanism for Red Emission Carbon Dots: Hydrogen Bond Dominated Molecular States Emission. *Nanoscale* **2017**, *9* (35), 13042−13051.
(138) Jiang, K.; Sun, S.; Zhang, L.; Lu, Y.; Wu, A.; Cai, C.; Lin, H. Red, Green, and Blue Luminescence by Carbon Dots: Full-Color Emission Tuning and Multicolor Cellular Imaging. *Angew. Chem.* **2015**, *127* (18), 5450−5453.
(139) Liu, H.; Yang, J.; Li, Z.; Xiao, L.; Aryee, A. A.; Sun, Y.; Yang, R.; Meng, H.; Qu, L.; Lin, Y.; Zhang, X. Hydrogen-Bond-Induced Emission of Carbon Dots for Wash-Free Nucleus Imaging. *Anal. Chem.* **2019**, *91* (14), 9259−9265.
(140) Kundu, A.; Park, B.; Oh, J.; Sankar, K. V.; Ray, C.; Kim, W. S.; Chan Jun, S. Multicolor Emissive Carbon Dot with Solvatochromic Behavior across the Entire Visible Spectrum. *Carbon N Y* **2020**, *156*, 110−118.
(141) Mukherjee, S.; Prasad, E.; Chadha, A. H-Bonding Controls the Emission Properties of Functionalized Carbon Nano-Dots. *Phys. Chem. Chem. Phys.* **2017**, *19* (10), 7288−7296.
(142) Miao, S.; Liang, K.; Zhu, J.; Yang, B.; Zhao, D.; Kong, B. Hetero-Atom-Doped Carbon Dots: Doping Strategies, Properties and Applications. *Nano Today* **2020**, *33*, No. 100879, DOI: 10.1016/j.nantod.2020.100879.
(143) Hu, C.; Liu, D.; Xiao, Y.; Dai, L. Functionalization of Graphene Materials by Heteroatom-Doping for Energy Conversion and Storage. *Prog. Natural Sci.: Mater. Int* **2018**, *28*, 121−132, DOI: 10.1016/j.pnsc.2018.02.001.
(144) Niu, Y.; Li, J.; Gao, J.; Ouyang, X.; Cai, L.; Xu, Q. Two-Dimensional Quantum Dots for Biological Applications. *Nano Res.* **2021**, *14*, 3820−3839, DOI: 10.1007/s12274-021-3757-5.
(145) Zhang, R.; Chen, W. Nitrogen-Doped Carbon Quantum Dots: Facile Synthesis and Application as a "Turn-off" Fluorescent Probe for Detection of Hg^{2+} Ions. *Biosens Bioelectron* **2014**, *55*, 83−90.
(146) Zhao, S.; Lan, M.; Zhu, X.; Xue, H.; Ng, T.-W.; Meng, X.; Lee, C.-S.; Wang, P.; Zhang, W. Green Synthesis of Bifunctional Fluorescent Carbon Dots from Garlic for Cellular Imaging and Free Radicals Scavenging. *ACS Appl. Mater. Interfaces* **2015**, *7*, 17054 DOI: 10.1021/acsami.5b03228.
(147) Xu, Q.; Pu, P.; Zhao, J.; Liu, Y.; Dong, C.; Gao, C.; Chen, Y.; Chen, J.; Zhou, H. Preparation of Highly Photoluminescent Sulfur-Doped Carbon Dots for Fe(III) Detection. *J. Mater. Chem. A* **2015**, *3*, 542−546, DOI: 10.1039/C4TA05483K.
(148) Xu, Q.; Niu, Y.; Li, J.; Yang, Z.; Gao, J.; Ding, L.; Ni, H.; Zhu, P.; Liu, Y.; Tang, Y.; Lv, Z. P.; Peng, B.; Hu, T. S.; Zhou, H.; Xu, C. Recent Progress of Quantum Dots for Energy Storage Applications. *Carbon Neutrality* **2022**, *1*, No. 13, DOI: 10.1007/s43979-022-00002-y.
(149) Liu, Y.; Wei, J.; Yan, X.; Zhao, M.; Guo, C.; Xu, Q. Barium Charge Transferred Doped Carbon Dots with Ultra-High Quantum Yield Photoluminescence of 99.6% and Applications. *Chin. Chem. Lett.* **2021**, *32* (2), 861−865.
(150) Choudhary, S.; Sharma, K.; Sharma, V.; Kumar, V. Grafting Polymers. In *Reactive and Functional Polymers Vol. Two: Modification Reactions, Compatibility and Blends*; Springer International Publishing, 2020; Vol. *2*, pp 199−243. DOI: 10.1007/978-3-030-45135-6_8.
(151) Paszkiewicz, S.; Szymczyk, A. Graphene-Based Nanomaterials and Their Polymer Nanocomposites. In *Nanomaterials and Polymer Nanocomposites: Raw Materials to Applications*; Elsevier, 2019; pp 177−216. DOI: 10.1016/B978-0-12-814615-6.00006-0.
(152) Fawaz, J.; Mittal, V. Synthesis of Polymer Nanocomposites: Review of Various Techniques. In *Synthesis Techniques for Polymer Nanocomposites*; Wiley, 2015.
(153) Jalili, R.; Amjadi, M. Bio-Inspired Molecularly Imprinted Polymer−Green Emitting Carbon Dot Composite for Selective and Sensitive Detection of 3-Nitrotyrosine as a Biomarker. *Sens Actuators B Chem.* **2018**, *255*, 1072−1078.
(154) Rivadeneyra, A.; Salmeron, J. F.; Murru, F.; Lapresta-Fernández, A.; Rodríguez, N.; Capitan-Vallvey, L. F.; Morales, D. P.; Salinas-Castillo, A. Carbon Dots as Sensing Layer for Printed Humidity and Temperature Sensors. *Nanomaterials* **2020**, *10* (12), 2446.
(155) Carvalho, J.; Santos, L. R.; Germino, J. C.; Terezo, A. J.; Moreto, J. A.; Quites, F. J.; Freitas, R. G. Hydrothermal Synthesis to Water-Stable Luminescent Carbon Dots from Acerola Fruit for Photoluminescent Composites Preparation and Its Application as Sensors. *Mater. Res.* **2019**, *22* (3). DOI: 10.1590/1980-5373-mr-2018-0920.
(156) Ma, S.; Zheng, H.; Chen, Y.; Zou, J.; Zhang, C.; Wang, Y. Nanocomposite Polymer Hydrogels Reinforced by Carbon Dots and Hectorite Clay. *Journal Wuhan University of Technology, Materials Science Edition* **2020**, *35* (2), 287−292.
(157) Shauloff, N.; Bhattacharya, S.; Jelinek, R. Elastic Carbon Dot/Polymer Films for Fluorescent Tensile Sensing and Mechano-Optical Tuning. *Carbon N Y* **2019**, *152*, 363−371.
(158) Rimal, V.; Shishodia, S.; Srivastava, P. K. Novel Synthesis of High-Thermal Stability Carbon Dots and Nanocomposites from Oleic Acid as an Organic Substrate. *Applied Nanoscience (Switzerland)* **2020**, *10* (2), 455−464.
(159) Zheng, X.; Ding, G.; Wang, H.; Cui, G.; Zhang, P. One-Step Hydrothermal Synthesis of Carbon Dots-Polymer Composites with Solid-State Photoluminescence. *Mater. Lett.* **2019**, *238*, 22−25.
(160) Fernandes, D.; Heslop, K. A.; Kelarakis, A.; Krysmann, M. J.; Estevez, L. In Situ Generation of Carbon Dots within a Polymer Matrix. *Polymer (Guildf)* **2020**, *188*, 122159.
(161) Tian, Z.; Li, D.; Ushakova, E. V.; Maslov, V. G.; Zhou, D.; Jing, P.; Shen, D.; Qu, S.; Rogach, A. L. Multilevel Data Encryption Using Thermal-Treatment Controlled Room Temperature Phosphorescence of Carbon Dot/Polyvinylalcohol Composites. *Adv. Sci.* **2018**, *5* (9), No. 1800795, DOI: 10.1002/advs.201800795.
(162) Issa, M. A.; Abidin, Z. Z. Sustainable Development of Enhanced Luminescence Polymer-Carbon Dots Composite Film for Rapid Cd^{2+} Removal from Wastewater. *Molecules* **2020**, *25* (15), 3541.
(163) Wang, M.; Gao, M.; Deng, L.; Kang, X.; Yang, L.; Quan, T.; Xia, Z.; Gao, D. Composite Material Based on Carbon Dots and Molecularly Imprinted Polymers: A Facile Probe for Fluorescent Detection of 4-Nitrophenol. *Nano* **2020**, *15* (8), 2050105.
(164) Belbruno, J. J. Molecularly Imprinted Polymers. *Chem. Rev.* **2019**, *119*, 94−119, DOI: 10.1021/acs.chemrev.8b00171.
(165) Turiel, E.; Esteban, A. M. Molecularly Imprinted Polymers. In *Solid-Phase Extraction*; Elsevier, 2019; pp 215−233. DOI: 10.1016/B978-0-12-816906-3.00008-X.
(166) Vasapollo, G.; Del Sole, R.; Mergola, L.; Lazzoi, M. R.; Scardino, A.; Scorrano, S.; Mele, G. Molecularly Imprinted Polymers: Present and Future Prospective. *International Journal of Molecular Sciences.* **2011**, *12*, 5908−5945.
(167) Akgönüllü, S.; Kılıç, S.; Esen, C.; Denizli, A. Molecularly Imprinted Polymer-Based Sensors for Protein Detection. *Polymers* **2023**, *15*, 629 DOI: 10.3390/polym15030629.
(168) Wu, Q.; Wang, X.; Rasaki, S. A.; Thomas, T.; Wang, C.; Zhang, C.; Yang, M. Yellow-Emitting Carbon-Dots-Impregnated Carboxy Methyl Cellulose/Poly-Vinyl-Alcohol and Chitosan: Stable, Freestanding, Enhanced-Quenching Cu2+-Ions Sensor. *J. Mater. Chem. C Mater.* **2018**, *6* (16), 4508−4515.
(169) Devadas, B.; Imae, T. Effect of Carbon Dots on Conducting Polymers for Energy Storage Applications. *ACS Sustain Chem. Eng.* **2018**, *6* (1), 127−134.
(170) Wang, M.; Gao, M.; Deng, L.; Kang, X.; Zhang, K.; Fu, Q.; Xia, Z.; Gao, D. A Sensitive and Selective Fluorescent Sensor for 2,4,6-Trinitrophenol Detection Based on the Composite Material of Magnetic Covalent Organic Frameworks, Molecularly Imprinted Polymers and Carbon Dots. *Microchemical J.* **2020**, *154*, 104590.

https://doi.org/10.1021/acsomega.3c07612
ACS Omega 2024, 9, 11050−11080

(171) Wang, C.; Hu, T.; Chen, Y.; Xu, Y.; Song, Q. Polymer-Assisted Self-Assembly of Multicolor Carbon Dots as Solid-State Phosphors for Fabrication of Warm, High-Quality, and Temperature-Responsive White-Light-Emitting Devices. *ACS Appl. Mater. Interfaces* **2019**, *11*, 22332.
(172) Li, Y.; Li, S.; Zhang, K. Influence of Hydrophilic Carbon Dots on Polyamide Thin Film Nanocomposite Reverse Osmosis Membranes. *J. Membr. Sci.* **2017**, *537*, 42−53.
(173) Li, Y.; Huang, Z. Z.; Weng, Y.; Tan, H. Pyrophosphate Ion-Responsive Alginate Hydrogel as an Effective Fluorescent Sensing Platform for Alkaline Phosphatase Detection. *Chem. Commun.* **2019**, *55* (76), 11450−11453.
(174) Wang, H.; Yi, J.; Yu, Y.; Zhou, S. NIR Upconversion Fluorescence Glucose Sensing and Glucose-Responsive Insulin Release of Carbon Dot-Immobilized Hybrid Microgels at Physiological PH. *Nanoscale* **2017**, *9* (2), 509−516.
(175) Kazemifard, N.; Ensafi, A. A.; Rezaei, B. Green Synthesized Carbon Dots Embedded in Silica Molecularly Imprinted Polymers, Characterization and Application as a Rapid and Selective Fluorimetric Sensor for Determination of Thiabendazole in Juices. *Food Chem.* **2020**, *310*, 125812.
(176) Koulivand, H.; Shahbazi, A.; Vatanpour, V.; Rahmandoust, M. Development of Carbon Dot-Modified Polyethersulfone Membranes for Enhancement of Nanofiltration, Permeation and Antifouling Performance. *Sep. Purif. Technol.* **2020**, *230*, 115895.
(177) Yuan, Z.; Wu, X.; Jiang, Y.; Li, Y.; Huang, J.; Hao, L.; Zhang, J.; Wang, J. Carbon Dots-Incorporated Composite Membrane towards Enhanced Organic Solvent Nanofiltration Performance. *J. Membr. Sci.* **2018**, *549*, 1−11.
(178) Sun, X.; Lei, Y. Fluorescent Carbon Dots and Their Sensing Applications. *TrAC - Trends in Analytical Chemistry* **2017**, *89*, 163−180, DOI: 10.1016/j.trac.2017.02.001.
(179) Ansari, S.; Masoum, S. Recent Advances and Future Trends on Molecularly Imprinted Polymer-Based Fluorescence Sensors with Luminescent Carbon Dots. *Talanta* **2021**, *223*, No. 121411, DOI: 10.1016/j.talanta.2020.121411.
(180) Peng, Z.; Han, X.; Li, S.; Al-Youbi, A. O.; Bashammakh, A. S.; El-Shahawi, M. S.; Leblanc, R. M. Carbon Dots: Biomacromolecule Interaction, Bioimaging and Nanomedicine. *Coord. Chem. Rev.* **2017**, *343*, 256−277, DOI: 10.1016/j.ccr.2017.06.001.
(181) Zu, F.; Yan, F.; Bai, Z.; Xu, J.; Wang, Y.; Huang, Y.; Zhou, X. The Quenching of the Fluorescence of Carbon Dots: A Review on Mechanisms and Applications. *Microchimica Acta* **2017**, *184*, 1899−1914, DOI: 10.1007/s00604-017-2318-9.
(182) Barman, S.; Sadhukhan, M. Facile Bulk Production of Highly Blue Fluorescent Graphitic Carbon Nitride Quantum Dots and Their Application as Highly Selective and Sensitive Sensors for the Detection of Mercuric and Iodide Ions in Aqueous Media. *J. Mater. Chem.* **2012**, *22* (41), 21832−21837.
(183) Wang, X.; Zhang, J.; Zou, W.; Wang, R. Facile Synthesis of Polyaniline/Carbon Dot Nanocomposites and Their Application as a Fluorescent Probe to Detect Mercury. *RSC Adv.* **2015**, *5* (52), 41914−41919.
(184) Xi, L. L.; Ma, H. B.; Tao, G. H. Thiourea Functionalized CdSe/CdS Quantum Dots as a Fluorescent Sensor for Mercury Ion Detection. *Chin. Chem. Lett.* **2016**, *27* (9), 1531−1536.
(185) Song, Y.; Zhu, S.; Xiang, S.; Zhao, X.; Zhang, J.; Zhang, H.; Fu, Y.; Yang, B. Investigation into the Fluorescence Quenching Behaviors and Applications of Carbon Dots. *Nanoscale* **2014**, *6* (9), 4676−4682.
(186) Yang, P.; Zhao, Y.; Lu, Y.; Xu, Q. Z.; Xu, X. W.; Dong, L.; Yu, S. H. Phenol Formaldehyde Resin Nanoparticles Loaded with CdTe Quantum Dots: A Fluorescence Resonance Energy Transfer Probe for Optical Visual Detection of Copper(II) Ions. *ACS Nano* **2011**, *5* (3), 2147−2154.
(187) Lu, W.; Qin, X.; Liu, S.; Chang, G.; Zhang, Y.; Luo, Y.; Asiri, A. M.; Al-Youbi, A. O.; Sun, X. Economical, Green Synthesis of Fluorescent Carbon Nanoparticles and Their Use as Probes for Sensitive and Selective Detection of Mercury(II) Ions. *Anal. Chem.* **2012**, *84* (12), 5351−5357.
(188) Cui, X.; Zhu, L.; Wu, J.; Hou, Y.; Wang, P.; Wang, Z.; Yang, M. A Fluorescent Biosensor Based on Carbon Dots-Labeled Oligodeoxyribonucleotide and Graphene Oxide for Mercury (II) Detection. *Biosens Bioelectron* **2015**, *63*, 506−512.
(189) Costas-Mora, I.; Romero, V.; Lavilla, I.; Bendicho, C. In Situ Building of a Nanoprobe Based on Fluorescent Carbon Dots for Methylmercury Detection. *Anal. Chem.* **2014**, *86* (9), 4536−4543.
(190) Mohapatra, S.; Sahu, S.; Sinha, N.; Bhutia, S. K. Synthesis of a Carbon-Dot-Based Photoluminescent Probe for Selective and Ultrasensitive Detection of Hg2+in Water and Living Cells. *Analyst* **2015**, *140* (4), 1221−1228.
(191) Wang, L.; Li, B.; Xu, F.; Shi, X.; Feng, D.; Wei, D.; Li, Y.; Feng, Y.; Wang, Y.; Jia, D.; Zhou, Y. High-Yield Synthesis of Strong Photoluminescent N-Doped Carbon Nanodots Derived from Hydrosoluble Chitosan for Mercury Ion Sensing via Smartphone APP. *Biosens Bioelectron* **2016**, *79*, 1−8.
(192) Zhou, M.; Zhou, Z.; Gong, A.; Zhang, Y.; Li, Q. Synthesis of Highly Photoluminescent Carbon Dots via Citric Acid and Tris for Iron(III) Ions Sensors and Bioimaging. *Talanta* **2015**, *143*, 107−113.
(193) Zhu, S.; Meng, Q.; Wang, L.; Zhang, J.; Song, Y.; Jin, H.; Zhang, K.; Sun, H.; Wang, H.; Yang, B. Highly Photoluminescent Carbon Dots for Multicolor Patterning, Sensors, and Bioimaging. *Angewandte Chemie - International Edition* **2013**, *52* (14), 3953−3957.
(194) Qu, K.; Wang, J.; Ren, J.; Qu, X. Carbon Dots Prepared by Hydrothermal Treatment of Dopamine as an Effective Fluorescent Sensing Platform for the Label-Free Detection of Iron(III) Ions and Dopamine. *Chem.—Eur. J.* **2013**, *19* (22), 7243−7249.
(195) Lu, W.; Yang, Z.; Zhang, Y.; Hu, Q.; Shuang, S.; Dong, C.; Choi, M. M. F. High-quality water-soluble luminescent carbon dots for multicolor patterning, sensors, and bioimaging. *RSC Adv.* **2015**, *5*, 16972 DOI: 10.1039/C4RA16233A.
(196) Zhang, H.; Chen, Y.; Liang, M.; Xu, L.; Qi, S.; Chen, H.; Chen, X. Solid-Phase Synthesis of Highly Fluorescent Nitrogen-Doped Carbon Dots for Sensitive and Selective Probing Ferric Ions in Living Cells. *Anal. Chem.* **2014**, *86* (19), 9846−9852.
(197) Lu, W.; Gong, X.; Nan, M.; Liu, Y.; Shuang, S.; Dong, C. Comparative Study for N and S Doped Carbon Dots: Synthesis, Characterization and Applications for Fe^{3+} Probe and Cellular Imaging. *Anal. Chim. Acta* **2015**, *898*, 116−127.
(198) Ju, J.; Chen, W. Synthesis of Highly Fluorescent Nitrogen-Doped Graphene Quantum Dots for Sensitive, Label-Free Detection of Fe (III) in Aqueous Media. *Biosens Bioelectron* **2014**, *58*, 219−225.
(199) Wang, Z. X.; Yu, X. H.; Li, F.; Kong, F. Y.; Lv, W. X.; Fan, D. H.; Wang, W. Preparation of Boron-Doped Carbon Dots for Fluorometric Determination of Pb(II), Cu(II) and Pyrophosphate Ions. *Microchimica Acta* **2017**, *184* (12), 4775−4783.
(200) Dong, Y.; Wang, R.; Li, G.; Chen, C.; Chi, Y.; Chen, G. Polyamine-Functionalized Carbon Quantum Dots as Fluorescent Probes for Selective and Sensitive Detection of Copper Ions. *Anal. Chem.* **2012**, *84* (14), 6220−6224.
(201) Sun, H.; Gao, N.; Wu, L.; Ren, J.; Wei, W.; Qu, X. Highly Photoluminescent Amino-Functionalized Graphene Quantum Dots Used for Sensing Copper Ions. *Chem.—Eur. J.* **2013**, *19* (40), 13362−13368.
(202) Zhu, A.; Qu, Q.; Shao, X.; Kong, B.; Tian, Y. Carbon-Dot-Based Dual-Emission Nanohybrid Produces a Ratiometric Fluorescent Sensor for in Vivo Imaging of Cellular Copper Ions. *Angewandte Chemie - International Edition* **2012**, *51* (29), 7185−7189.
(203) Yen, Y. Te; Lin, Y. S.; Chen, T. Y.; Chyueh, S. C.; Chang, H. T. Carbon Dots Functionalized Papers for High-Throughput Sensing of 4-Chloroethcathinone and Its Analogues in Crime Sites. *R Soc. Open Sci.* **2019**, *6* (9), 191017.
(204) Chu, C.-S.; Hsieh, M.-W.; Su, Z.-R. Optical Sensing of H_2O_2 Based on Red-Shift of Emission Wavelength of Carbon Quantum Dots. *Opt Mater. Express* **2016**, *6* (3), 759.
(205) Wang, J.; Li, D.; Qiu, Y.; Liu, X.; Huang, L.; Wen, H.; Hu, J. An Europium Functionalized Carbon Dot-Based Fluorescence Test

https://doi.org/10.1021/acsomega.3c07612
ACS Omega 2024, 9, 11050−11080

Paper for Visual and Quantitative Point-of-Care Testing of Anthrax Biomarker. *Talanta* **2020**, *220*, 121377.
(206) Wu, F. F.; Zhou, Y.; Wang, J. X.; Zhuo, Y.; Yuan, R.; Chai, Y. Q. A Novel Electrochemiluminescence Immunosensor Based on Mn Doped Ag_2S Quantum Dots Probe for Laminin Detection. *Sens Actuators B Chem.* **2017**, *243*, 1067−1074.
(207) Fu, Y.; Wu, S.; Zhou, H.; Zhao, S.; Lan, M.; Huang, J.; Song, X. Carbon Dots and a CdTe Quantum Dot Hybrid-Based Fluorometric Probe for Spermine Detection. *Ind. Eng. Chem. Res.* **2020**, *59* (4), 1723−1729.
(208) Zhang, L.; Han, Y.; Zhu, J.; Zhai, Y.; Dong, S. Simple and Sensitive Fluorescent and Electrochemical Trinitrotoluene Sensors Based on Aqueous Carbon Dots. *Anal. Chem.* **2015**, *87* (4), 2033−2036.
(209) Shen, P.; Xia, Y. Synthesis-Modification Integration: One-Step Fabrication of Boronic Acid Functionalized Carbon Dots for Fluorescent Blood Sugar Sensing. *Anal. Chem.* **2014**, *86* (11), 5323−5329.
(210) Zhu, P.; Liu, Y.; Tang, Y.; Zhu, S.; Liu, X.; Yin, L.; Liu, Q.; Yu, Z.; Xu, Q.; Luo, D.; Wang, J. Bi-Doped Carbon Quantum Dots Functionalized Liposomes with Fluorescence Visualization Imaging for Tumor Diagnosis and Treatment. *Chin. Chem. Lett.* **2024**, *35*, No. 108689.
(211) Xu, B.; Zhao, C.; Wei, W.; Ren, J.; Miyoshi, D.; Sugimoto, N.; Qu, X. Aptamer Carbon Nanodot Sandwich Used for Fluorescent Detection of Protein. *Analyst* **2012**, *137* (23), 5483−5486.
(212) Ma, N.; Jiang, W.; Li, T.; Zhang, Z.; Qi, H.; Yang, M. Fluorescence Aggregation Assay for the Protein Biomarker Mucin 1 Using Carbon Dot-Labeled Antibodies and Aptamers. *Microchimica Acta* **2015**, *182* (1−2), 443−447.
(213) Xu, S.; Su, Z.; Zhang, Z.; Nie, Y.; Wang, J.; Ge, G.; Luo, X. Rapid Synthesis of Nitrogen Doped Carbon Dots and Their Application as a Label Free Sensor Array for Simultaneous Discrimination of Multiple Proteins. *J. Mater. Chem. B* **2017**, *5* (44), 8748−8753.
(214) Freire, R. M.; Le, N. D. B.; Jiang, Z.; Kim, C. S.; Rotello, V. M.; Fechine, P. B. A. NH2-Rich Carbon Quantum Dots: A Protein-Responsive Probe for Detection and Identification. *Sens Actuators B Chem.* **2018**, *255*, 2725−2732.
(215) Xiaoyan, Z.; Zhangyi, L.; Zaijun, L. Fabrication of Valine-Functionalized Graphene Quantum Dots and Its Use as a Novel Optical Probe for Sensitive and Selective Detection of Hg^{2+}. *Spectrochim Acta A Mol. Biomol Spectrosc* **2017**, *171*, 415−424.
(216) Li, M.; Wang, Q.; Shi, X.; Hornak, L. A.; Wu, N. Detection of Mercury(II) by Quantum Dot/DNA/Gold Nanoparticle Ensemble Based Nanosensor via Nanometal Surface Energy Transfer. *Anal. Chem.* **2011**, *83* (18), 7061−7065.
(217) Li, Q.; Chen, B.; Xing, B. Aggregation Kinetics and Self-Assembly Mechanisms of Graphene Quantum Dots in Aqueous Solutions: Cooperative Effects of PH and Electrolytes. *Environ. Sci. Technol.* **2017**, *51* (3), 1364−1376.
(218) Feng, Z.; Adolfsson, K. H.; Xu, Y.; Fang, H.; Hakkarainen, M.; Wu, M. Carbon Dot/Polymer Nanocomposites: From Green Synthesis to Energy, Environmental and Biomedical Applications. *Sustainable Mater. Technol.* **2021**, *29*, No. e00304, DOI: 10.1016/j.susmat.2021.e00304.
(219) Eftekhari, E.; Wang, W.; Li, X.; A, N.; Wu, Z.; Klein, R.; Cole, I. S.; Li, Q. Picomolar Reversible Hg(II) Solid-State Sensor Based on Carbon Dots in Double Heterostructure Colloidal Photonic Crystals. *Sens Actuators B Chem.* **2017**, *240*, 204−211.
(220) Kumar, A.; Chowdhuri, A. R.; Laha, D.; Chandra, S.; Karmakar, P.; Sahu, S. K. One-Pot Synthesis of Carbon Dot-Entrenched Chitosan-Modified Magnetic Nanoparticles for Fluorescence-Based Cu2+ Ion Sensing and Cell Imaging. *RSC Adv.* **2016**, *6* (64), 58979−58987.
(221) Shao, J.; Yu, Q.; Wang, S.; Hu, Y.; Guo, Z.; Kang, K.; Ji, X. Poly(Vinyl Alcohol)−Carbon Nanodots Fluorescent Hydrogel with Superior Mechanical Properties and Sensitive to Detection of Iron(III) Ions. *Macromol. Mater. Eng.* **2019**, *304* (11), No. 1900326, DOI: 10.1002/mame.201900326.
(222) Guo, X.; Xu, D.; Yuan, H.; Luo, Q.; Tang, S.; Liu, L.; Wu, Y. A Novel Fluorescent Nanocellulosic Hydrogel Based on Carbon Dots for Efficient Adsorption and Sensitive Sensing in Heavy Metals. *J. Mater. Chem. A Mater.* **2019**, *7* (47), 27081−27088.
(223) Li, S.; Zhou, S.; Xu, H.; Xiao, L.; Wang, Y.; Shen, H.; Wang, H.; Yuan, Q. Luminescent Properties and Sensing Performance of a Carbon Quantum Dot Encapsulated Mesoporous Silica/Polyacrylonitrile Electrospun Nanofibrous Membrane. *J. Mater. Sci.* **2016**, *51* (14), 6801−6811.
(224) Yuan, H.; Peng, J.; Ren, T.; Luo, Q.; Luo, Y.; Zhang, N.; Huang, Y.; Guo, X.; Wu, Y. Novel Fluorescent Lignin-Based Hydrogel with Cellulose Nanofibers and Carbon Dots for Highly Efficient Adsorption and Detection of Cr(VI). *Sci. Total Environ.* **2021**, *760*, 143395.
(225) Gogoi, N.; Barooah, M.; Majumdar, G.; Chowdhury, D. Carbon Dots Rooted Agarose Hydrogel Hybrid Platform for Optical Detection and Separation of Heavy Metal Ions. *ACS Appl. Mater. Interfaces* **2015**, *7* (5), 3058−3067.
(226) Li, M.; Li, X.; Jiang, M.; Liu, X.; Chen, Z.; Wang, S.; James, T. D.; Wang, L.; Xiao, H. Engineering a Ratiometric Fluorescent Sensor Membrane Containing Carbon Dots for Efficient Fluoride Detection and Removal. *Chemical Engineering Journal* **2020**, *399*, 125741.
(227) Dolai, S.; Bhunia, S. K.; Jelinek, R. Carbon-Dot-Aerogel Sensor for Aromatic Volatile Organic Compounds. *Sens Actuators B Chem.* **2017**, *241*, 607−613.
(228) Bai, J.; Ren, W.; Wang, Y.; Li, X.; Zhang, C.; Li, Z.; Xie, Z. High-Performance Thermoplastic Polyurethane Elastomer/Carbon Dots Bulk Nanocomposites with Strong Luminescence. *High Perform Polym.* **2020**, *32* (7), 857−867.
(229) Wang, M.; Fu, Q.; Zhang, K.; Wan, Y.; Wang, L.; Gao, M.; Xia, Z.; Gao, D. A Magnetic and Carbon Dot Based Molecularly Imprinted Composite for Fluorometric Detection of 2,4,6-Trinitrophenol. *Microchimica Acta* **2019**, *186* (2), No. 86, DOI: 10.1007/s00604-018-3200-0.
(230) Dai, J.; Dong, X.; Fidalgo de Cortalezzi, M. Molecularly Imprinted Polymers Labeled with Amino-Functionalized Carbon Dots for Fluorescent Determination of 2,4-Dinitrotoluene. *Microchimica Acta* **2017**, *184* (5), 1369−1377.
(231) Li, H.; Zhao, L.; Xu, Y.; Zhou, T.; Liu, H.; Huang, N.; Ding, J.; Li, Y.; Ding, L. Single-Hole Hollow Molecularly Imprinted Polymer Embedded Carbon Dot for Fast Detection of Tetracycline in Honey. *Talanta* **2018**, *185*, 542−549.
(232) Xu, X.; Xu, G.; Wei, F.; Cen, Y.; Shi, M.; Cheng, X.; Chai, Y.; Sohail, M.; Hu, Q. Carbon Dots Coated with Molecularly Imprinted Polymers: A Facile Bioprobe for Fluorescent Determination of Caffeic Acid. *J. Colloid Interface Sci.* **2018**, *529*, 568−574.
(233) Wang, J.; Qiu, F.; Wu, H.; Li, X.; Zhang, T.; Niu, X.; Yang, D.; Pan, J.; Xu, J. A Novel Water-Soluble Chitosan Linked Fluorescent Carbon Dots and Isophorone Diisocyanate Fluorescent Material toward Detection of Chromium(Vi). *Analytical Methods* **2016**, *8* (48), 8554−8565.
(234) Sun, X.; Liu, Y.; Niu, N.; Chen, L. Synthesis of Molecularly Imprinted Fluorescent Probe Based on Biomass-Derived Carbon Quantum Dots for Detection of Mesotrione. *Anal Bioanal Chem.* **2019**, *411* (21), 5519−5530.
(235) Zhang, Y.; Li, S.; Ma, X. T.; He, X. W.; Li, W. Y.; Zhang, Y. K. Carbon Dots-Embedded Epitope Imprinted Polymer for Targeted Fluorescence Imaging of Cervical Cancer via Recognition of Epidermal Growth Factor Receptor. *Microchimica Acta* **2020**, *187* (4), No. 228, DOI: 10.1007/s00604-020-4198-7.
(236) Shariati, R.; Rezaei, B.; Jamei, H. R.; Ensafi, A. A. Application of Coated Green Source Carbon Dots with Silica Molecularly Imprinted Polymers as a Fluorescence Probe for Selective and Sensitive Determination of Phenobarbital. *Talanta* **2019**, *194*, 143−149.

https://doi.org/10.1021/acsomega.3c07612
ACS Omega 2024, 9, 11050−11080